The Lithological and Structural Characterisation of the Sperlingputs Shear Zone in Southern Namibia.

by
Jason Linekela Indongo

Thesis presented in fulfilment of the requirements for the degree of Master of Science in the Faculty of Science at Stellenbosch University

Supervisor: Dr. Jodie Miller

Co-Supervisor: Dr. Paul Macey

December 2017

DECLARATION

This thesis is a presentation of my original research work. Wherever contributions of others are involved, every effort is made to indicate this clearly, with due reference to the literature, and acknowledgement of collaborative research and discussions. I declare that I am the sole author thereof (save to the extent explicitly otherwise stated), that reproduction and publication thereof by Stellenbosch University will not infringe any third party rights and that I have not previously in its entirety or in part submitted it for obtaining any qualification.

Date: December 2017

ACKNOWLEDGEMENTS

In this very special occasion I would like to express my deepest gratitude and appreciation to Dr Jodie A. Miller (University of Stellenbosch) for supervising this project. I cannot extend my appreciation enough for all your help and patience over difficult few years. Acknowledging you for the valuable time, advice, criticism and correction that you gave to this thesis from the beginning up to the end of the writing. I would like to thank Dr. Paul Macey for the invaluable input in this study. I would also like to extend my appreciation to the members of the southern Namibia joint mapping project between the Geological Survey of Namibia and Council for Geosciences, South Africa. Finally, thanks are also due to my fiancée, daughter, family and colleagues. Thank you all.

Table of Content

Table of Figures

ABSTRACT

The Richtersveld Magmatic Arc (RMA) forms a major ~200km wide Palaeoproterozoic block within the Mesoproterozoic Namaqua Metamorphic Province (NMP). The RMA consist of rafts of Orange River Group volcanic rocks intruded by voluminous coeval Vioolsdrif Suite granitoids (1905-1865 Ma, [1]). The RMA is further subdivided into two domains with equivalent stratigraphic units but different metamorphic grade and deformation. In the west are low grade greenschist-facies rocks affected only by D1 which have been termed the Vioolsdrif Domain. These rocks are separated by a km wide tectonic zone termed the Southern Namaqua Front from the amphibolite-facies Pella Domain in the NE. The Pella Domain is strongly transposed by the main ductile D_2 phase of the Namaqua Orogeny at ~1215Ma. As part of a regional scale mapping program by the Namibian Geological Survey and the Council for Geoscience, the Southern Namaqua Front has been re-examined and redefined. The Southern Namaqua Front in fact coincides with the northern margin of a ~15 km deformation zone termed the Sperlingputs Shear Zone System (SPSZS). The SPSZS consists of three main WNW-trending, steeply dipping shear zones that cross-cut the Vioolsdrif Domain and truncate the Haib porphyry Cu deposit. Collectively the SPSZS represents an anastomosing zone of deformation that mainly follows the less competent Orange River Group volcanic rocks that are sheared into fissile cataclasites and mylonites and wrap around largely unsheared blocks of bedded lava and, more often, granitoids of the Vioolsdrif Suite. The northernmost shear zone termed Fontal-SPSZS reworks the Southern Namaqua Front and cross-cuts the penetrative Pella Domain fabrics and structures, and thus post-dates D_2. The rocks on the north of the F-SPSZS have a gneissic and schistose texture, with an overall mid to upper amphibolite-facies mineral assemblage, whilst those on the south of the F-SPSZS, are weakly deformed with a lower greenschist-facies mineral assemblage. The dominant steeply south plunging lineation along with various shear sense indicators suggest a significant a dextral sense of movement, which is the transpression regime. However, in some areas, the shear zones are accompanied by the development of vertical lineation with a suggesting a vertical component to the shear with an overall top to the south sense of movement. The SPSZS is intruded by pegmatite dykes and large plugs, both deformed and undeformed, which suggests intrusion during and soon after shearing - a relationship similar to that in other large shear zones in the area (Marshall Rocks-Pofadder Shear Zone (MRPSZ), Eureka shear Zone(ESZ)). Assuming that these pegmatites are equivalent to those in other parts of the Pella Domain (MRPSZ and ESZ), the SPSZS developed during the late Namaqua D_4-dextral shearing event

between ca. 1005 and 950 Ma, together with the also NW-trending Marshall Rocks-Pofadder and Eureka Shear Zones.

Table of contents

CHAPTER 1: INTRODUCTION

1.1 INTRODUCTION

The study of shear zones offers a unique opportunity to study the progressive development of geological structures that occur at all scales, from sub-microscopic shear bands and slips planes in minerals to wide zones of intense deformation, tens of kilometres wide (e.g. Bak et al., 1975; Wakefield, 1977; Davis and Reynolds, 1996; Passchier, 2005). Shear zones are known to play a crucial role in recording deformation processes and rheological behaviours at a variety of pressure and temperature conditions (Carreras, 2001; Means, 1995; Passchier and Trouw, 2005; Ramsay, 1980; Simpson and De Paor, 1993). In many terranes, deformation is not homogeneously distributed and during terrane amalgamation, deformation is often concentrated in shear zones that absorb the strain by accommodating the movement of relatively rigid terrane blocks (Passchier, 2005). Understanding the evolution of shear zones therefore helps us to understand the initiation and growth of orogenic belts as deformation tends to be concentrated on pre-existing structures, which end up with long-lived histories (White et al., 1979; Davis and Reynolds, 1996; Katsuyoshi & David, 2004). In addition, shear zones tend to reactivate repeatedly instead of new ones initiating (Davis and Reynolds, 1996), hence can also be central to unravelling the tectonic histories of orogenic belts.

What the above implies, is that shear zones are often likely to form on the boundary between two tectonic blocks or terranes. However, because of the complex interplay between the location of the terrane boundary and the physical properties of the terranes on either side of the boundary, this is not always the case. Firstly, differences in the rheological properties of the rocks in either side of the terrane boundary often result in strain being preferentially partitioned into one rock type or a series of similar rock types because of differences in the yield strength of different rocks and minerals (e.g. Durham & Goetze, 1977; Bai et al.,1991). Secondly, the orientation of the compressive stress relative to any pre-existing rock fabric strongly influences the rock fabric's strength (Wendt et al., 1998). This suggests that the existence of an earlier rock fabric could influence the development of new rock fabrics (e.g. Katsuyoshi & David, 2004). In both cases, it is the existence of pre-existing anisotropies, either lithological or structural (rock fabrics), which strongly influence where deformation is partitioned.

In southern Namibia, several tectonic terranes or blocks with different geological histories suggest that there is some type of large-scale terrane amalgamation. Whilst the details of this terrane amalgamation are still being debated (Blignault, 1977; Joubert, 1986; Colliston et al., 1991, Colliston

and Schoch, 2000; Macey et al., 2015), it is clear that there are a number of crustal scale shear zones that lie approximately parallel to the boundary between the Richtersveld Magmatic Arc (the old Richtersveld Subprovince) and the Kakamas Domain (the old Gordonia Subprovince). These include the well-known Marshall Rocks Pofadder Shear Zone as well as the Eureka Shear Zone to the north and the Sperlingsputs Shear Zone to the south (Macey et al., 2015). Whilst the position of the Marshall-Rocks Pofadder Shear Zone is not clearly linked to one specific pre-existing structure, Angombe (2016) found that the Eureka Shear Zone exploited a pre-existing tectonic boundary between the Kakamas and Pella domains. The position of the Sperlingsputs Shear Zone also appears to be linked to a pre-existing structure in the form of the Southern Namaqua Front (SNF), a kilometre scale transitional zone between the Pella and Vioolsdrif domains of the Richtersveld Magmatic Arc, first identified by Beukes (1973).

The SNF is defined as the southern boundary of where a homogeneous gneissic foliation has developed as part of the Namaqua Orogeny. However, the position and origin of the SNF is ambiguous and hence it has not been clear how to indicate it on regional maps (Moen and Toogood, 2007; Minnaar et al., 2012; Macey et al.,2015). What is clear, is that parts of the SNF are being reworking by shear zones belonging to the Sperlingsputs Shear Zone system. It could be that, as a zone of intense deformation, the SNF focusses subsequent deformation events, accounting for the presence of the SPSZS. The position of the SPSZS could also be the result of lithological anisotropies (and hence rheological differences) between the gneissic rocks of the Pella Domain, and the volcanics and plutonics that make up the Vioolsdrif Domain. This reason might also explain why deformation is partitioned into the rocks with the lowest competency (volcanic sequences), since plutonic rocks and gneissic rocks can have similar rheological properties.

Recent mapping has identified a more complex series of shear zones within the SPSZS and cast doubt on the extend and size of the Southern Namaqua Front. This study will re-evaluate the geological character and context of the SPSZS and reinterpret the significance of the Southern Namaqua Front. The main focus of this project will be on describing the detailed relationship between the different lithologies and lithological packages that host the SPSZS and the distribution and intensity of shear zones and shear fabrics. This will help us to establish the processes behind the nucleation of the SPSZS and how the evolution of the SPSZS relates to the broader tectonic processes operating during the Namaqua Orogeny.

1.2 PROBLEM STATEMENT

Historically, the SPSZS has been known for some time, but the driving forces behind the nucleation and evolution of the shear zone are not clearly understood. Until we understand the driving forces behind the nucleation and evolution of the SPSZS it is not possible to assess its relationship to larger-scale tectonic processes and hence it is not clear how the SPSZS is related to the Namaqua Orogeny. In addition, the SNF and the SPSZS have not been differentiated in the literature and to do this requires a detailed structural analysis of all the structural elements in both features to determine if there is a causal link between the two. Once this is established, it will be possible to outline the overall internal structural architecture of both the SPSZS and SNF and to link this to the structural architecture of the Namaqua Metamorphic Province generally. This is turn should shed further light on the causal relationship between the SPSZS in particular and other late Namaquan shear zone systems, such as the Marshall Rock-Pofadder Shear Zone and Eureka Shear Zone.

1.3 RESEARCH AIMS AND OBJECTIVES

Objective One: To determine the range of lithologies in the study area and to assess the role of lithology in the development of shear zone networks that form the Sperlingsputs Shear Zone System

- What are the lithologies present within the study area, can their protoliths be identified and how do they relate to the Richtersveld magmatic arc?
- What is the extent, distribution and interconnectivity of shear zones within the study area?
- What is the relationship between lithology and shear zone development and how does this vary spatially within the study area?

Objective Two: To characterise the internal structural architecture of individual shear zones within the broader Sperlingsputs Shear Zone System and their relationship to one another.

- What are the structural elements and types of fault rocks associated with individual shear zones in the broader Sperlingsputs Shear Zone System and do they vary spatially?
- What deformation microtextures are present in the faults rocks and can this tell us about the conditions of shear zone development?
- What are the kinematics of each shear zone individually, how consistent are they across the individual shear zones, and what does this imply about the overall shear sense in the Sperlingsputs Shear Zone System?

- What role does lithology play in determining the type of structural architecture that is developed?

Objective Three: To determine whether there is a link between the Frontal Sperlingsputs Shear Zone and the SNF within the study area

- What are the lithological and structural variations across these frontal zones?
- What differentiates the Frontal Sperlingsputs Shear Zone and the SNF within the study area?
- How does the position of the Frontal Sperlingsputs shear zone and the SNF relate to the boundary between the Pella Domain and the Vioolsdrif Domain and what does this imply about the relative timing of these features?

Objective Four: To determine the tectonic evolution of the broader Sperlingsputs Shear Zone System and its relationship to the Marshall Rocks-Poffader Shear Zone.

1.4 LOCATION OF THE STUDY AREA

The study area is located in the Warmbad District of the Karas Region in southern Namibia immediately north of the Orange River (Fig 1-1). It lies between 18°00' and 18°15'E and between 28°45' and 28°25'45" in the remote, desert and mountains area between Haib and Warmbad district. The north western boundaries are defined by the contact of the Precambrian basement and the overlying cover rocks of the Karoo Supergroup. The study area measures a total area of approximately 1800 km² that includes the 1:50 000 scale map sheet 2818CA and parts of 2817 DA and 2817DB.

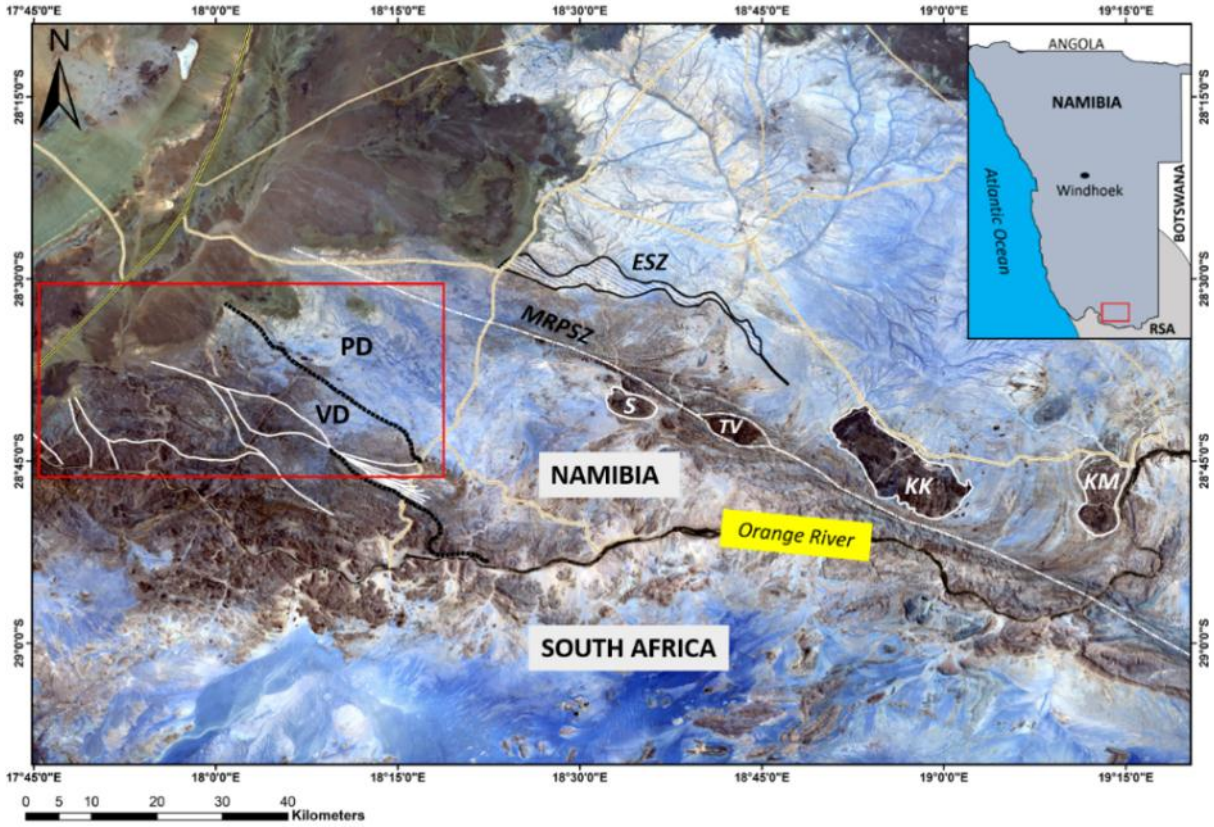

Figure 1-1: Locality map of the study area within the wide dispersed Namaqua Metamorphic Province in the southern Namibia immediately north of the Orange River. The map is indicating the position and extent of the SPSZS (white sold lines) and other major relative shear zones such as Marshall Rocks Pafadder shear zone (MRPZS) and Eureka shear zone (ESZ) delineated from the stacked Landsat Image (RGB 321). The bolded dotted line represented the southernmost edge of the Southern Namaqua Front, that marks the tectonic boundary between the Vioolsdrif domain (VD) and Pella domain (PD) within Richtersveld Magmatic Arc (RMA). In the adjacent area to the study area, are the four Gordonia Klippen namely; Keimasmond (KM), Kum kum (KK), Tantalite Valley (TV) and Sandfontein (S). The red rectangle block represent the study area which approximately 1800 Km^2 whereby the 1: 50 000 geological map was produced as a part of this project.

Geographically; the SPSZS are situated in the Vioolsdrif domain of the NMP and along its tectonic boundary with the Pella domain south west of the MRPSZ and ESZ. The Vioolsdrif and Pella domains consist of Paleoproterozoic rocks that were variably deformed and metamorphosed during the Mesoproterozoic Namaqua Metamorphic Orogeny (see Chapter 2)

1.5 METHODOLOGY

This study initiated from the mapping project Precambrian basement rocks of the Namaqua Metamorphic Province at 1:50 000 scale that the Council for Geoscience (South Africa) conducted under contract, in collaboration with the Geological Survey of Namibia. Under this project, the

author mapped an area of approximately 1800 Km^2 as part of his MSC studies and the resultant geological map is provided in appendix A

1.5.1 Geodatabase and field work

Remote sensing data used in this study were Google Earth Image, magnetic and radiometric images, ASTER and hyperspectral image (Fig 1-2). The Hyperspectral and ASTER images were process using different band combinations and band ratios to enhance different rock types and a range of structures. These images were incorporated in the digital database, newly published and unpublished results from previous CGS/GSN mapping of adjacent areas detailed in Macey et al. (2013). The existing geochemical and geochronological data from the mapping area and adjacent areas were also included in the current database. Fieldwork was carried out over a period of 50 days, spread over two field visits between May 2014 and June 2015. The highly mountainous and difficult to access areas were in part mapped by using high resolution HYMAP and Google Earth imagery.

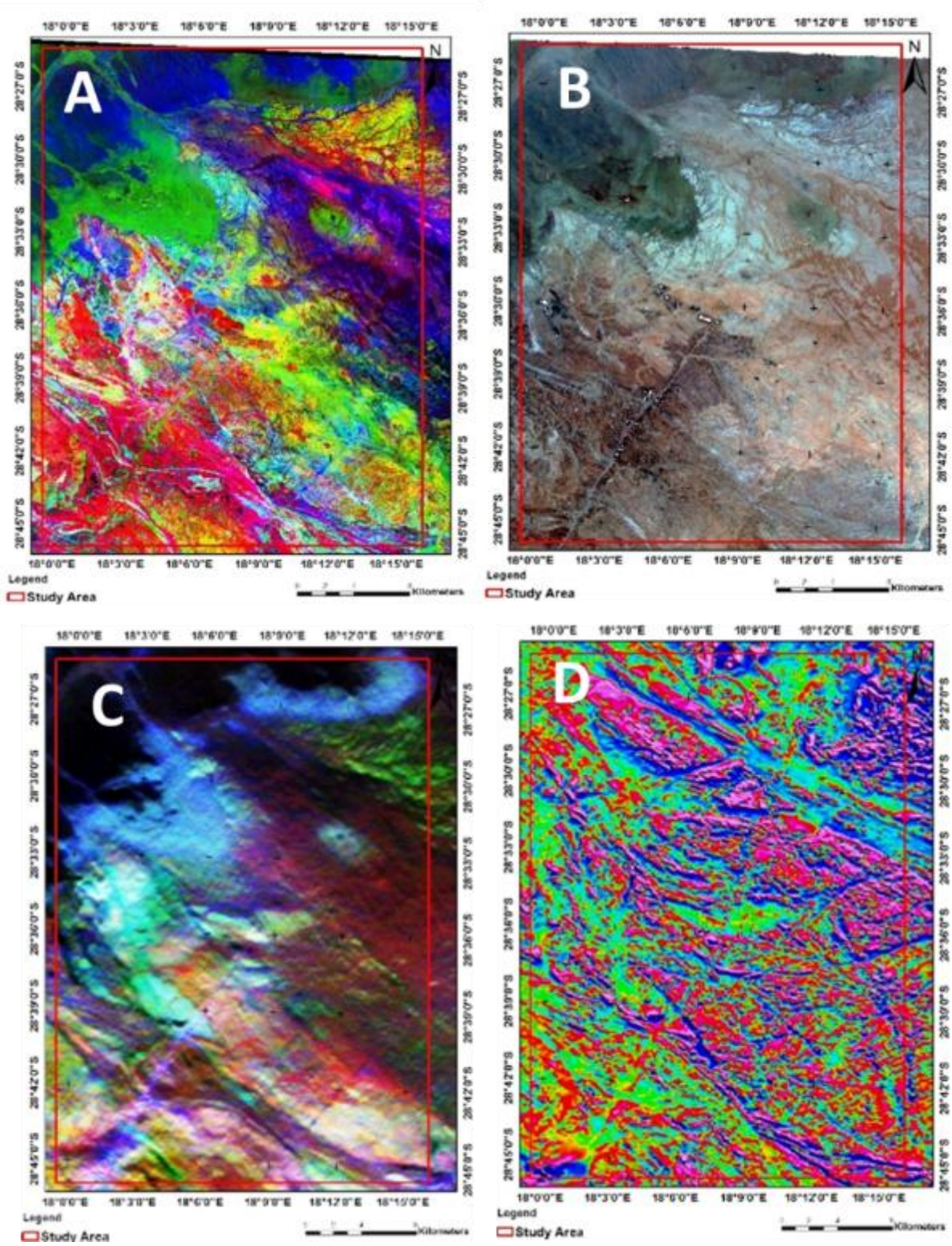

Figure 1-2: Various remote sensing dataset used partly in the study area (2818CA): A. high resolution hyperspectra false color (2_3_4) band combination, B. Hyperspectral Near-true colour (RGB 28_9_3) image. C; Radiometric ternary image and D; Magnetic (First Derivative) image. Sourced from GSN database

1.5.2 Analytical Techniques

Suitable samples were selected for petrographic section preparation and geochemical analysis. Eighty-five samples were submitted for normal and oriented thin section preparation at the Council for Geoscience and Geological Survey of Namibia laboratory. XRF major element analysis of 36 rock samples was carried out at the Council for Geoscience Laboratories in Pretoria. The samples milled (<75 µ fraction) and roasted at 1000 °C for at least 3 hours to oxidise Fe^{2+} and S, and to determine the loss on ignition (L.O.I.). Glass disks were prepared by fusing 1.5 g roasted sample and 9 g flux consisting of 66.67% $Li_2B_4O_7$, 32.83% $LiBO_2$ and 0.50% LiI at 950 °C. All geochemical data have been captured in a database together with data from previous studies (Minnaar, 2007 and Reid, 1977). Most of the existing geochemical data were acquired by Reid (1977), who analysed approximately 160 samples within and adjacent to the current study area.

CHAPTER 2 – REGIONAL GEOLOGY

2.1 THE NAMAQUA-NATAL PROVINCE

Namaqua-Natal Province is approximately 1400 km long and 400 km wide, NW-SE trending Proterozoic metamorphic belt that extends beneath the phanorozoic Karoo Supergroup (Blignault, 1977; Blignault et al., 1983; Cornell et al., 2006; Frimmel, 2000; Hartnady et al., 1985; Joubert, 1986; Miller, 2008; Thomas et al., 1994). The province is deeply eroded and extends from southern Namibia across the Orange River into South Africa through the west up to KwaZulu-Natal in the east (Miller, 2008). The Namaqua-Natal Province comprises of Proterozoic metamorphic rocks that were metamorphosed during the Namaqua Orogeny between circa 1200 and 1000 Ma relative to the formation of the supercontinent Rodinia (Hartnady et al., 1985; Hoffman, 1991; Stockwell *et al*., 1970) and occurred through a polyphase of deformation and metamorphism referred to as D_2, D_3 and D_4 (Joubert, 1986). The formation of the supercontinent Rodinia was associated with a series of crustal blocks that were accreted onto the southern and southwestern margin of the Kaapvaal Craton in southern Namibia and South Africa (Hartnady, 1985; Joubert, 1986; Humphreys & Van Bever Donker, 1987; Eglington & Armstrong, 2003; Colliston & Schoch, 2013). This orogenic domain represents a fold and thrust belt consisting of distinct tectono-stratigraphic terranes that have undergone subhorizontal ductile shear deformation at mid-crustal conditions (Colliston *et al*., 1991; Colliston & Schoch, 2000).

Karoo sediments separate the Namaqua-Natal Province into the Namaqua sector and the Natal sector (Thomas *et al*., 1994; Frimmel, 2000; Eglington & Armstrong, 2003; Cornell *et al*., 2006). The Natal Sector lies adjacent to the southeastern margin of the Archean Kaapvaal craton, and is further divided from north to south into the Tugela, Mzumbe and Margate terranes. The three terranes were differentiated on the base of metamorphic grade and structural domains. The Namaqua sector is adjacent to the southwest of the Natal sector. The study area is located in the Namaqua sector, of the Namaqua-Natal Province, in southern Namibia.

2.2 THE NAMAQUA SECTOR

Namaqua Sector is an approximately 400-km-wide belt of high-grade tectono-metamorphic terranes that stretch from southern Namibia south-eastward into the Northern Cape Province of South Africa. The NMP has traditionally been subdivided into a number of tectonostratigraphic ‘subprovinces’,

'terranes' or 'domains' that are separated by major tectonic boundaries and are distinguished on the basis of different lithostratigraphy, tectonic history and metamorphic grade (Hartnady *et al*., 1985; Colliston & Schoch, 1996; Cornell *et al*., 2006; Miller, 2008). The Richtersveld Subprovince (Richtersveld Magmatic Arc [RMA]) is a tectonically bounded sliver of crust that lies 'sandwiched' between the Bushmanland Province to the south and the Kakamas Domain to the north (Macey *et al*., 2017). The two provinces (Richtersveld and Bushmanland subprovinces) are separated from each other by the Groothoek Thrust (Van Aswegen *et al*., 1987; Colliston & Schoch, 1996). The Bushmanland Subprovince is the southernmost subprovince of the NMP in the Namaqua sector, located in South Africa. The province is dominated by amphibolite to granulite facies gneisses and granites dated at between 1210 and 1020 Ma but with ~1.85 Ga Paleoproterozoic migmatitic gneisses locally present (e.g. Robb *et al*., 1999; Cornell *et al*., 2006; Eglington, 2006). The Kakamas Domain is the northernmost domain in the NMP and consists of granulite-facies gneisses and granitoids, separated from the underlying RMA by a wide, extensive imbricate zone known as the Lower Fish River-Onseepkaans Thrust Zone (LFROTZ) (Macey *et al*., 2015).

In the past, different authors have used different names to refer to the tectonostratigraphic classification within the NMP. McDaid (1978), Hartnady *et al*. (1985), Joubert (1986), Thomas *et al*. (1994) and Cornell *et al.* (2006) all used the term 'Richtersveld Subprovince'; however, Blignault *et al*. (1983) and Moen and Toogood (2008) used 'Orange River Sequence' and 'Bushmanland Subprovince' respectively to represent the same subprovince. 'Gordonia Thrust Stack' replaces terms such as 'Gordonia Subprovince' (e.g. Hartnady *et al*., 1985; Moen, 2007; Miller, 2008), 'Kakamas Terrane' (e.g. Thomas *et al*., 1994; Cornell *et al*., 2006) and 'Grunau Terrane' (e.g. Colliston & Schoch, 2000) that cover similar areas. Table 2-1 represents a summary of the tectonostratigraphic nomenclature used by various researchers over the past years. The rise of different names for the tectonostratigraphy in the NMP has led to considerable confusion and controversy amongst researchers in this region; therefore, for this study the names highlighted in blue are used.

Table 2- 1: Tectonostratigraphic nomenclature used by researchers

Nomenclature used in this study	Richtersveld Magmatic Arc	Vioolsdrif Domain	Pella Domain	Gordonia Thrust Stack	Gordonia Klippe	Kakamas Domain	Sperrlingsputs Shear Zones	Onseepkans Thrust	Marshall Rocks Pofadder Shear Zone
Beukes (1973)							Namaqua Front		Pofadder Shear Zone
Jackson (1976)									Kuckaus mylonite belt
Blignaut (1977)					Central zone	Central zone	Front zone		
McDaid (1978)									Haalenberg SZ
Hartnady et al. (1985)	Richtersveld Subprovince			Gordonia Subprovince					
Joubert (1986)	Richtersveld Subprovince	Vioolsdrif Terrane	Pella Terrane	Gordonia Subprovince	Aus Terrane	Aus Terrane		Tantalite Valley line	Pofadder Lineament
Thomas et al. (1994)	Richtersveld Subprovince				Kakamas Terrane	Kakamas Terrane			
Colliston & Schoch (1996, 1998)		Pofadder Terrane: Richtersveld Domain	Pofadder Terrane		Grünau Terrane	Grünau Terrane		Klein Fish-Hartbeesriver Thrust	Tantalite Valley Shear Zone
Cornell et al (2006)	Richtersveld Subprovince				Kakamas Terrane	Kakamas Terrane		Hartbeesriver Thrust	Pofadder Shear Zone
Miller (2008)	Richtersveld Subprovince	Vioolsdrif Terrane	Pella Terrane		Aus Terrane	Aus Terrane	Southern Front		
Moen and Toogood (2008)	Bushmanland Subprovince				Grunau Terrane	Grunau Terrane		Onseepkans Thrust	Pofadder Shear zone
Corner (2008)				Gordonia Subprovince					Pofadder-Marshall rocks SZ
Macey et al. (2015)	Richtersveld Magmatic Arc	Vioolsdrif Domain	Pella domain	Kakamas Domain	Gordonia Klippe	Kakamas Domain	Southern Namaqua Front	Onseepkans Thrust	Marshall Rocks pofadder shear zone

2.2.1 Richtersveld Magmatic Arc

The RMA (Joubert, 1986; Macey et al., 2015) is defined as an isolated remnant sandwiched between the highly deformed and metamorphosed rocks of the Bushmanland and Kakamas Domains to the southwest and northeast, respectively (Fig 2-1). In Namibia, the arc forms a tectonic boundary with the Kakamas Domain along the LFROTZ to the northeast within the Tantalite Valley area and extends farther southwest across the Orange River into South Africa. The RMA is further subdivided into the low-grade greenschist facies Vioolsdrif Domain to the southwest and the medium-grade amphibolite

facies Pella Domain to the northeast (Thomas *et al*., 1994; Reid, 1997; Minnaar, 2011; Macey *et al*., 2015). These domains are both made up of Paleoproterozoic (~1880 Ma) near-juvenile calc-alkaline volcanic (Orange River Group) and intrusive (Vioolsdrif Intrusive Suite) rocks.

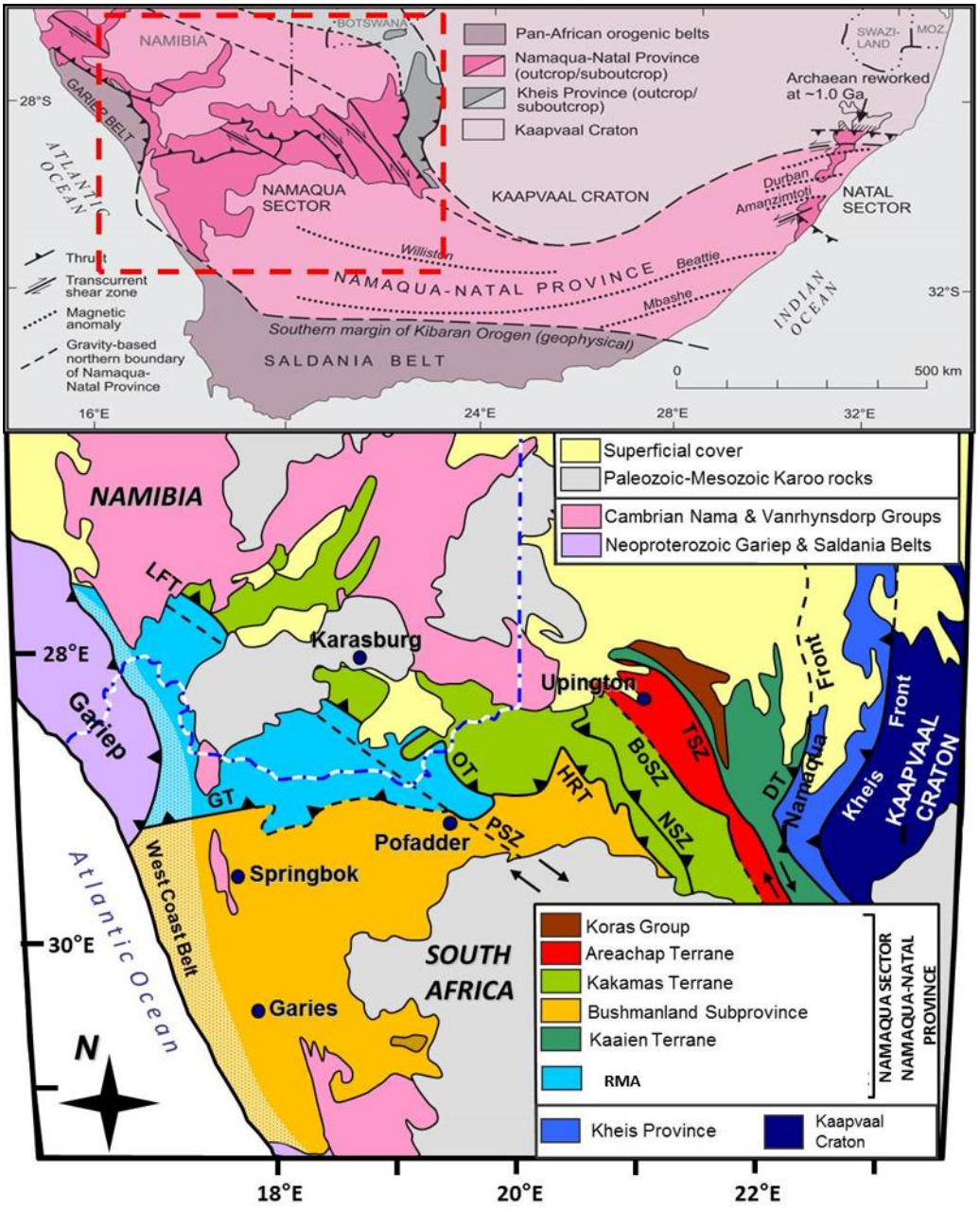

Figure 2-1: Tectonostratigraphic position of the RMA of the Namaqua sector of the NMP, modified from Macey et al. (2015) after Hartnady et al. (1985), Thomas et al. (1994), Cornell et al. (2006) and Moen and Toogood (2007)

2.2.1.1 Orange River Group

The Orange River Group represents a spectrum of calc-alkaline volcanic rocks types, ranging in composition from basalt to rhyolite (e.g. Reid, 1977; Reid et al., 1987, 1997). The ORG within the low-grade Vioolsdrif Domain has a simple stratigraphy, subdivided into four main units: (1) the De Hoop Subgroup; (2) the Haib Subgroup; (3) the Hom Subgroup; and (4) the Rosyntjieberg Formation (Beukes, 1973; Blignault, 1974, 1977; Reid, 1977; Ritter, 1977 1980; SACS, 1980). Of these, only the Haib Subgroup is present in the study area. The Haib Subgroup was divided into the Nous and Tsams formations by Blignault (1977), with the Nous Formation being made up of predominantly basaltic-andesite and andesite lavas, minor leucocratic intercalations and minor volcanic breccia and tuffs, whilst the Tsams Formation is made up of a mixed volcanic package of dacite and rhyolite with minor andesite. The Nous Formation is well exposed and forms individual mappable units. These units also define a kilometre-scale fold structure extending from the Nababeep Plateau in the west to the eastern side of Goodhouse farm, with the units becoming more deformed farther to the east. Where they are deformed, most of the primary volcanic features are completely lost through the development of a strong penetrative regional foliation (Blignault, 1977). The Tsams Formation is farther north than the Nous Formation and crops out in the Haib area and to the east thereof (Miller 2008). The Tsams Formation was further classified into three units: (1) a lower feldspar porphyry; (2) a middle volcaniclastics member; and (3) an upper feldspar porphyry that grades into quartz-feldspar porphyry (Blignault, 1977). However, this volcanic stratigraphy is very difficult to identify in areas where the rocks have been moderately to strongly deformed as in the current study area.

2.2.1.2 Vioolsdrif Intrusive Suite

The Vioolsdrif Intrusive Suite intrudes the Orange River Group rocks. The suite is believed to have formed in a juvenile calc-alkaline volcanic arc terrane together with the Orange River Group volcanic rocks (Reid, 1977, 1997; Cornell *et al*., 2006; Minnaar, 2012). The suite consists of subvolcanic rocks ranging from ultrabasic to highly acidic in composition. In the low grade greenschist facies Vioolsdrif Domain, these intrusive rocks preserved their intrusive contacts well, allowing the reconstruction of the relative timing of the different phases. The leuco-granite and quartz porphyry are the youngest, and the more mafic phases are older (Miller, 2008). Based on that, Strydom *et al*. (1987) were able to subdivide the intrusive suite into the Vuurdood, Goodhouse and Ramansdrif subsuites.

The Vuurdood Subsuite is largely represented by basic members, forming the earliest members of the Vioolsdrif Intrusive Suite (Blignault, 1977). Several authors such as Gevers *et al*. (1937), De Villiers and Söhge (1959) and Beukes (1973) mentioned that the subsuite contained serpentinites,

hornblendites and gabbroic rocks. In most places, especially in the Lower Fish River and Haib areas, the gabbroids are absent and the hornblendites and diorites are sparsely dispersed as small bodies within the Vioolsdrif Domain (Blignault, 1977). The dioritic member was further detached from the basic member by Cilliers (1989), naming it the Goabis Subsuite. The Goabis Subsuite consists of two varieties of dioritic rocks: (1) a coarse mela-diorite that is quartz free, mainly associated with hornblendite, and (2) a fine to medium, even-grained quartz diorite. The Vuurdood Subsuite in the study area forms numerous isolated bodies of limited extent hosted within the dominant Goodhouse Subsuite.

Goodhouse Subsuite (Strydom *et al*., 1987) consists of granodiorites and adamellite phases of the Vioolsdrif Intrusive Suite. The phases signify the biotite and hornblende granite of Gevers *et al*. (1937), the basement granodiorites of Coetzee (1942), the grey gneissic granite of De Villiers and Söhge (1959) and Von Backstrom and Villiers (1972), the Gn2 of Middlemost (1963), the Vioolsdrif granite of De Villiers and Burger (1967) and Mcmillan (1963) and the older mesocratic Vioolsdrif granite of Beukes (1973).

Recent work (Minnaar, 2012; Macey *et al*., 2015) subdivided the Goodhouse Subsuite into subtypes that are mainly noticeable within the Vioolsdrif Domain. The two subtype are (1) the Gaarseep Granodiorite and (2) the Khoromus Tonalite/Porphyry. Both subtypes were first documented by Marais *et al*. (2001) who named them Khoromus and Gaarseep ‘gneiss’. Then, in the less deformed Vioolsdrif Domain, Minnaar *et al*. (2012) modified the names to ‘Khoromus Tonalite’ and ‘Gaarseep Granodiorite’, based on the average composition and deformation intensity respectively. The Khoromus Tonalite is defined by a homogeneous grey weathered surface, medium-coarse-grained porphyritic tonalitic-granodiorite, associated with dark mineral cumulates, and tabular white feldspar phenocrysts, while the Gaarseep Granodiorite is characterised as a coarse-grained equigranular and porphyritic granodiorite coupled with mafic enclaves (Macey *et al.*, 2015). Both the Vuurdood and Goodhouse intrusive bodies are intruded by the younger member alkaline granites of the Ramansdrif Subsuite. The Ramansdrif Subsuite, in general is dominated by medium-coarse-grained equigranular or porphyritic alkaline granites. According to Blignault (1977), the porphyritic alkaline granite variety has a limited distribution and in places is associated with copper mineralisation.

2.2.1.3 Vioolsdrif Domain versus Pella Domain

The Vioolsdrif Domain within the RMA is characterised by low-grade, greenschist-facies rocks of the Orange River Group and the Vioolsdrif Intrusive Suite. The domain is bounded by the Southern

Namaqua Front Zone to the north and by thrusts or subvertical shear zones, which juxtapose it with the higher grade Bushmanland Subprovince, to the south (Beukes, 1973). The domain was mostly unaffected by the main penetrative deformation of the Namaqua Orogeny (~1200 Ma) and preserves the older low-grade greenschist facies Paleoproterozoic (~1880 Ma) Orange River orogeny (Macey *et al*., 2013). Many of the original volcanic textures are preserved within this domain.

The Pella Domain within the RMA is represented by pretectonic rocks of both the Orange River Group and the Vioolsdrif Intrusive Suite and syntectonic Namaqua granitoids (Macey, 2014). These rocks were metamorphosed at amphibolite-facies to granulite-facies conditions. In comparison with the low-grade Vioolsdrif Domain, the lithostratigraphy of the Pella Domain becomes more complex and controversial. Various researchers, including Beukes (1973), Blignault (1974; 1977), Blignault *et al*. (1974; 1983), Strydom *et al*. (1987), Reid (1977; 1979), Cilliers (1989) and Moen and Toogood (2007), who worked in this domain proposed different stratigraphies. These authors identified the supercrustal rocks of the Orange River Group and the intrusive rocks of the Vioolsdrif Intrusive Suite in the Pella Domain. Beukes (1973), Blignault *et al*. (1974; 1983) and Blignault (1977) recognised the Orange River supercrustal rocks in the Pella Domain; however, Beukes grouped the gneisses and schists into the Umeis Formation while Blignault classified them as the gneisses of the Pella Domain. The Vioolsdrif Intrusive rocks also extend into the high-grade domain; Strydom *et al*. (1987) and Colliston (1989) recognised them as 'undifferentiated Vioolsdrif' orthogneisses, while Moen and Toogood (2007) categorised these different orthogneisses into the Hoogoor Suite and Coboop, Noudap and Pipeline gneisses. Macey *et al*. (2014) further divided the subsuite of the Vioolsdrif Intrusive Suite in the Pella Domain into subunits based on the composition, the macroscopic gneissic textures and the proportion of, and variety of, mafic minerals present. For instance, the Goodhouse Subsuite was divided into 10 subunits that represent compositional end-member orthogneisses, whereby four of the ten subunits, represent compositional end-member orthogneissess that recognised on the basis of, composition (tonalite, granodiorite, granite and leucogranite), macroscopic textures, such as augen, streaky and coarse graine equigranuklar orthogneisses and proportion of, and variety of, mafic minerals present (hornblende/ biotite orthogneiss).

2.2.2 Gordonia Thrust Stack

The Gordonia Thrust Stack (Macey *et al*., 2015) consists of rocks of the Kakamas Domain preserved as southwest-verging thrust sheets and nappes of high-grade supracrustal gneisses and intrusive rocks (Joubert, 1986; Macey *et al*., 2015). During D_2 Namaqua orogeny, the Kakamas Domain was thrust over the Paleoproterozoic RMA along the LFROTZ. The rocks within the Kakamas Domain

(Macey *et al*., 2015) are believed to have been derived from the pre-existing older crust of the Paleoproterozoic Richtersveld and early Mesoproterozoic Areachab Arcs that were completely reworked through high grade metamorphism and intense plutonism during the mid-Mesoproterozoic and then imbricated during the mid- to late-Mesoproterozoic D_2 Namaqua Orogeny. The Kakamas Domain is mainly characterised by pelitic and psammitic gneisses that were deformed at granulite facies. The Domain (thrust stack) is very complex and has been intruded by Mesoproterozoic intrusive igneous suites (e.g. Kum Kum, Endoorn, Beenbreek, Tantalite Valley, etc.).

2.2.3 The regional structural division of the Namaqua Sector

The regional structural subdivision of the Namaqua Sector of the NMP was established by Joubert (1971; 1986) who subdivided the sector into four major tectonic events, D_1 to D_4, associated with lineations (L), foliations (S) and folds (Table 2-2). Macey *et al*. (2015) placed emphasis on the regional tectonostratigraphy of the NMP in southern Namibia and identified another late deformation episode of Neoproterozoic brittle structures, D_5. The current study focused on the boundary between the Vioolsdrif and Pella domains (Fig 2-2). The Vioolsdrif Domain is a low-grade greenschist facies domain and preserves volcanic and sedimentary bedding structures and the early fabrics of the D_1 deformation episode. In the amphibolite-facies Pella Domain, the D_2 and D_4 phases of the Namaqua Orogeny strongly overprint the early fabrics. The D_1 fabrics are thought to have developed in the Paleoproterozoic coeval with the development of the RMA and have been named the Orange River Orogeny (Blignault, 1977; Blignault *et al*., 1983). The D_2 and D_4 deformations are considered phases of the Mesoproterozoic Namaqua Orogeny, with the D_2 deformation forming a penetrative gneissic fabric (Joubert, 1986); D_3 is a kilometre-scale F_3 fold structure with a localised foliation and lineation. The D_4 deformations are large-scale Late-Namaqua dextral transcurrent shear zones of which the Marshall Rocks-Pofadder Shear Zone (MRPSZ) is the largest (Macey *et al*., 2014); the Sperlingsputs Shear Zone System (SPSZS) is also one of the major shear zones and formed the focus of this study.

Table 2- 2 Summary of the tectonic events within the Namaqua Sector of the NMP (Joubert, 1971; Blignault, 1977 and Macey et al., 2015)

	Deformation Episodes	Pella domain	Vioolsdrif domain
NAMAQUA OROGENY	D_5	Brittle Deformation represented by Fault and Joints	Brittle Deformation represented by Fault and Joints
	D_4	Dextral km-scale shear zones	Dextral km-scale shear zones
	D_3	Localised Km-scale anticline & Syncline dome and basin structures (F_3)	Not developed
	D_2	Penetrative S_2 gneissic fabric associated with moderately to sub-horizontal plunging L_1	Not developed
ORANGE RIVER OROGENY	D_1	Transposed by D_2 and D_4	Axial plane cleavage (S_1) in accompany with open to close folds (F_1 & L_1)
	Bedding	Transposed by D_2 and D_4	Millimetre to metres scale composition and colour variation bedding (S_0)

2.2.4 Lower Fish River-Onseepkaans Thrust Zone in the Onseepkaans area

The LFROTZ (Macey *et al*., 2015) is a 1–10 km wide structurally and lithologically complex zone of roughly southwest-verging, imbricate thrust sheets. The megastructure can be traced from the Ai-Ais area (Blignault, 1977; Blignault *et al*., 1983) to southeast of Onseepkans (Slabbert *et al*., 1989; Moen & Toogood, 2007), separating the Kakamas Domain (hanging wall) from the RMA and the Bushmanland Block (footwall). Recent work by Macey *et al*. (2015) in the Onseepkaans area defined the LFROTZ as significantly separating the older rocks of the Kakamas Domain on top from the underlying Pella Domain rocks. The LFROTZ consists of variably sheared rocks from both granulite- and amphibolite-facies domains and is further divided into the upper thrust and the basal thrust. The upper thrust is termed the Kerelbed-Tafelkop Thrust that separates the LFROTZ from the overlying Kakamas Domain rocks while the basal thrust is referred to as the Lower Fish River Onseepkaans Thrust (Macey *et al*., 2015).

The geometry and structure of the fabric of the LFROTZ are also variably and often strongly reoriented and distorted by the megascale F_3 folding and D_4 shearing. The subhorizontal thrust zones at places are deformed by the F_3 folding event into kilometre-scale dome and basin structures that are eroded and form structure-like ‘ear’ and ‘eye’ klippe (Macy *et al*., 2015). The basal thrust

(LFROTZ) in the Onseepkaans area is totally reworked by the nearby D_4 MRPSZ, transposed dextrally along a vertical shear plane.

2.2.5 The Southern Namaqua Front

The Southern Namaqua Front was first recognised by Beukes (1973) who named it the 'Front Zone'. It separates the low-grade Richtersveld (now referred to as the Vioolsdrif Domain) rocks from the intensely deformed medium- to high-grade Namaqualand Province (now referred to as the Pella Domain). Beukes (1973) defined the boundary in the Lower Fish River-Ai-Ais area as a 1.5–5-km-wide zone of variably sheared rocks and described its southern boundary as located exactly where the homogeneous gneissic foliation began developing. However, the exact position of the Front Zone in this area is, in places, ambiguous, and this seems to be related to reworking of the zone by the D_4 shearing events. Beukes (1973) indicated that the SNF is well preserved north and west of Haakiesdoorn and becomes thinner and less well developed towards the southeast. However, Joubert (1986) extended the Southern Namaqua Front farther southeast across the Namibian border into South Africa and joined it up with the well-known Groothoek Thrust of Van der Merwe (1986), thereby enclosing the Vioolsdrif Domain.

Conversely, Moen and Toogood (2007) did not show the boundary on the Onseepkans geological (2818 map sheet), South Africa. They thought that such a structure could not be identified on the basis of field relationships to represent the boundary between the two domains. However, Minnaar *et al*. (2012) recognised the boundary in South Africa but again as a vague and poorly defined zone between the two domains. The authors traced this boundary north of, and not joining with, the Groothoek Thrust. To avoid confusion with the 'Namaqua Front', which is the boundary between the Kaapvaal Craton and the Namaqua Metamorphic Province, Macey *et al*. (2014) recommended using the term 'Southern Namaqua Front' to represent the boundary between the two domains (Vioolsdrif and Pella) and this terminology is adopted in this study.

2.2.6 Late-stage Namaqua shearing

During the later stage of the Namaqua Orogeny, when the rocks had already been intensely deformed and a regional penetrative gneissic fabric and kilometre-scale folds had already formed, numerous ductile, dextral NW-SE-trending shear zones formed (Joubert, 1986; Macey *et al*., 2014). These shear zones are believed to have formed as a result of unroofing of the Namaqua Orogeny that led to the cooling of the NMP rocks to temperatures below approximately 350 °C by 950–980 Ma (Barton & Burger, 1983; Cornell *et al*., 1990, 1992; Grantham *et al*., 1993; Eglington, 2006).

Lateral escape tectonics were proposed as the mechanism whereby this occurred as a result of the nonstop southward depression of the rigid Kaapvaal Craton into the newly accreted NMP (De Beer & Meyer, 1984; Humphreys & Van Bever Donker, 1987; Jacobs *et al*., 1993; Jacobs & Thomas, 1994). The MRPSZ is the most widespread and best exposed example of these late-tectonic D_4 shear zones. Macey *et al*. (2014) used the structural architecture of the MRPSZ as an analogue for other late-stage Namaqua shear zones within the Namaqua Sector, principally the ESZ (Angombe, 2016) and shear zones spatially associated with the Southern Namaqua Front, here termed the SPSZS, which is the subject of this study.

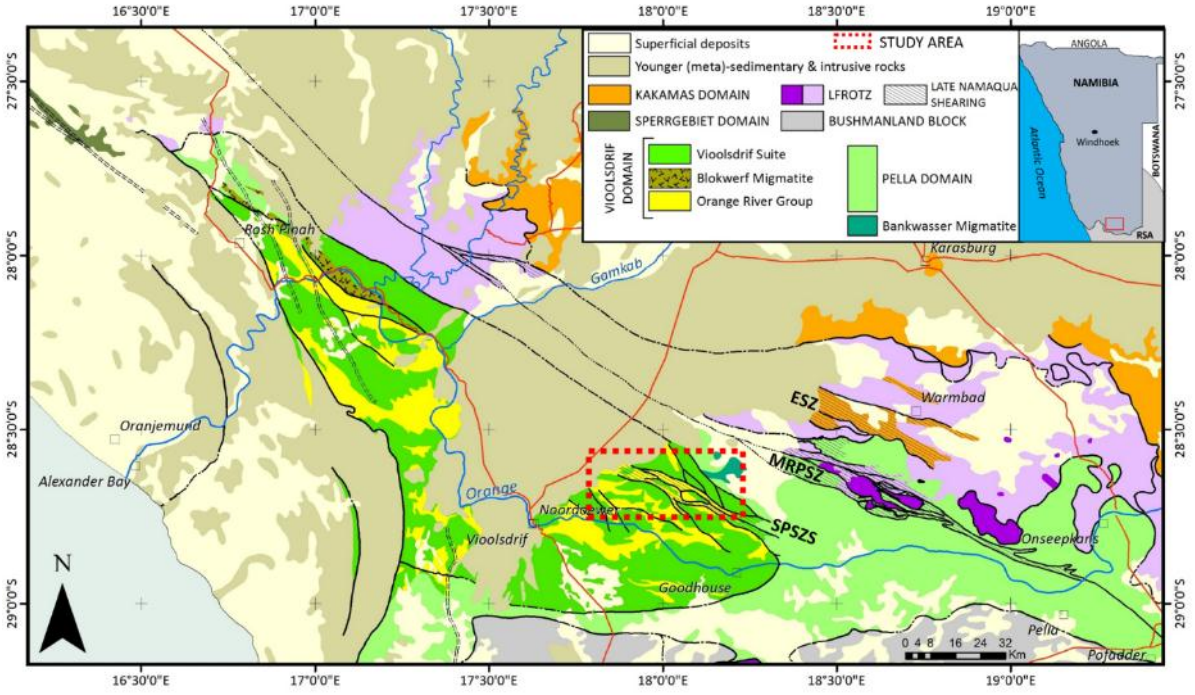

Figure 2-2: The tectonostratigraphic map showing the extent of the SPSZS (red dotted rectangle) in relationship with two other Namaqua sector shear zones, namely the ESZ and the MRPSZ, compiled from the recent 1:50 000 scale of Macey et al. (2015) and Thomas et al. (2016).

2.2.6.1 Marshall Rocks-Pofadder Shear Zone

The MRPSZ has previously been referred to as the Pofadder Shear Zone (Lambert, 2013), the Pofadder-Marshal Rocks Lineament (Miller, 2008) and the Tantalite Valley Mylonite Belt (Joubert, 1975). The MRPSZ extends for over 500 km, from the Atlantic seaboard in southern Namibia to the Northern Cape of South Africa (Moen & Toogood, 2007; Miller, 2008). The shear zone trends in an NW-SE direction and is characterised by a 2–7-km-wide core of amphibolite- and greenschist-facies mylonite (Lambert, 2013). This wide NE-dipping mylonitic core is dominated by a subhorizontal SEE and NWW shallowly plunging lineation (Lambert, 2013). The polyphase deformed (D_2–D_3)

orthogneisses and supracrustals adjacent to the mylonitic core are transposed into parallelism with the high-strain mylonite core (Toogood, 1976; Moen & Toogood, 2006; Miller, 2008; Lambert, 2013). Both the large-scale drag features as well as small-scale microstructures indicate dextral movement sense dominated by wrench faulting and localised dip-slip faulting (Colliston & Schoch, 2013; Lambert, 2013; Macey *et al*., 2015). The MRPSZ together with the other late-stage Namaqua shear zones (ESZ and SPSZ) displays retrograde deformation fabrics with a mineral assemblage of broadly greenschist-facies conditions (Toogood, 1976; Van Bever Donker, 1980; Stowe, 1983; Humphreys & Van Bever Donker, 1990; Geringer *et al*., 1994; Lambert, 2013). Previous work on the MRPSZ (e.g. Beukes, 1973, Joubert, 1974, 1975; Jackson, 1976; Mclaren, 1988) was largely done at a regional scale, and most of the work was centred on the copper-nickel deposits of the Tantalite Valley Complex. However, Toogood (1976) did detailed work on the structural and metamorphic evolution of the gneissic terrain around this shear zone. This study highlighted the strain partitioning within the MRPSZ and discriminated noncoaxial from coaxial strain domains.

Recent work by Colliston and Schoch (2013), Lambert (2013) and Macey *et al*. (2015) documented four principal deformation episodes, namely D_{4a}, D_{4b}, D_{4c} and D_{4d}. The D_{4a} deformation episode is dominated by ductile deformation and is responsible for the dragging, folding and rotation of the pre-existing penetrative D_2 gneissic fabric of the wall rocks to the shear zone (Lambert, 2013). The D_{4b} deformation mainly takes place within the core shear zone, dominated by a ductile-brittle deformation manner overprinting D_{4a}, and is therefore accountable for the development of mylonite and cataclasite rocks. It retrogrades from amphibolite facies to greenschist facies (Lambert, 2013). D_{4c} deformation is mainly restricted to the Pella Domain and forms 1–30 m wide distinct shear zones of mylonite-ultramylonite and cross-cuts and overprints the previous late D_4 fabrics at an angle (Macey *et al*., 2015). D_{4d} is a brittle deformation episode overprinting the D_{4c} episode, resulting in brecciation of the D_{4c} mylonite-ultramylonite (Lambert, 2013; Melosh *et al*., 2014; Macey *et al*., 2015).

2.2.6.2 The Eureka Shear Zone

The ESZ (Macey *et al*., 2014; Angombe, 2016) is located north of the MRPSZ and is about 5 km wide and at least 50 km long. The shear zone is NW-SE trending and is mainly associated with a dextral, brittle-ductile, tectonic melange of early Neoproterozoic Age (Angombe, 2016). The ESZ reworked the LFROTZ, which represents the tectonic boundary between the Pella Domain and Kakamas Domain (Angombe *et al*., 2016). It differs from the MRPSZ by its associated sigmoidal-shaped lithotectonic slices of the interlayered mafic and quartz feldspathic gneiss and Eureka complex, and

its dominant cataclasite-brittle shear fabric subjected to greenschist facies. Previous researchers recognised the high-strain zone (Blignault *et al*., 1983; Colliston & Schoch, 2000) but did not recognise its significance in reworking the boundary between the Kakamas Domain and the RMA.

2.2.6.3 The Sperlingsputs Shear Zone System

The SPSZS documented by Blignault (1977) termed 'Tsams Thrust' is poorly understood, with no kinematic interpretations in the existing literature. This study recognised the same shear zone system but named it the SPSZS, after Sperlingsputs farm. The Tsams Thrust name is not used in this study since it is already used for a formation (Tsams Formation) in the Orange River Group. In addition to this, the SPSZS forms relatively subvertical district shear planes, not thrusts.

Blignault et al. (1983) defined the shear zone system as a major zone of movement within the Haib area, rotating and steepening eastwards the pre-existing D_1 Orange River Orogeny structures. The authors further described the shearing intensity of the shear zone in intrusive and extrusive rocks. The shearing was developed more in the volcanic rocks of the Orange River Group with narrow anastomosing mylonite zones within the competent granitoids of the Vioolsdrif Suite. The study also found the SPSZS to be a south-dipping (45˚) shear plane with a near down-dip line of movement. The study by Blignault et al., 1983, applied Ramsay and Graham's (1970) technique to determine the displacement associated with the SPSZS, which was interpreted to be 11 km displacement.

2.2.7 Pegmatite

Pegmatites within the Namaqua sector of the NMP are been economically important, and their exploitation dates back to 1925 when mining activities commenced in the area south of Vioolsdrif in South Africa and the Karas Region in southern Namibia. Along the Orange River, pegmatites form a roughly east-west-trending domain that extends from Vioolsdrif on the western side of South Africa through the Karas Region in Namibia to Kenhardt in South Africa at its eastern extremity (Macey, 2014).

Pegmatites in southern Namibia form part of an extensive territory of pegmatite intrusion known as the Orange River Pegmatite in the Northern Cape Province of South Africa and southern Namibia (Gevers, 1936; Gevers *et al*., 1937; Hugo, 1970; Schutte, 1972; Blignault, 1977; Minnaar, 2005; Cornell *et al*., 2006; Cornell & Pettersson, 2007). Pegmatites were formed together with late-stage granite (Warmbad granite) during the late shearing and unroofing of the NMP (Macey, 2015). They are products of primary melts generated during partial melting of granitic plutons during the late

stages of the Namaqua orogeny rather than products of late fluids generated during crystallisation (Macey *et al*., 2015). Generally, they occur as elongated/irregular bodies that can be in the form of either a vein or a dyke (Macey, 2015). However, in places (Warmbad area) they occasionally occur as bulbous-shaped and rootless patch leucosome bodies within the earlier rocks (Lambert, 2013).

CHAPTER 3: LITHOSTRATIGRAPHY

3.1 INTRODUCTION

In this chapter, the detailed lithostratigraphy as mapped as part of this study is presented and each rock unit as identified in the study area is described. The lithostratigraphy of the study area is very complex, consisting of Orange River Group volcanic rocks and the Vioolsdrif Intrusive rocks, that are of diverse- ages and metamorphic grade. The less deformed greenschist-facies rock units are restricted on the southern part of the study area whilst the equivalent stratigraphic high-grade amphibolite-facies rock units are limited on the northern part of the study area (Fig 3-1). In this section, the major rock units in the field area are described in terms of their lithological characteristics and structural features and the spatial relationship between them is explained with reference to the Pella and Vioolsdrif domains, the position of the Southern Namaqua Front and the location of the Sperlingsputs Shear Zone System.

3.2 MAJOR ROCK UNITS WITHIN LOWER GRADE REGION (VIOOLSDRIF DOMAIN)

The Vioolsdrif Domain is made up of weakly deformed basement volcanic rocks of the Orange River Group (ORG) that are intruded by rocks of the Vioolsdrif Intrusive Suite (VIS). Both the ORG and the VIS are cross cut by numerous NNE trending discontinuous Neoproterozoic doleritic and gabbroic Gannakouriep dykes.

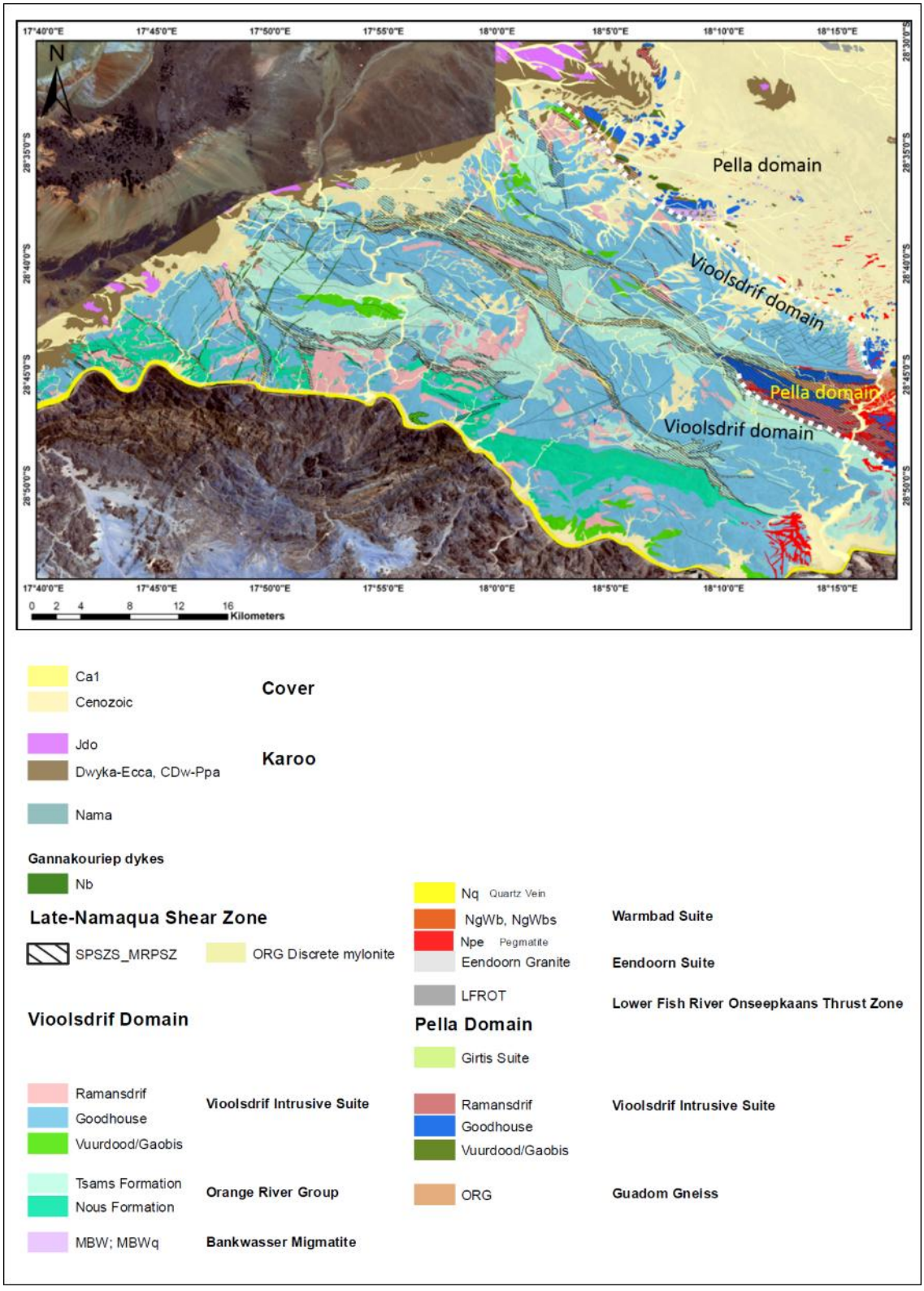

*Figure 3-1: The simplified lithological map for the entire study area compiled from the 1: 50 000 scale geological of 2818CA, (Indongo et al., 2014) 2817DA and 2817DB (Indongo & shifotoka et al., 2015). The map is showing the position of all the major rocks of the Orange River Group and the Vioolsdrif Intrusive Suite. In addition, the map also shows the position of the Southern Namaqua Front (**white dotted line**) that mark the boundary between Pella and Vioolsdrif Domain.*

3.2.1 Orange River Group (ORG)

Volcanic rocks of the ORG within the study area are compositionally represented by mafic, intermediate and felsic units, although intermediate and felsic compositions dominate. The volcanic rocks are locally sheared in deformation zones that are associated with the Sperlingsputs Shear Zone System (*SPSZS*), and mainly occur as west to northwest-trending supracrustal belts extending for more than 10km, intruded by the VIS granitoids. They also occur as mega-xenoliths and mega-autoliths of different sizes within the VIS granitoids. In places, the volcanic rocks are subjected to an extensive weathering, alteration and are coated in desert vanish. For this reason, some of the volcanic rocks are not easy to distinguish in the field. In the southernmost part of the study area, the volcanic rocks tend to preserve their primary structures in comparison to the central part of the study area along the Kromrivier and in the northernmost part of the study area, where the primary structures have been destroyed by D4 and D2 respectively (Fig 3-1). In addition, to the volcanic lavas, felsic and intermediate pyroclastic rock have also identified within the study area.

The ORG volcanic rock units identified in the study area, belong to the Haib Subgroup, which is further divided into the Tsams and Nous Formation on the basis of the geographical location and proportion of the felsic to intermediate and mafic volcanic rock units. The Nous Formation dominated by basalt, basaltic andesite and andesite and is located on the southern part of the study area (Fig 3-2), whilst the Tsams Formation extends from Haib area (Map sheet 2818 DB) across the Witsputs farm into the Sperlingsputs farm (Map sheet 2818 CA & 2818 CC) and is mainly dominated by dacite and rhyolite.

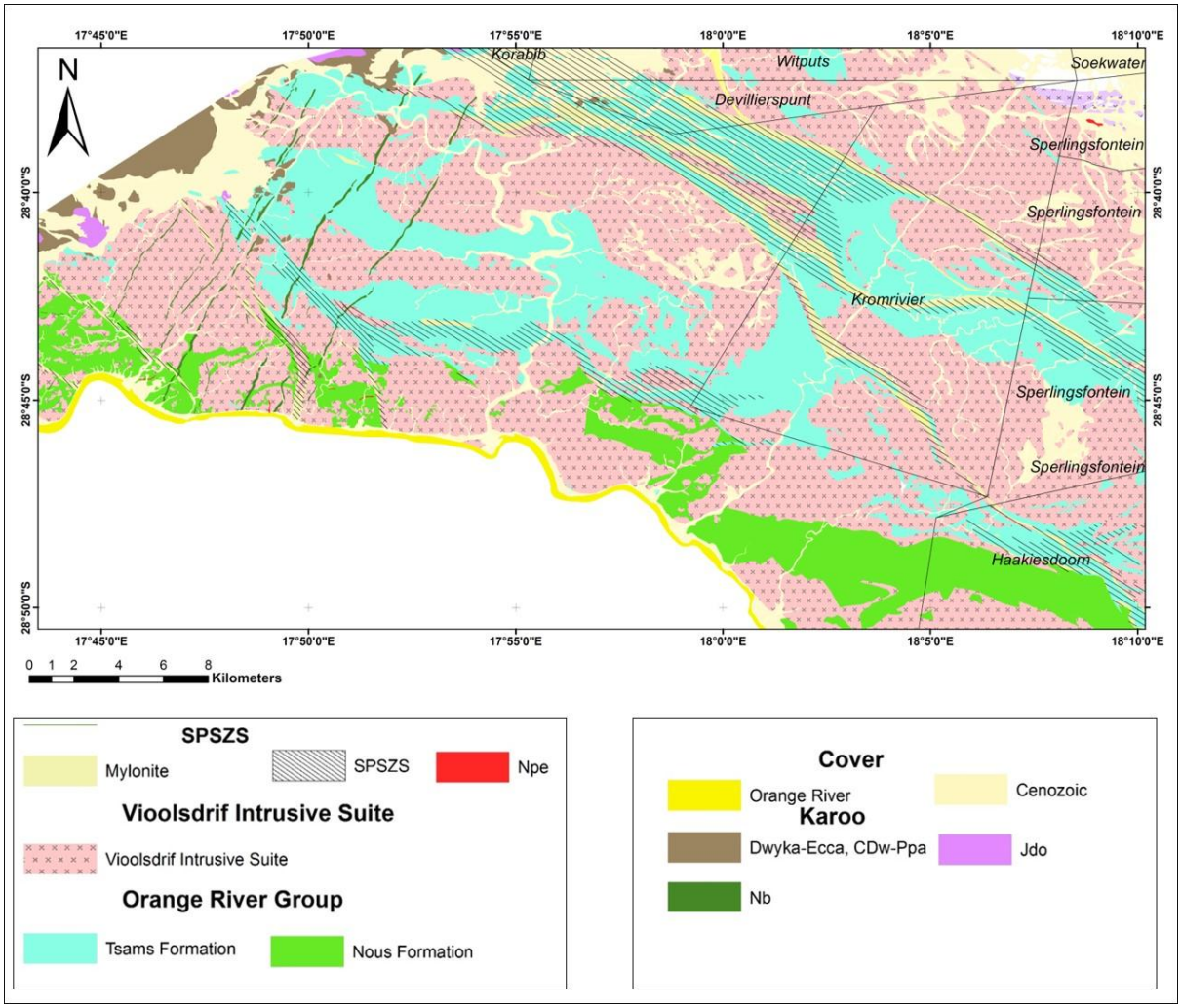

Figure 3-2: The simplified geological map of the southern part of the study area, showing the position of Nous and Tsams formation.

3.2.1.1 Basalt – Basaltic-Andesite & Andesite

Basalt and basaltic –andesite represent the mafic phase of the ORG and are the smallest component within the study area. The basalt dominantly occurs as 1 to 5 m un-mappable lenses at 1: 50 000 scale, even though, along the Orange River at the northwest edge of the 28 17 DD map sheet (Fig 3-2), the basalt was observed forming 10 - 15 m thick beds together with andesite and basaltic andesite, and together represent the Nous formation. Overall, mafic phase of the ORG is dominant in the southern part of the study area. In places, especially around the farm Kromrivier, the basaltic andesite forms 1 to 10 m thick beds interlayered with andesite, rhyolite and dacite, with the felsic units dominant. However, in the Haib area toward the Orange River, the basaltic andesite forms 3 to 50 m thick beds, again interlayered with andesitic, rhyolitic and dacitic lavas, but now form the dominant component. Both basalt and basaltic-andesite primarily consist of fine grained (aphanitic)

and medium grained rocks with locally porphyritic textures (Fig 3-3 a, b, c & e). The rocks are typically characterised by dark-grey to black fresh surfaces and dark-grey dull to shiny weathered surfaces. Where the rocks are weakly to moderately deformed, they preserved their amygdale and primary layering structures (Fig 3-3 d & e). The amygdales range from 3mm to 25 mm in diameter and filled by quartz, epidote and chlorite. The plate minerals (mica) are weakly oriented and anastomosing along the margin of amygdales features (Fig 3-3 e). The primary layering observed at both macro- and microscopic scale, defined by centimetre to millimetre scale arranged biotite rich layers, that alternating with quartz and feldspar rich layers.

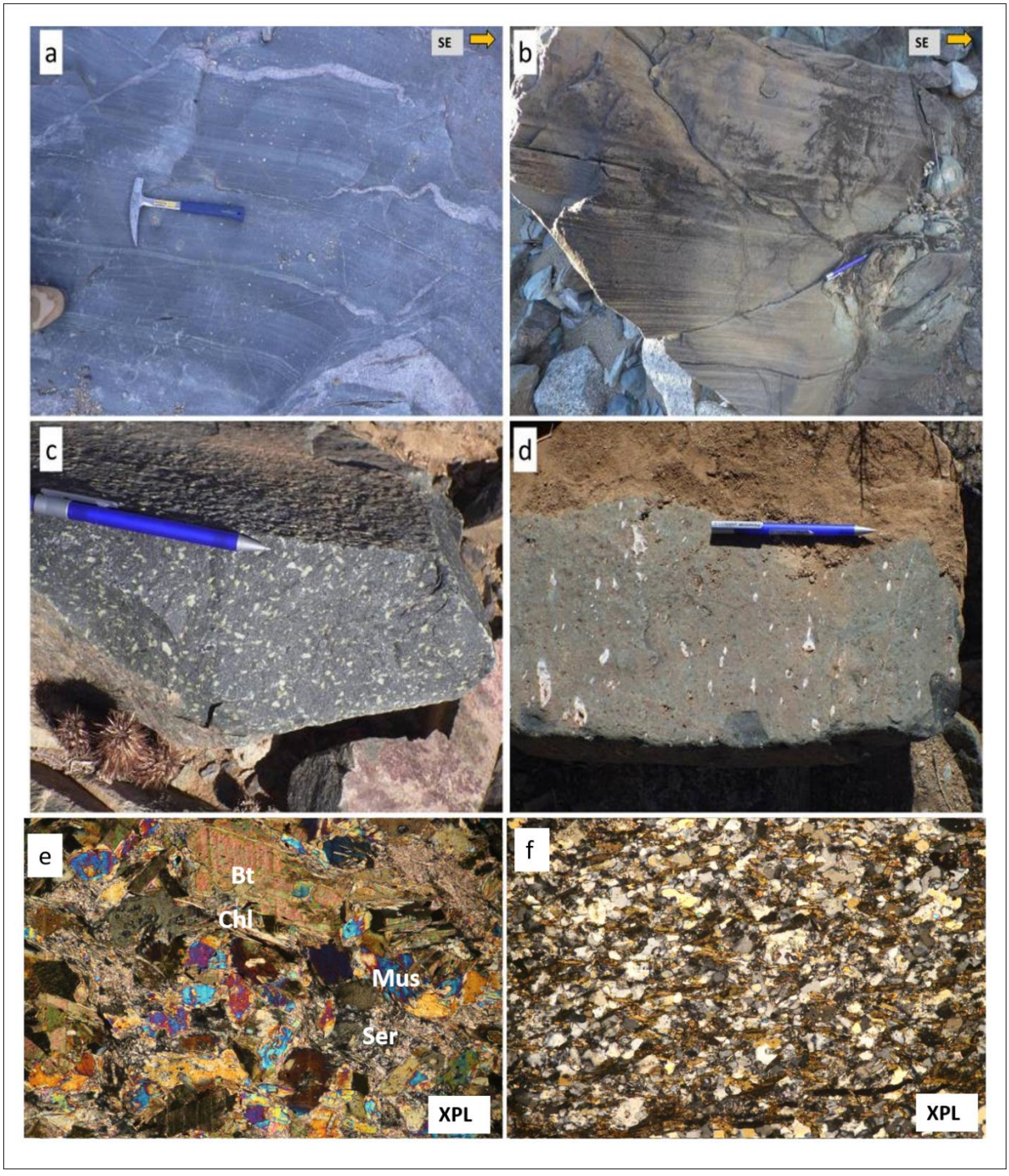

Figure 3-3: Weakly to un-deformed basalt & basaltic-andesite of the ORG within the lower grade greenschist Vioolsdrif domain of the RMA. (a) & (b); un-disrupted millimetre to centimetre scale volcanic primary structures (flow bands) within the basalt. (c); un-deformed 2 mm to 1 cm plagioclase porphyroclasts within the basaltic andesite. (d); the mm to 2 cm elongated quartz filled amygdales. (e); photomicrograph (FOV=4.5 mm) of the porphyritic basaltic andesite consists hornblende and sausseritized plagioclase porphyroclasts sit within the fine grained intermediate-mafic groundmass. (f) Photomicrograph (FOV=4.5 mm) of the medium-fine grained basaltic andesite, consists of mm scale laminar of hornblende and biotite band verses feldspar dominant band.

Andesitic lava dominates the ORG volcanic section and largely occurs as sheared units. They are well exposed within the Krom River with the largest outcrops in the southernmost part the study area. The unsheared andesites are mainly preserved as 20 to 200m wide rigid bodies within the network of Sperlingsputs shear zone stystem, and as mega-zenoliths within the Vioolsdrif intrusive rocks. More often, the andesitic volcanic rocks are interlayered with rhyolite at about 5 to 100 m thick layers and are characterised by a weathered light-grey to greyish surface, with a dull dark grey fresh surface. Texturally; they are fine-medium grained, and composed of hornblende, biotite, quartz, plagioclase and epidote. The porphyritic varieties contain igneous hornblende and feldspar phenocrysts and sit within a fine-grained matrix of plagioclase (30%), biotite (35%) and quartz (15%), whilst chlorite and sericite occur as secondary minerals. The plagioclase phenocryts are usually sausseritized. Some outcrops contain pyroclastic material with irregular-shaped volcanic clasts ranging from 2 to 15 cm in size (see also section 3.2.1.3)

3.2.1.2 Rhyolite-Dacite

Rhyolite and dacite represent the felsic phase of the ORG. Within the study area, the felsic volcanic rocks occur throughout the study area, but are mostly distributed in the central and northern part of the study area, where they chiefly occur as sheared bodies within the Sperlingsputs Shear Zone System. They also occur as minor NWW-SEE trending elongated rigid bodies, together with the andesitic volcanic rocks. In general, unsheared rhyolite and dacite are less commonly found within the study area. In the central-most part of the study area, about 500 m west of the Krom Rivier, the rhyolitic-dacite rocks are represented by a 300 m wide unit that is in contact with the andesite. The rhyolite-dacite rocks show variable colours and are commonly dark-grey to brownish on fresh surfaces and brownish to pinkish weathered tints. Outside the SPSZS, they occur in 1 - 200 m thick units again interlayered with intermediate and mafic lavas. The rhyolite and dacite are characterised by a fine- to medium-grained texture, and consist of quartz (~55%), K-feldspar (30%) and plagioclase (5%), with biotite, sericite, epidote and oxides mostly occurring as minor or accessory components. In places, the subhedral to euhedral feldspars are randomly oriented, but are oriented toward and along the shear zones. The felsic volcanic member is represented by two textural types: (1) aphanitic and (2) porphyritic. The porphyritic variety is represented by 2 to 5 mm angular to rounded fragments of quartz and plagioclase grains within a very fine-grained felsic groundmass. Overall, these fragments are weakly internally deformed and they are randomly oriented with their net orientation parallel to the flow magmatic foliation. The aphanitic variety is associated with fine to medium flow banding on a millimetre- to centimetre-scale (Fig 3-4). The aphanitic variety appear to resemble a mylonitic foliation, but the quartz grains retain their angular shape differentiating them

from the porphyroblasts in mylonite that are always elongated and ribbon-shaped. The magmatic flow foliation is shown by a well pronounced crystallographic preferred orientation of biotite and feldspar grains (Fig 3-4 f).

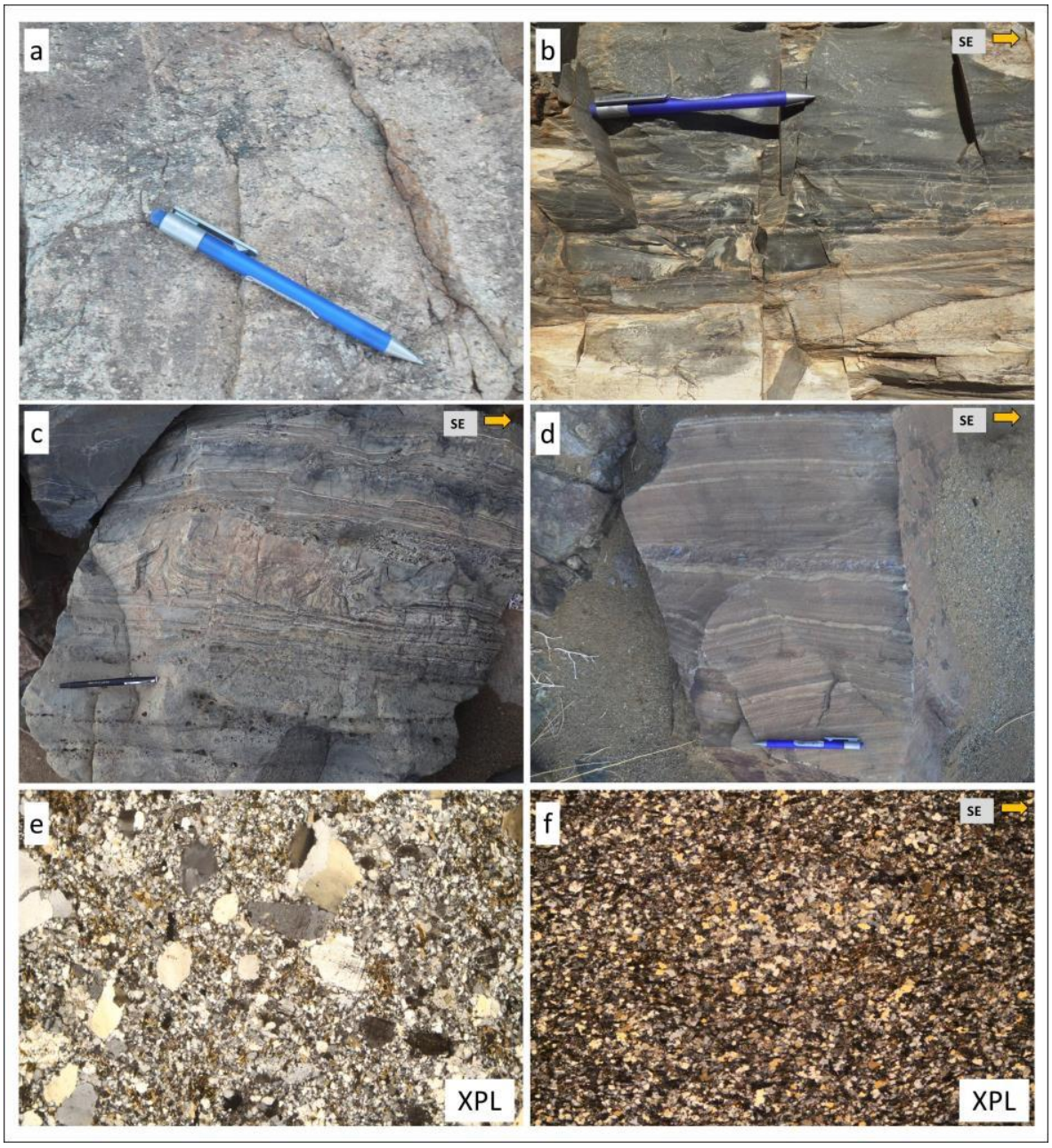

Figure 3-4: The rhyolite variant across the study area, (a) fine to medium grained weakly sheared quartz-feldspar porphyry, (b) a millimetre scale flow bands of the aphanitic rhyolite with conchoidal fractures, (c) & (d) weakly deformed millimetre to centimetre scale flow bands within the rhyolite, (e) photomicrograph (FOV=4.5 mm) shows a porphyritic texture, revealed by sub-angular to rounded quartz phenocrysts within the fine grained groundmass of feldspar, biotite and quartz. The quartz phenocrysts have weak endulose extinction and the feldspar also displayed a poorly developed twinning. (f) Photomicrograph (FOV=4.5 mm) of the very fine-medium grained (aphanitic-dacite), showing aligned small sub-vertical elongated aggregates of biotite verses feldspar and quartz, resembling a millimetre scale lamination.

3.2.1.3 Pyroclastic volcanic rocks

Pyroclastic rocks are scarce within the study area. They are mainly found in the southernmost part of the study area, occurring as 1 m to 10 m wide "strain free" layered units together with both felsic and intermediate clast-free volcanic rocks. In general, they have a very fine-grained groundmass composed of slightly elongated, generally 1 cm to 15 cm (rarely up to 30 cm) long glass shards (Fig 3-5). The glass shards are commonly angular and irregular in shape and are flattened and elongated parallel to layering (Fig 3-5 c & d). The pyroclastic volcanic rocks have both felsic and intermediate units. They do not show any systematic variation in size, shape and abundance across the units. In summary the pyroclastic rocks along the study area, range from the largest agglomerates, to very fine ashes and tuffs.

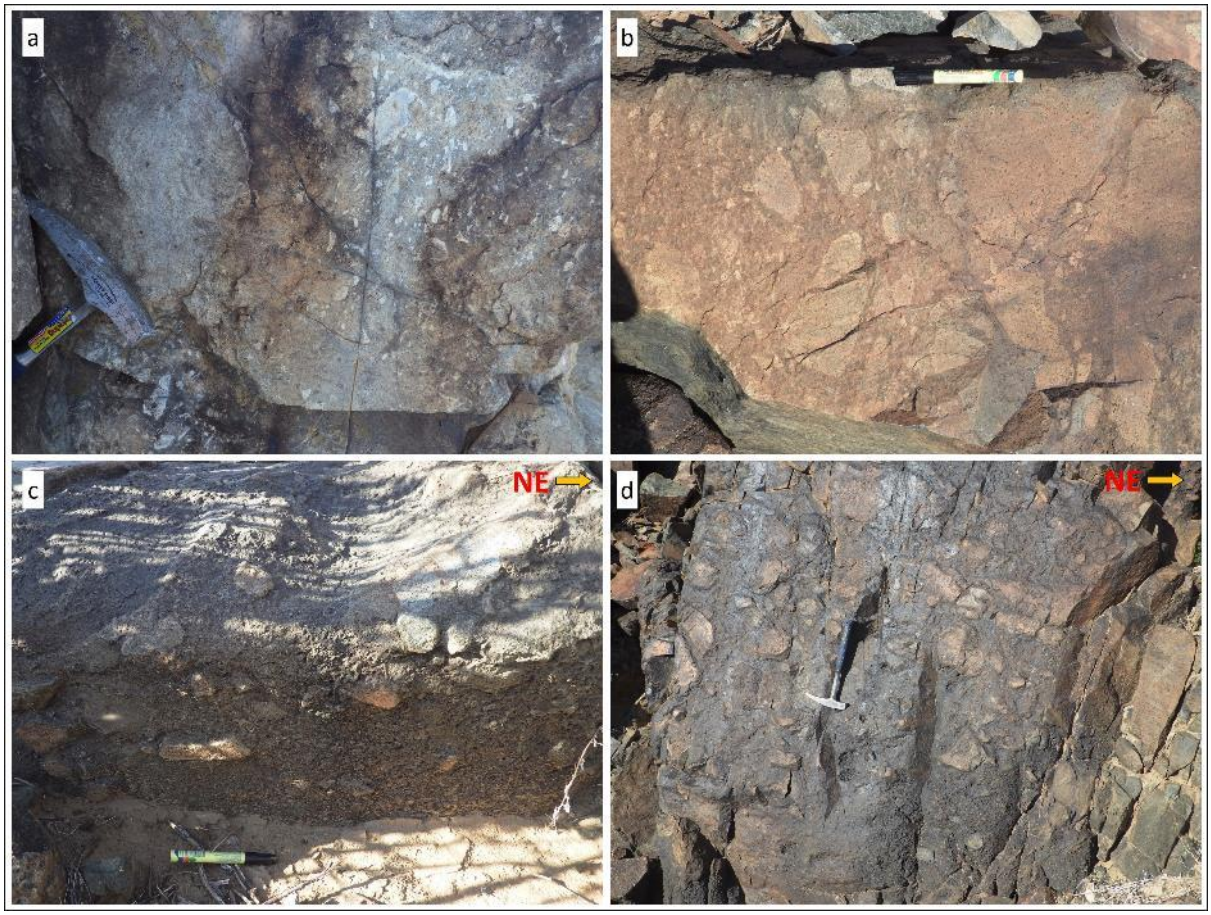

Figure 3-5: (a) & (b); the felsic and intermediate pyroclastic volcanic rocks with 0.5 cm to 6 cm irregular to sub-angular randomly oriented rhyolitic to andesitic fragments. (c) & (d); the layered elongated 2cm to 30 cm long, basaltic and andesitic fragments within the very fine to glass mafic matrix (agglomerate).

In summary the ORG rocks within the Vioolsdrif Domain preserved their primary composition, however in place where these rocks are metamorphosed, the igneous minerals are dominantly transformed into chlorite, muscovite, sericite, epidotes and biotite.

3.2.2 Vioolsdrif Intrusive Suite

Vioolsdrif Intrusive Suite (VIS) rocks are dominated by granitic and granodioritic compositions with minor gabbroic and tonalitic rocks. The VIS intruded the ORG, forming batholiths, dykes and sheets. Outcrops are generally NWW-SEE trending ellipsoid rigid bodies within the Sperlingsputs Shear Zone System and range in width from 5 m to 2 km.

3.2.2.1 Mafic Intrusive Subsuite (Vuurdood and Gaobis)

The Vuurdood and Gaobis subsuites are interpreted to be the early phase of the Vioolsdrif Intrusive Suite. The mafic intrusive units are limited within the study area, consisting of intrusive bodies that intrude the volcanic units and range from 10 to 200 m width on outcrop (Fig 3-6 a). Compositionally, they have a wide range from mafic-ultramafic, but mainly range from diorite to gabbro, occurring as numerous of isolated bodies of limited extend. They also occur as autoliths/xenoliths within the granodioritic and granitic intrusive rocks. At 1:50 000 scale most of the gabbroic rocks are un-mappable and therefore, only the larger intrusive bodies of this subsuite are represented on the geological map of the study area.

In most instances, they occur as un-sheared bodies, often intruded or enclosed by intermediate and felsic intrusive rocks. Coarse- to very coarse-grained gabbro is the most common variety, while diorites occur as dykes cross-cutting the volcanic rock unit. Compositionally, plagioclase (45%) and igneous hornblende (35%) dominate and are partly altered into epidote and chlorite and texturally, they range from medium grained equigranular- to very coarse grained porphyritic- texture (Fig 3-6 c & d) The mafic rock units are commonly closely associated with the intermediate intrusive rock units (granodiorites). Where they are found together, they intermingle and form randomly distributed mafic blocks of variable size (2 to 15 cm) and shape within the equigranular granodiorites.

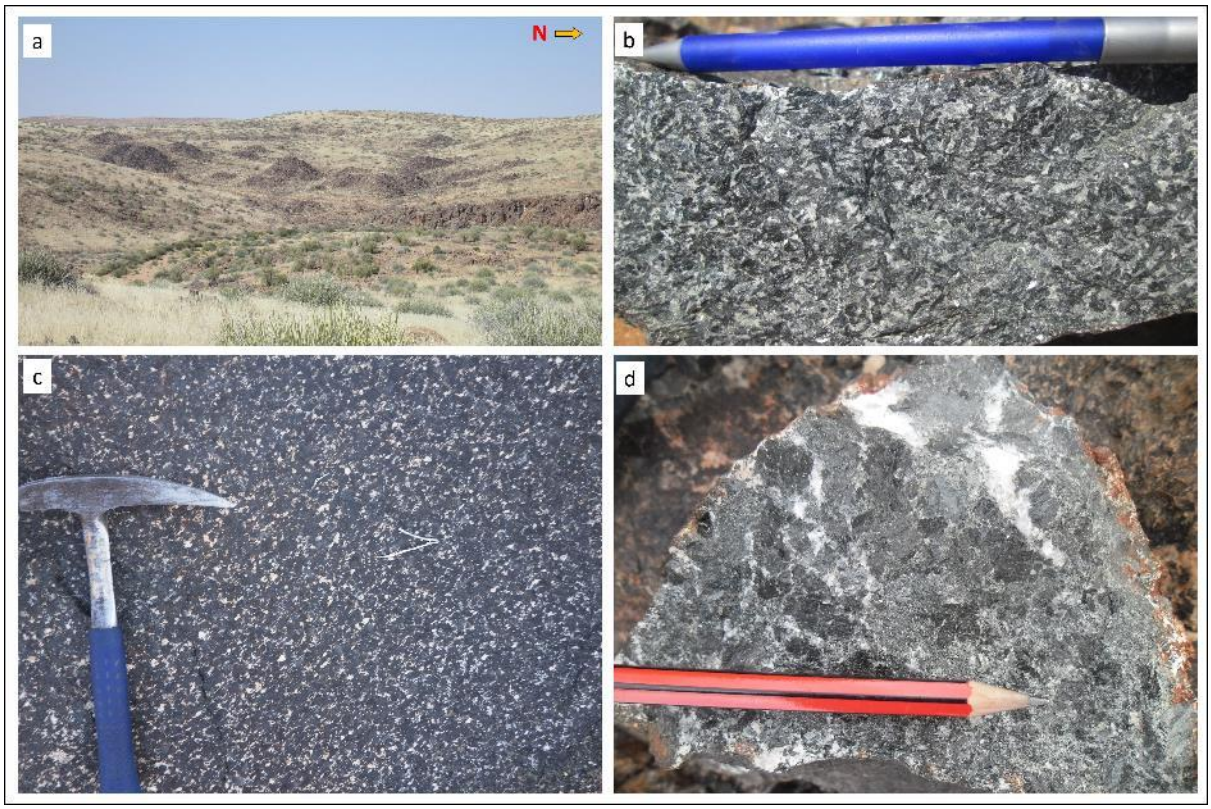

Figure 3-6: (a) plane view picture of the Vuursdood gabbros forming 20 m to 100 m wide intrusive bodies within the Orange river Group volcanic rocks. (b) & (c); close look pictures of the weakly deformed medium grained micro gabbro, (d) very coarse grained gabbro.

3.2.2.2 Intermediate Granitoids Intrusive Subsuite (Goodhouse)

Intermediate intrusive rocks volumetrically dominate the VIS. Based on field observations the intermediate intrusions were further classified into two different granodioritic units; (1) medium to coarse grained equigranular granodiorite and (2) coarse-grained porphyritic- granodiorites and tonalitic-granodiorites. The tonalitic-granodiorite only occur in the southeast of the study area within the Kromrivier farm. In the field, intrusive contacts between the two are not clear but distinctions on the map are made where possible.

3.2.2.2.1. Porphyritic Granodiorite

The porphyritic variety is widely distributed across the study area and appears to dominate the Goodhouse Subsuite. It is medium-grey to grey when fresh but brownish–grey on weathered surfaces. On mountain sides it gives rise to rounded, bouldery blocks that appear quite homogeneous. The porphyritic texture is defined by 2mm to 4cm K-feldspar (35%) phenocrysts within a finer-grained groundmass of biotite (30%), quartz (20%), plagioclase (15%) and k-feldspar. The porphyritic granodiorite is massive, unfoliated and locally contains sparse rounded enclaves of Orange River Group lavas, ranging from 2 cm to 1m in diameter. The porphyritic Granodiorite is composed of glassy quartz, greenish saussuritized plagioclase, sub-rounded K-feldspar, biotite and hornblende, with a colour index of about 30%. Titanite occurs as an accessory mineral, while chlorite, epidote and muscovite are the most common secondary minerals.

The granodiorite on average is made of feldspar (~40%), quartz (~ 25%), biotite (~20%) and hornblende (~ 10%) ± oxides (Fig 3-7). The microscopic observations show plagioclase and k-feldspar mainly altered into sericite and chlorite aggregates. Quartz crystals occur as recrystallized aggregates of sub-grains surrounding most of the primary minerals (Fig 3-7 e & f). Again at microscope scale, the granodiorite dominated by a coarse grained porphyritic texture defined by 0.2 to 0.8 mm anhedral k-feldspar phenocrysts sitting in a medium grained matrix of mostly quartz and biotite crystals.

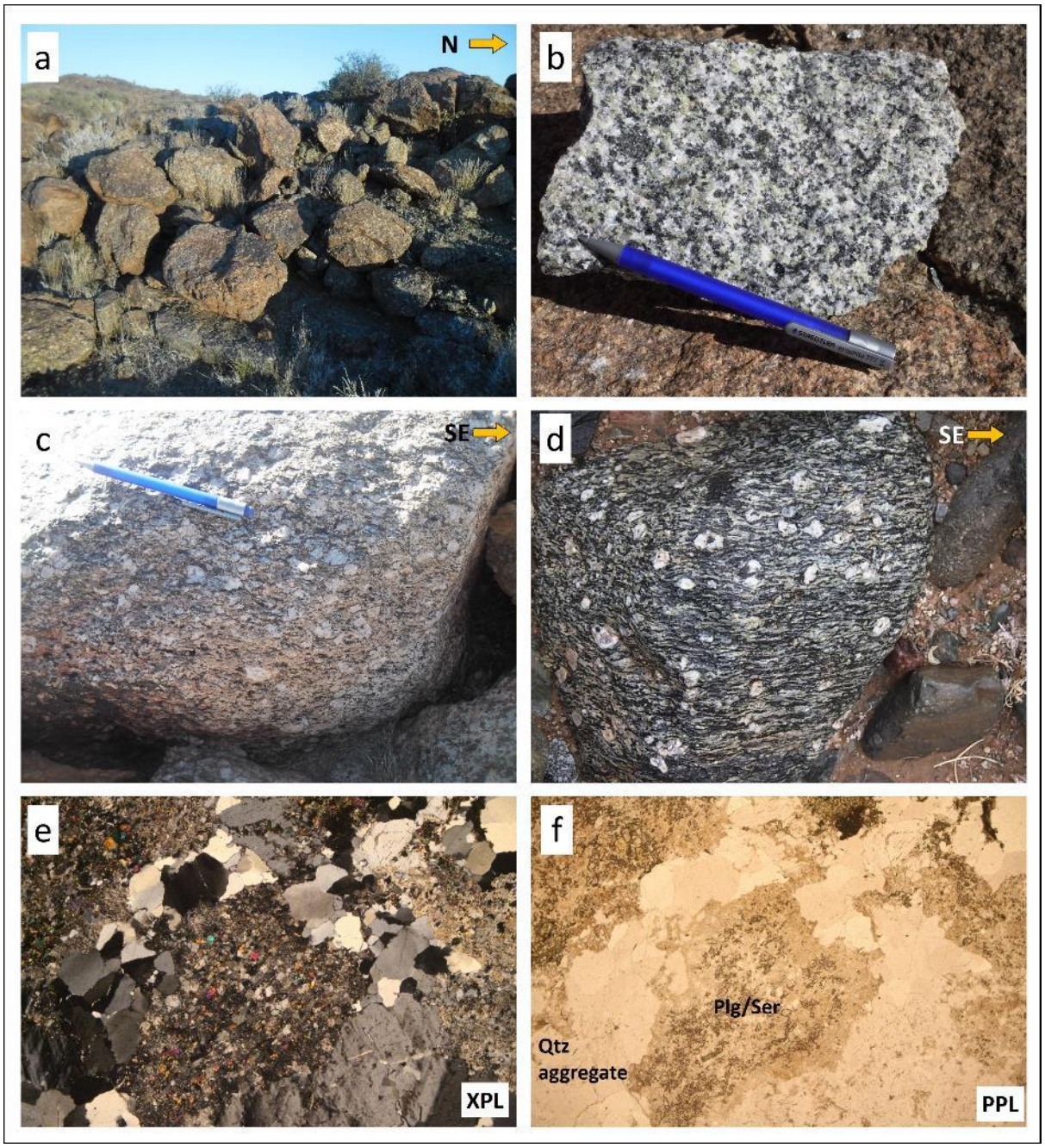

Figure 3-7: field photographs of the Porphyritic Granodiorite of the Goodhouse Subsuite within the Vioolsdrif domain. (a) plane view image of the rigid granodiorite bobs within the SPSZS. (b, c & d); close look photographs showing the porphyritic texture, biotite variety and the unstable plagioclase that mainly altered into epidote at field observation scale. (e) & (f) Photomicrographs (FOV=4.5 mm) of the very Coarse grained porphyritic granodiorite, whereby the porphyritic texture defined by 2mm wide altered plagioclase phenocrysts set within the medium grained groundmass of the recrystallized aggregates of sub+grains quartz.

3.2.2.2.2 Equigranular Granodiorite

The equigranular texture variety of the granodiorite also occurs as rigid bodies within the Sperlingsputs network of shear zones or as large intrusive bodies. They form NW-SE trending

outcrops, that range from 10 m to 500 m in width (Fig 3-1). Across the study area considerable compositional and textural variation was observed, which is reflected in variable proportions of the major mineral phases, quartz, plagioclase, K-feldspar, hornblende, and biotite, with accessory opaque minerals. Epidote, chlorite and muscovite are secondary minerals replacing hornblende, plagioclase and biotite. Generally, the equigranular Granodiorite has a felsic to intermediate composition, but where the silicification process take place, the composition becomes dominantly felsic, making the distinction between these Granodiorites and the Granite difficult. The equigranular granodiorite is coarse- to very coarse-grained (3mm – 2cm) texture, however in places they are medium grained (Fig 3-7 c). Locally they also contain mega-zenoliths of volcanic rocks and mafic intrusive rocks and weakly deformed on overall, with a vague fabric, except in shear zones, where they are heavily strained into cataclasites and mylonites.

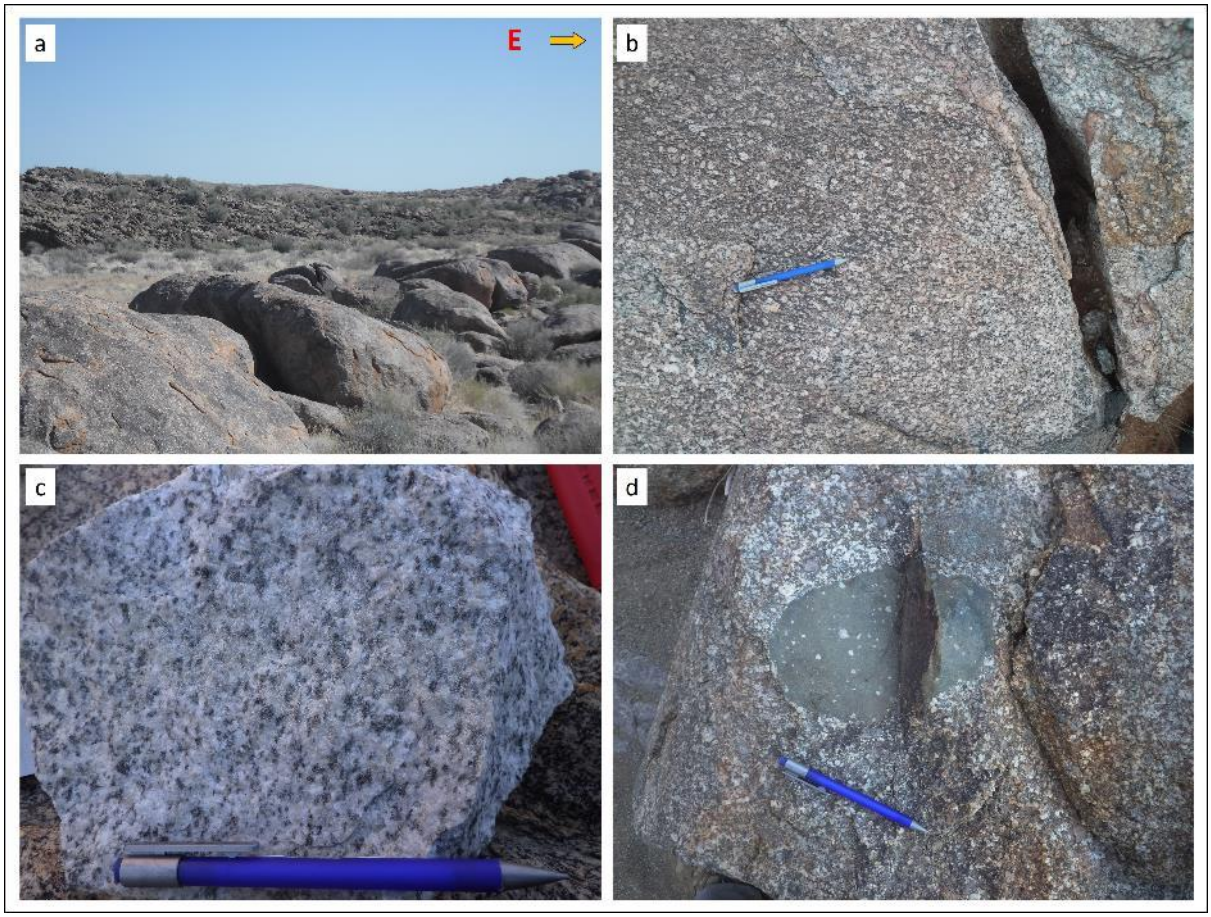

Figure 3-8: shows a textural and composition range of the equigranular granodiorite. (a) distance view photograph of the equigranular granodiorite (b) very coarse grained type granodiorite dominated by quartz and k-feldspar, with minor biotite and hornblende, (c) medium-coarse grained biotite-hornblende spotted granodiorite, (d) medium grained equigranular biotite-rich granodiorite consisting of ellipsoidal basalt xenolith.

3.2.2.3 Felsic Granitic Intrusive Subsuite (Ramansdrif Intrusive Subsuite)

Two distinct types of the granitic intrusive subsuite occur within the study area: (1) coarse-grained equigranular to porphyritic, alkaline granite and (2) fine- to medium-grained alkaline granite. While the former is one of the most dominant units within the subsuite and occurs on the south of the Northernmost Sperlingsputs Frontal shear zone, the latter is only rarely observed, mostly in the form of dykes. The granitic subsuite is the youngest member of the Intrusive Suite, and invaded both the volcanic rocks and the earlier intrusive phases of the intermediate and mafic subsuites. The granitic subsuite in general is mainly characterised by leucocratic pink colour.

3.2.2.3.1 Coarse-grained granite

The coarse-grained alkali granite phase of the subsuite is distributed throughout the map area, forming equigranular to porphyritic intrusive bodies 20 to 200 m wide. Mostly if not always these granites are associated with granodiorites of the Goodhouse Intrusive Subsuite. The whitish to brownish coarse-grained Granite weathers to a light-brown to pinkish colour. The mineral assemblage consists of quartz (30%), K-feldspar (35%), plagioclase (15%) and biotite (20%). Hornblende and muscovite are rarely observed, while magnetite and ilmenite are the accessory minerals. Epidote, sericite and chlorite occur as secondary minerals. The porphyritic variety is characterized by numerous 2 mm to 20 mm large, sub-rounded to rounded K-feldspar phenocrysts within the finer-grained pinkish groundmass (Fig 3-9). Locally, the alkali-feldspar phenocrysts have plagioclase rims forming a rapakivi-like texture. Within and adjacent to the SPSZS, K-feldspar phenocrysts are clearly reshaped into ellipsoidal crystals (augen), defining foliation and shear sense of movements. However, out of the shear zones the granite has a very poorly developed fabric, mainly delineated from the mica minerals. Most of the thin sections contain k-feldspar (microcline), plagioclase, quartz and biotite minerals. The plagioclase is mainly altered into sericite. Biotite is also unstable, since it forms a reaction rim with sericite. The overall texture is defined by k-feldspar (0.2-0.6mm) phenocrysts within a medium grained matrix of quartz (0.05-0.1 mm), and biotite.

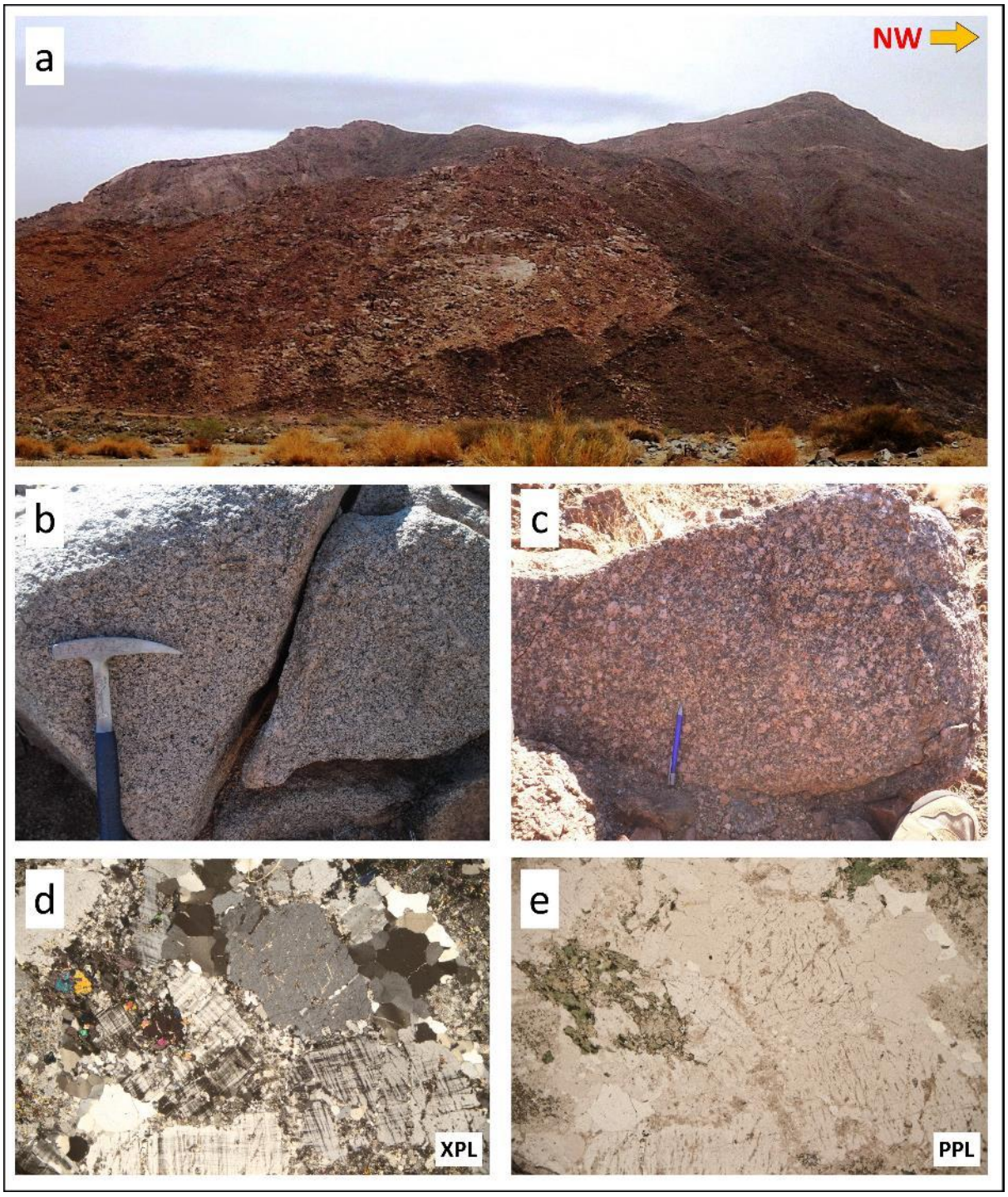

Figure 3-9: (a) distance plane view photograph of the batholitic Ramansdrif granite that forms a very sharp intrusive contact with the porphyritic granodiorite of the Goodhouse Subsuite along the Haib River toward the Orange River. (b) & (c) the variation of k-feldspar phenocrysts within the granite across the study area. (d) & (e) photomicrographs (FOV=4.5 mm) of porphyritic granite, consists of millimetre scale microcline phenocrysts set in a medium grained quartz aggregate groundmass.

3.2.2.3.2 Fine- to medium-grained alkali granite (aplitic dykes)

Although the aplitic dykes occur throughout the study area, they are most commonly found in the western part of the study area. The randomly trending dykes form one to 40 m thick linear bodies' cross-cutting volcanic units, as well as mafic, intermediate and felsic granitic intrusive subsuites. Generally they are fine-to medium-grained, with a pinkish to brownish weathered colour and pinkish to reddish colour when fresh (Fig 3-10). The mineralogical assemblage is dominated by K-feldspar (45%), with subordinate plagioclase (20%), quartz (25%), and biotite (8%) ± amphibolite. Within the shear zones, they are transformed into cataclasite or felsic mylonite, together with the older volcanic rocks. In areas of intense shearing, quartz has been plastically deformed into ribbon-like shapes, while feldspars are sheared into ellipsoidal crystals.

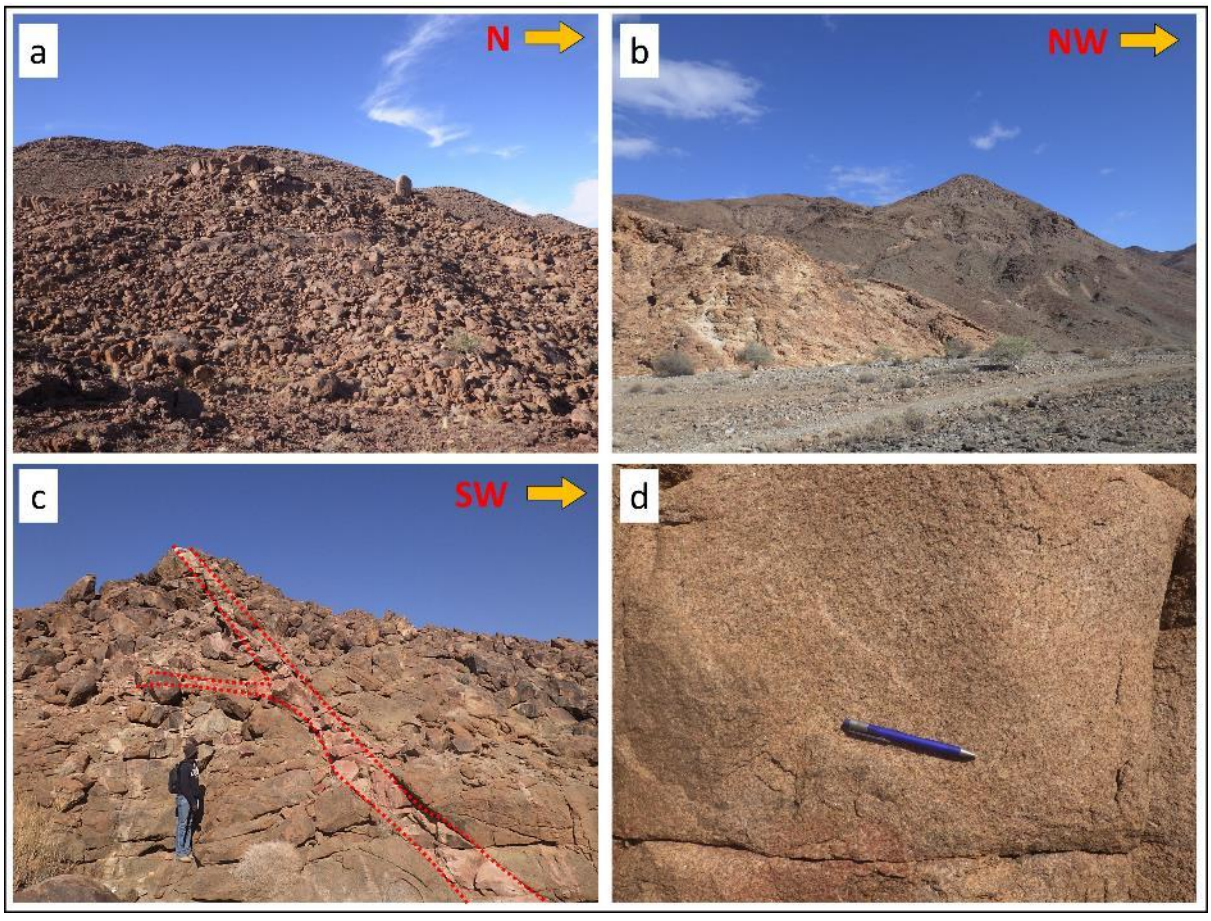

Figure 3-10 (a) & (b) distance view photograph of the medium-fine grained leucocratic alkali granitic dyke, cross-cut the early Vioolsdrif intrusive bodies and the ORG volcanic rocks. (c) metre wide fine to medium grained Ramansdrif dyke (Rd) within the coarse grained Ramansdrif granite. (d) outcrop photograph showing the medium grained alkaline dyke consists of plagioclase that is partly altered into epidote and fine grained shiny mica (sericite).

3.3. MAJOR ROCK UNITS WITHIN HIGH GRADE REGION (PELLA DOMAIN)

The Pella Domain is made up of amphibolite-facies gneisses that are interpreted to be equivalents of the lower grade Vioolsdrif domain. These rocks are found in the northern part of the study area and separated from the Vioolsdrif domain by a kilometre-wide transitional zone (the Southern Namaqua Front). The four rock types that out crop in the study area are: (1) Biotite-Hornblende gneiss; (2) migmatitic biotite-quartz-feldspathic gneiss; (3) Hornblendite agmatite; and (4) Cordierite-sillimanite-garnet bearing gneiss. Protoliths have been determined for each of these units and are indicated below.

3.3.1 Biotite-Hornblende gneiss

Biotite-hornblende gneisses are the dominant rock unit within the Pella domain and is restricted to the north of the Sperlingsputs Shear Zone, where it forms 20 m to 200 m wide hills. The gneisses are characterised by a dark-brownish to dark-grey fresh surface, with a brownish weathered surface. Petrographically they constituent two main types, one of which is derived from the granodiorite and one from the andesite. The first type, interpreted to be derived from the granodiorite (Fig 3-11 a, g & h) is mainly medium to coarse grained and consist of both igneous and metamorphic minerals. Plagioclase (30%), biotite (30%), quartz (19%) and ± pyroxene mostly occur as metamorphic minerals, whilst K-feldspar and hornblende either occur as altered igneous or metamorphic minerals. The metamorphic hornblende and k-feldspar are elongated with high aspect ratios. The gneissic texture is represented by mesocratic and leucocratic bands that range from 1 cm to 4 cm in thickness. The leucocratic bands are dominated by quartz and ellipsoidal feldspars, while the mesocratic bands consist mainly of metamorphic hornblende and biotite. In places, the gneisses are associated with a 'spotted' texture made of biotite and hornblende aggregates that are disseminated throughout the rock. The aggregates range from 5 mm to 2cm in size and are elongated with the long axis parallel to the gneissic fabric.

The second type, interpreted to be derived from the andesites (Fig 3-11 b, c, e &f), is medium grained and contains porphyroblastic hornblendes that are generally orientated parallel to the regional fabric but can in places be locally more randomly oriented. This type is interlayered at a metre scale with the cordierite-sillimanite and garnet-bearing quartz mica schists, which are interpreted to be the sediments associated with the volcaniclastics. Overall, these gneisses are highly strained and associated with a penetrative fabric defined by aligned mica and amphiboles. The gneisses, both consist of strongly twinned feldspars, and quartz with strong undulose extinction.

In places hornblende and biotite are strongly altered to chlorite. Two types of amphibolite were identified within these gneisses. The first type (hornblende) is oriented parallel to the feldspars, biotite and quartz, whilst the second type (actinolite) is overprinting the gneissic fabric and forms reaction rims and bulging structures with the feldspar and biotite.

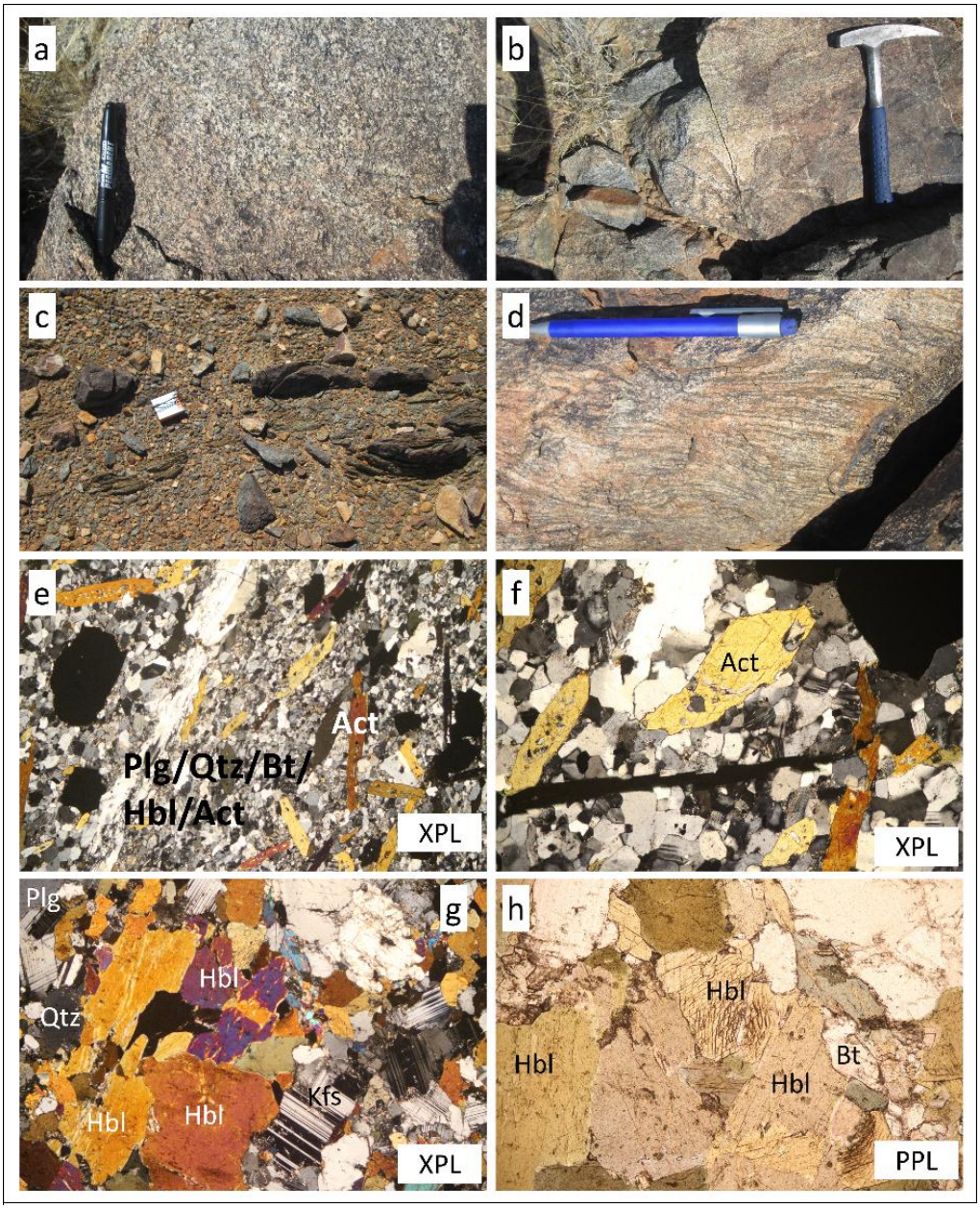

Figure 3-11: shows the petrography and texture variation of the biotite-hornblende gneisses within the Pella domain In the RMA. (a) medium-coarse grained biotite-hornblende gneiss interpreted derived from the granodiorite of the Goodhouse Subsuite, (b) & (c) medium-fine grained biotite-hornblende banded gneiss interpreted derived from the andesites of the ORG, (d) well-developed gneissic fabric (compositionally banded biotite-hornblende gneiss), (e) & (f) photomicrographs (XPL FOV 4.5 mm) from the medium-fine grained biotite-hornblende gneiss, consisting both aligned and randomly oriented amphiboles. (h) & (g) Photomicrographs (XPL FOV=4.5 mm) of the medium-coarse grained biotite –hornblende gneiss, constituent two types of biotites, that appear to form at different time.

3.3.2 Migmatitic biotite-quartz-feldspathic gneiss

Migmatitic quartz feldspathic gneisses occurs within the Pella domain, to the north of the Sperlingsputs Shear Zone. The rocks are poorly outcropping and occurs as isolated collections of small irregular bodies within the quaternary sands. Even though they are poorly outcropping within the study area, they are very easy to recognise, since they are always associated with a strong migmatitic texture (Fig 3-12 c, d &e). The mappable units of this migmatite, appear to have a SE-NW trend, extending from the farm Sperlingsputs across the farm Bankwasser and into the farm Soekwater (Fig XX). They form outcrops that range from 10 m to 300 m wide, with the biggest outcrop within the Sperlingsputs farm on the north-western side of the Kromrivier. The migmatitic texture is mainly defined by 5 mm to 2 cm thick leucosomes and melanosome bands (Fig 3-11 c & d). The leucosomes are dominated by segregations of quartz and feldspar, while the melanosomes are mainly rich in biotite and ± hornblende. In places, the neosomes are often folded into tightly, incoherent ptygmatic folds. They also appear to contain restitic xenoliths of the host rock that float within the melt. Mineralogically the gneiss is dominated by quartz and feldspar (plagioclase and k-feldspar) that are mainly bulgingly recrystallized to form a monomineralic reaction rim of sericite. Biotite retrogresses into chlorite and sericite.

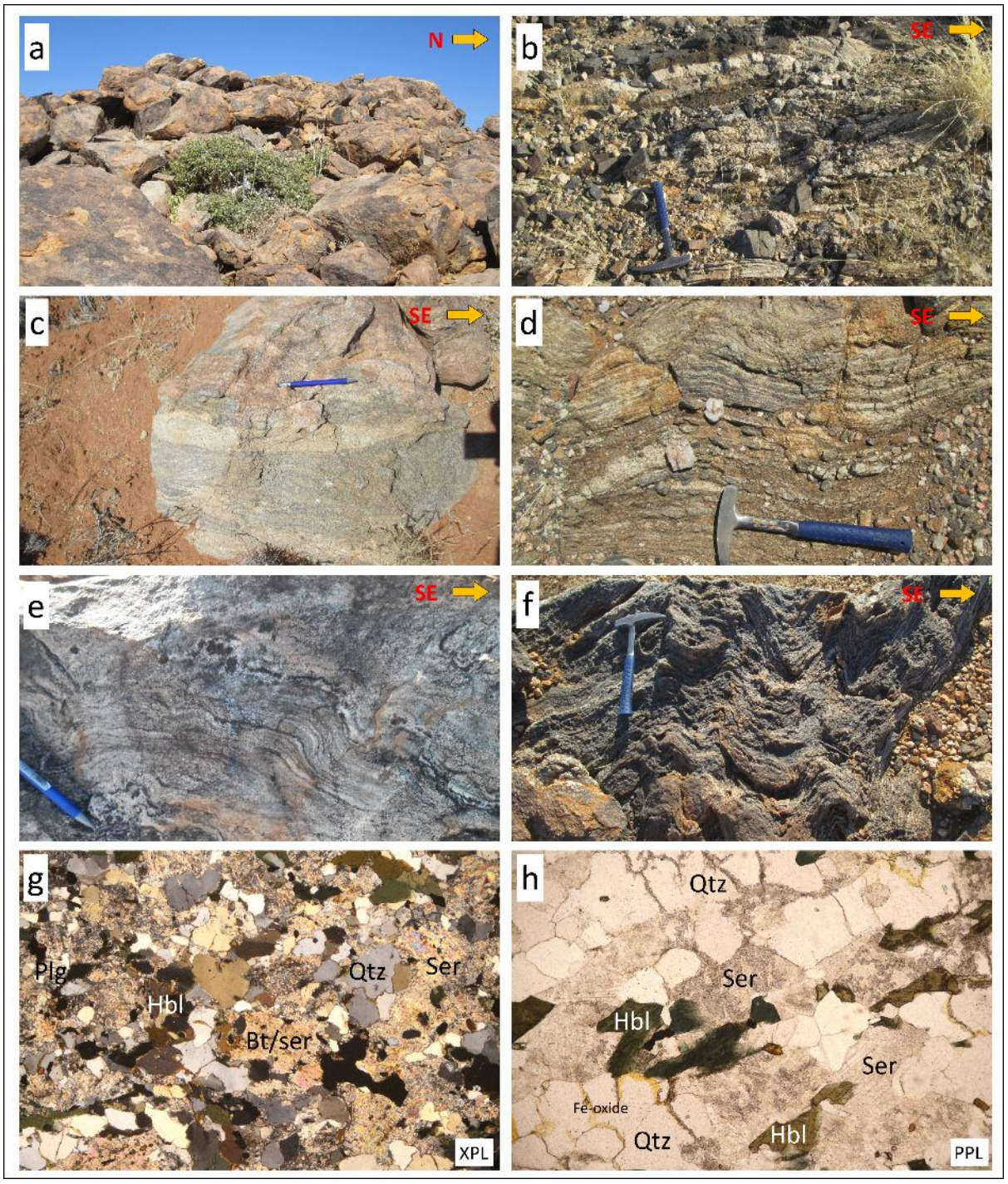

Figure 3-12: Field photographs and microscopic photomicrographs of the migmatitic biotite-quartz-feldspathic gneiss of the Pella domain. (a) mountain range photograph of the migmatite; (b), (c), (d) & (e) millimetre to centimetre scale leucosomes and melanosome bands; (f) open to close ptygmatic folds within the migmatite; (g) & (h) feldspar bulgingly recrystallized to form a monomineralic reaction rim of sericite in hands with biotite retrogrades into chlorite and sericite.

3.3.3 Hornbendite Agmatite

Hornbendite agmatite is a migmatitic rock characterized by 2 cm to 2 m wide paleosome of hornblendite set in granitic composition leucosome (Fig 3-13). The agmatites occur as numerous, albeit volumetrically small, boulder style out crops that range from 5 m to 200 m wide. However, numerous outcrops are too small to map at 1:50 000 scale. In these rocks, the melt is largely composed of recrystallised quartz and feldspar but in a few places contains calc-silicate. In places, the melt component from the migmatite becomes more volumetrically significant and forms small granitic intrusives containing blocks of the mafic host rocks (Fig 3-13 d). The paleosomes (or host rocks) are mainly hornblendite, but can be pyroxenite or gabbro. The hornblendes within the paleosomes are partially altered to actinolite.

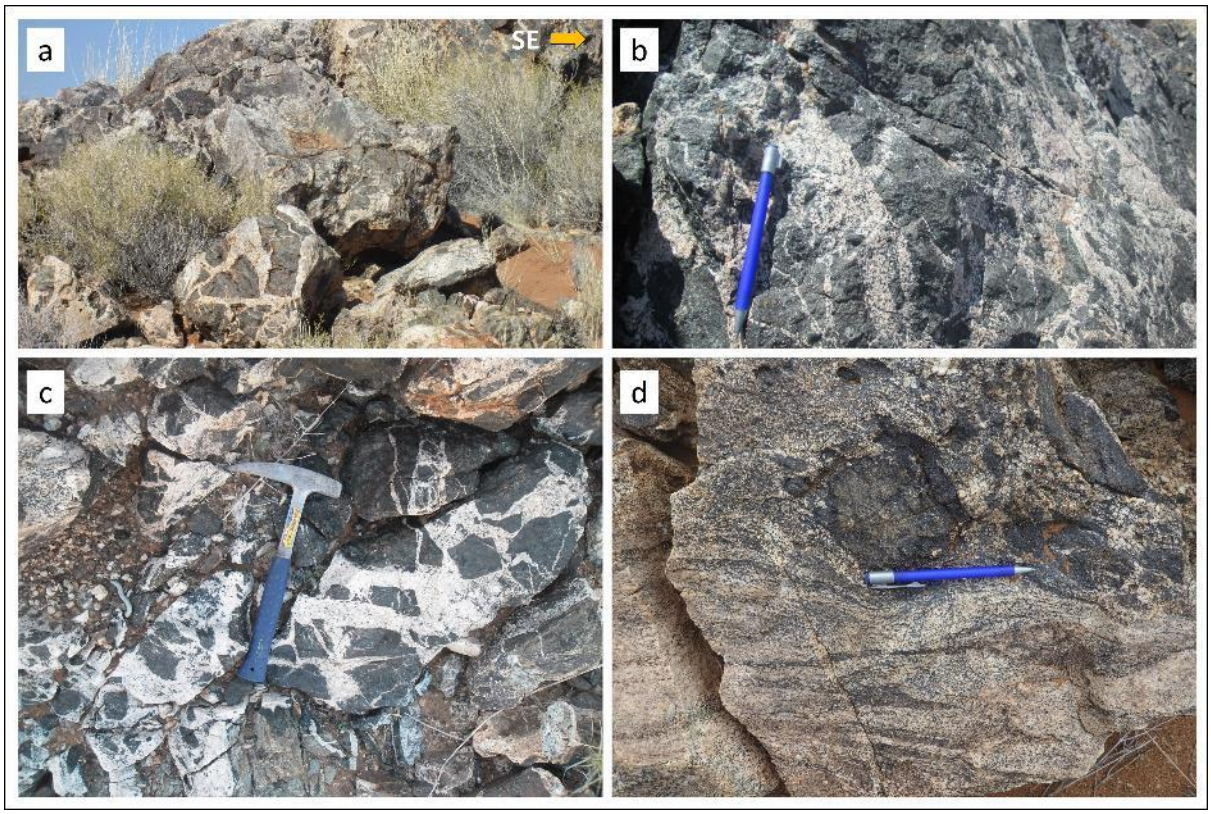

Figure 3-13: Field photographs of the hornbendite agmatite within the Pella domain. (a) small, sporadic, low-lying inselberg, set in a sea of young superficial sand. (b) & (c) the paleosomes dominant agmatite, (d) leucosome dominant agmatite. The paleosome in the photographs are coarsely oriented and mainly represented by horblendite, whilst the leucosome is granitic in composition.

3.3.4 Cordierite-sillimanite schist and garnet-bearing quartz mica Schist

The cordierite-sillimanite schist is interpreted to be a sedimentary rock associated with the pyroclastic and volcanic rocks because they occur as interbedded layers with the medium-grained biotite-hornblende gneisses. The garnet-bearing quartz-mica schist (Fig 3-14 a) may have been either a sedimentary rock but could also represent the metamorphosed equivalents of the felsic volcanic members . Both types of schist are on the north side of the Sperlingsputs Shear Zone but occur to the south east edge of the study area. The schists are mainly dominated by biotite and quartz, while the sillimanite, cordierite and garnet are largely concentrated in bands interlayered at a metre scale with the quartz mica schist. The cordierites range from 7 cm up to 20 cm wide and they occur as flattened boudinaged ovoid porphyroblastic clasts within the schist (Fig 3-14 b). The cordierite voids are mainly deformed into ellipsoidal shape, with mica around the margins. The long axis of some of the ellipsoidal cordierite are observed parallel to the regional L_2 stretching lineation.

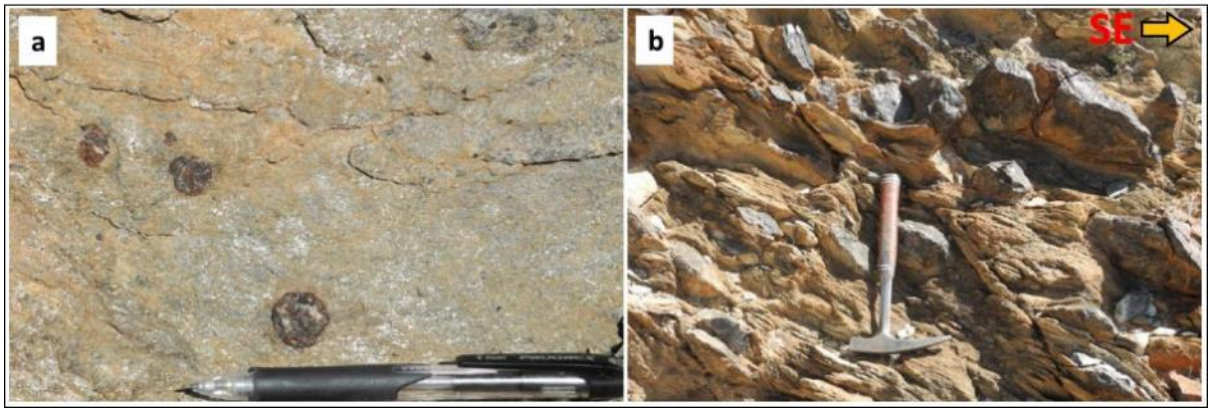

Figure 3-14: The interbedded pelitic rocks derived from the sedimentary rocks of the Orange River Group. (a) garnet porphyroblasts set within the sillimanite-cordierite mica schist in the Pella domain, (b) cobble sized flattened boundinage ovoid porphyroblastic clasts of cordierite within the mica schist.

3.4 PEGMATITES

Pegmatites are widely distributed in both Vioolsdrif and Pella domains, with more of pegmatites occurring in the northern part of the study area. Their composition is homogeneous, although in places they form a heterogeneous composition of multiple interlayering of quartz-rich zone and feldspar-mica-quartz zone. Along the SPSZS, pegmatites occur as laterally continuous sheet-like bodies that range 5 m to 100 m wide (Fig 3-15).

Figure 3- 15: Pegmatite consists of interlayered quartz-rich zone and feldspar-mica-quartz zone

3.5 GANNAKOURIEP DYKES

The Gannakouriep dyke swarm extends throughout the study area. They are well displayed on the Google Earth Image and they are more than 300 km across the Namibia-South Africa border. On satellite and other remotely sensed images the dykes are clearly visible (Fig 3-16) as 2 to 10 m wide and 100 to 500 m long, discontinuous, brownish-black, NNE-trending linear bodies. Most of the dykes are fairly straight; however, in some places they form irregular-shaped linear bodies. The dykes range from doleritic to gabbroic in composition; the latter are the most common in the study area.

They usually weather negatively and showing classic onion skin weathering features (Fig 3-16 f). The dykes are to be the youngest intrusive unit (Neoproterozoic) within the map area, cross-cutting both D_2, D_4 and D_5 structures. Chilled margins and cuspate-lobate igneous features are locally observed at the contacts between the dykes and their country rocks. The dykes have undergone partial silicification, sericitization or argillic alteration processes, especially towards the contacts. At microscopic scale, these dykes are observed to consists of pyroxene (mainly orthopyroxene), plagioclase, ± olivine, biotite, chlorite, epidote and opaque. Both plagioclase and olivine are partly altered into sericite and chlorite

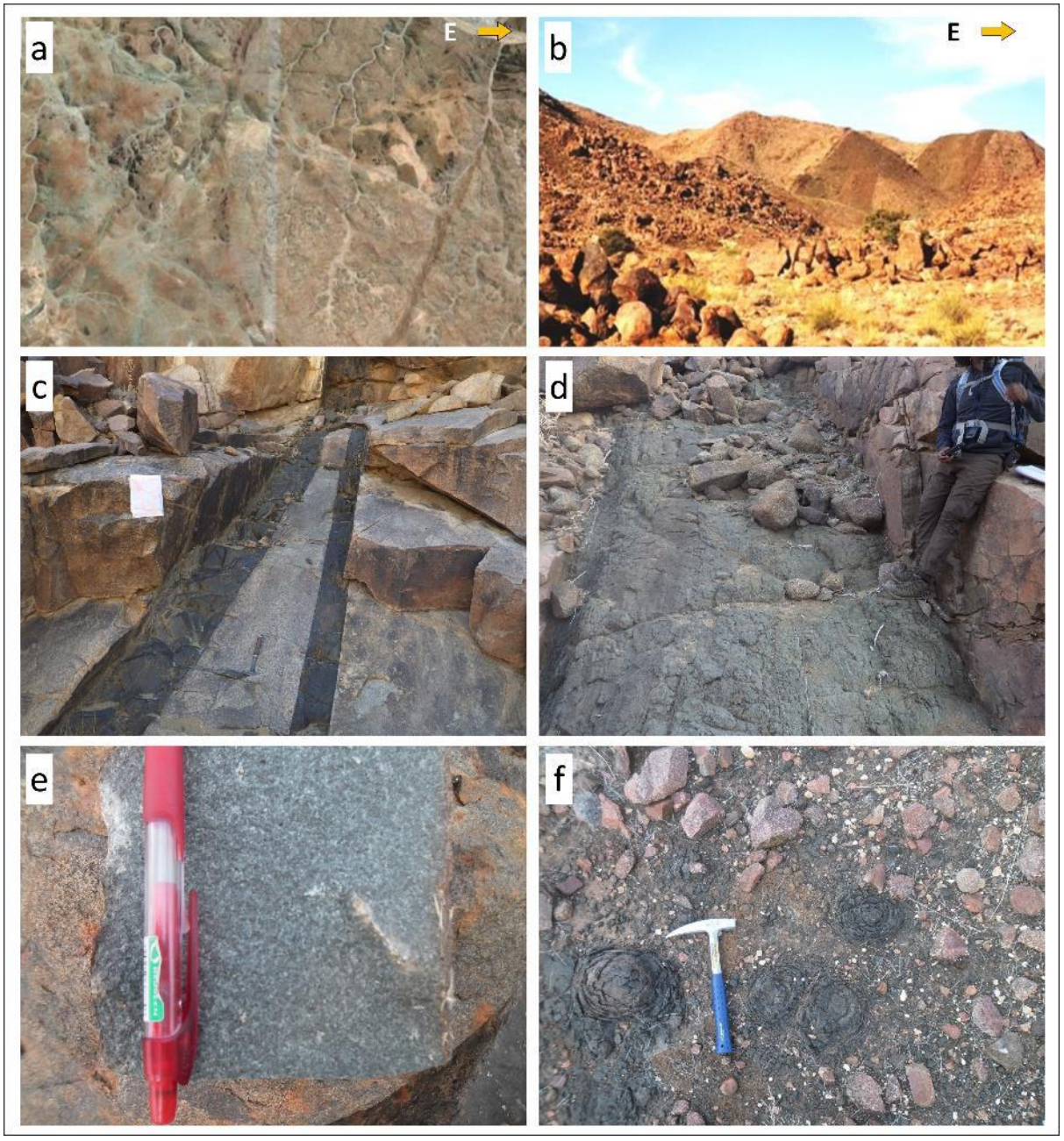

Figure 3-16: The Gannakouriep dyke satellite image and field photographs. (a) Google Earth Image (captured at < 2 m resolution), (b) plane view photograph showing the cross-cut relationship between the Gannakouriep dyke and the ORG volcanic rocks, (c) & (d) outcrop scale photographs of the doleritic Gannakouriep dyke, (e) close look photograph of the medium grained dolerite and (f) the overriding onion-like weathering texture of doleritic dyke.

3.6 GEOCHEMISTRY

The study area is largely covered by very fine grained volcanic rocks of the ORG and it's difficult to do a qualified classification of these different types of volcanic rocks, e.g. separating andesite from andesitic basalt using only field and microscope analyses. The geochemistry mechanism was used to examine the distribution of the chemical elements in these rocks that led us to the classification of all various types of very fine grained volcanic rocks within the study area.

Twenty-two volcanic rock samples were analysed for whole rock major element geochemistry. This study only collected samples for geochemistry analyses within the low grade greenschist facies Vioolsdrif domain and there was no sample taken from the high grade amphibolite facies Pella domain for this analysis. However, the geochemical data obtained from this study were presented together with the previous geochemistry data of Reid (1977), Celliers (1989), Minnaar (2012) and Macey et al (2014) to brace the data analysis. In the adjacent area to the study area, Macey et al (2014) plotted the same volcanic rocks together with their stratigraphy equivalent high grade Pella domain rocks on an AFM diagram and these rocks defined the calc-alkalinen trends (Fig 3-17). Base on that information, all our geochemical data presented straight on the total alkali versus silica plot (Fig 3-18).

From the TAS diagram, these volcanic rocks show a range in composition from rhyolite to andesitic basalt with the most of the samples plotting in the dacite area and the least within the andesitic basalt area. The TAS plot again shows a composition variation in volcanic rocks from the north to the south. Most of the samples collected from northern part of the study area predominately plotted within the dacite and rhyolite area, while the samples from the southern are more mafic, mainly the andesite and andesitic basaltic area.

For further analyses, the geochemical data of this study once more plotted on the TAS diagram (Fig 4-2) together with the compositional fields of the component of the Intrusive Suites (Vioolsdrif Intrusive Suites) in the lower grade greenschist facies domain for Reid (1977), Minnaar (2012) and Macey et al., (2014). The TAS diagram shows a range of overlapping compositions between the volcanic and the intrusive suites rocks and their trends absolutely overlap.

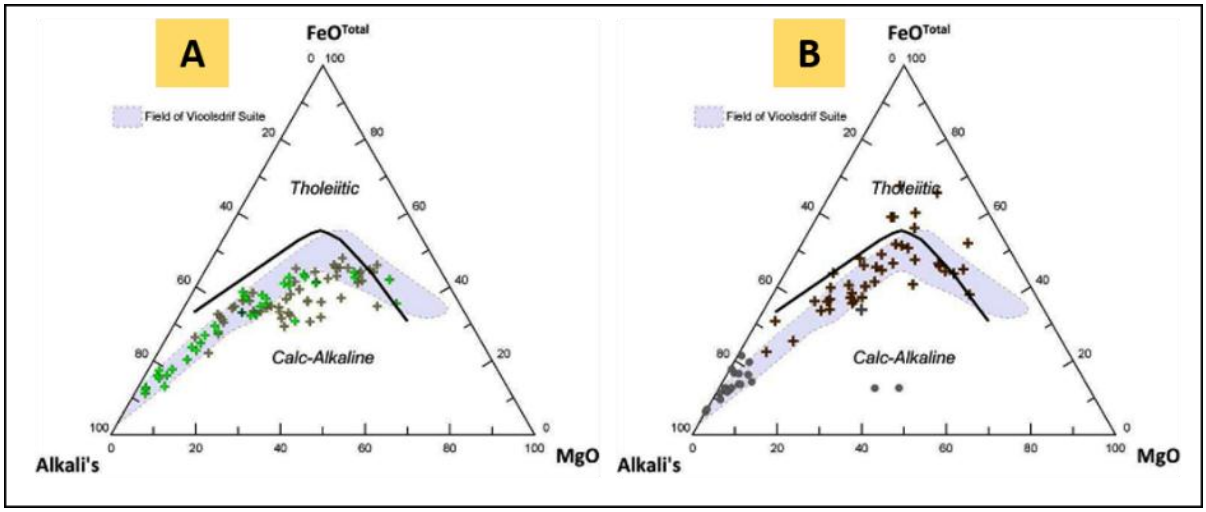

Figure 3-15: The AFM classification diagram of the rocks within the Richtersveld Subprovince of the Namaqua Metamorphic Province, with A-diagram representing the volcanic rocks and intrusive suites within the lower grade greenschist Vioolsdrif domain and B-diagram representing the meta-volcanic rocks in the high grade amphibolite faciesm Pella domain after Macey et al., (2014).

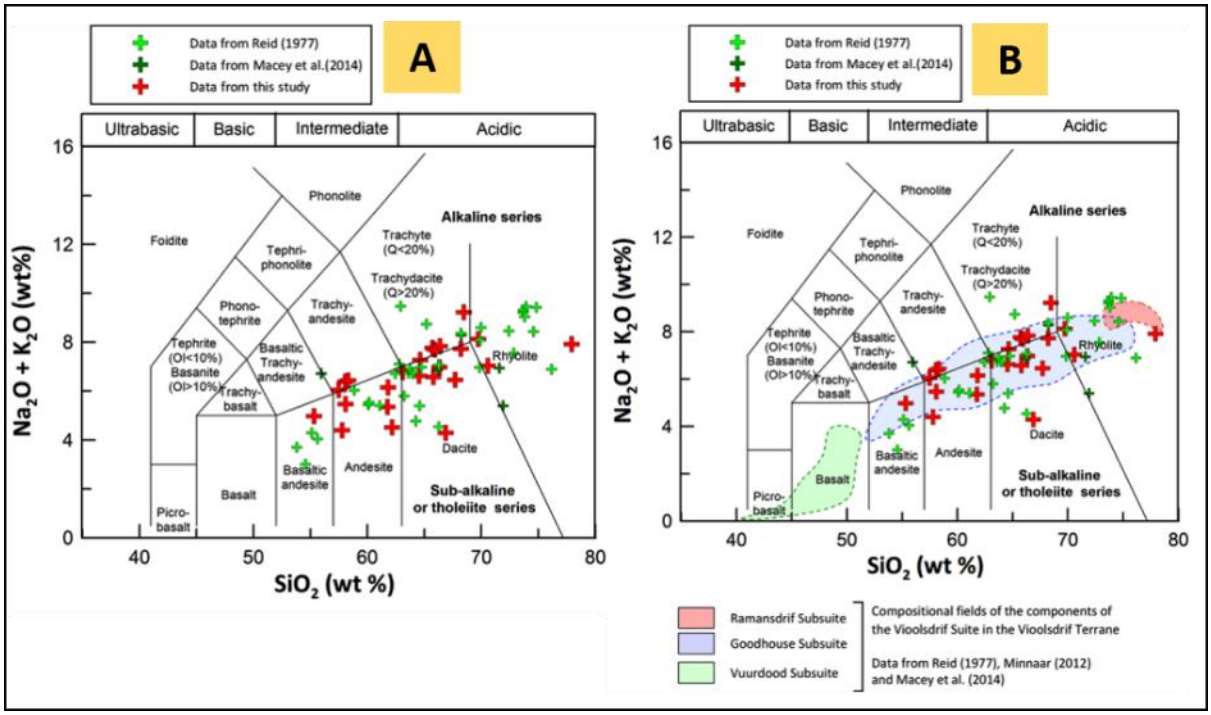

Figure 3-16: The TAS geochemistry diagrams show the composition range within the Paleo-Proterozoic volcanic and intrusive rocks within the study area. A; the total alkali versus silica plot diagram, showing a range in composition of the samples, from rhyolite to andesitic basalt, with more samples plotting within the dacite zone. B; TAS diagram presenting the geochemical data of the ORG volcanic rocks plotted together with the Vioolsdrif Intusive Suites compositional fields for Reid (1977), Minnaar (2012) and Macey et al., (2014).

CHAPTER 4: STRUCTURE

4.1 INTRODUCTION

The structural character of the study area is variable, ranging from brittle structures to brittle-ductile structures. In the study area, a pre-existing weakly developed fabric called S_1 is associated with open to close folds (F_1) that formed during the earliest recognised deformation event denoted D_1. The brittle-ductile fabrics post-date the earliest D_1 event fabrics and are further divided into two types; (1) amphibolite facies gneissic deformation event (D_2) and (2) low greenschist facies brittle ductile shear deformation event (D_4). The well-known mega-scale anticline and syncline dome and basin structures deformation event (D_3) that is well-preserved immediately south of the MRPSZ was not observed within the study area. The D_2 deformation event is defined by penetrative gneissic fabrics (S_2 & L_2) and is restricted within the Pella domain of the RMA, whereas the brittle ductile shear deformation event (D_4) is confined in the Vioolsdrif domain and reworked the D_2 event fabric plus the km-scale transitional tectonic boundary between the two domains. The D_2 deformation totally transposed the D_1 event fabrics in the Pella domain. The brittle-ductile shear deformation (D_4) in this study is assigned to the Sperlingsputs shear zone system, which is characterised by network of anastomosing discrete high-strain dextral shear zones. The brittle deformation event (D_5) are mainly fault and joints that cross-cut all the structures within the study area and suggested to be the youngest structures amongst others. In summary the tectonic events were characterised base on their field and microscopic relationships and were described base on the characteristic of structural fabrics as follow.

4.2 STRUCTURAL ELEMENTS

4.2.1 Foliations and Lineations

4.2.1.1 Bedding S_0

Bedding is well preserved within the Vioolsdrif domain, except where it is cross-cut by the brittle-ductile shear fabric. It is represented by volcanic layering and highlighted by primary millimetre-scale lithological banding (volcanic flow-banding) defined by variations in colour, grain size and composition (Fig 4-1). Since S_0 foliation has been locally overprinted by the S_4 shear fabric, it is now best preserved in unsheared domains between the SPSZS, specifically along the Kromrivier and Haib River. At individual outcrop scale, S_0 appears to be randomly oriented, but at larger scale has an

overall north-west trend, although this is not considered to be the original primary orientation because is in line with the direction of D_4 shear fabrics. In places, the S_0 fabric is folded into open to closed folds, cross-cut by a weakly developed cleavage interpreted to be S_1 (Fig 4-2 a). Within the shear zones, the S_0 fabric has been reworked, and primary layering within the volcanic rocks is obliterated and replaced with cataclastic and mylonitic textures. However, at a few rare locations within the shear zones, bedding has been preserved but deformed into inclined close to tight folds on a cm scale.

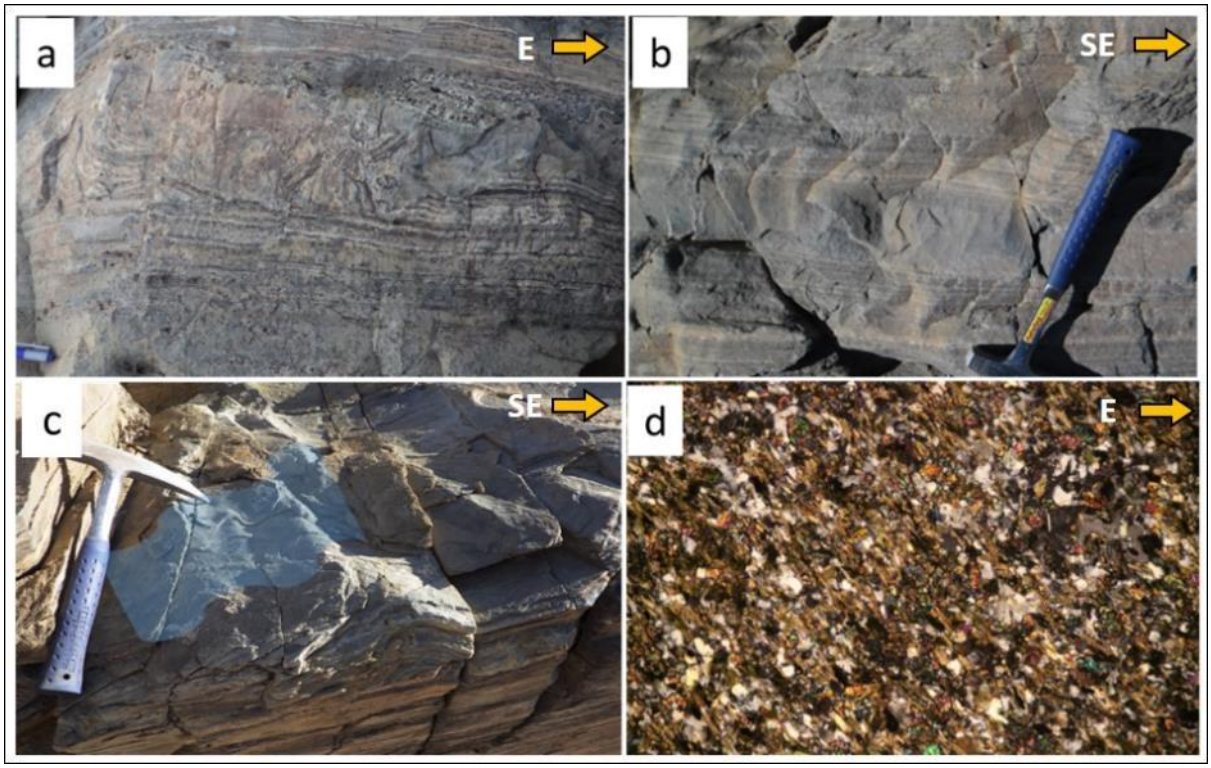

Figure 4-1: The S_0-bedding (volcanic layering) within the weakly deformed ORG volcanic rocks within the lower grade greenschist Vioolsdrif Domain in Haib Vicinity. (a) The sub-parallel reversed fault plane is evidenced by disruption of the millimetre to centimetre scale flow bands within the fine grained rhyolite. (b) The fine-grained flinty medium grey rhyolite shows mm-scale flow bands. (c) gentle to close folds in the ORG rocks displayed by cm scale compositional layering. (d) Volcanic layering at microscope scale, shown by interlayered biotite rich layer and feldspar-quartz layer.

4.2.1.2 D_1 fabric

The D_1 event is associated with a weakly developed lower-strain cleavage (S_1), defined dominantly by weakly aligned micas. The S_1 fabric developed at low grade greenschist facies conditions and as a result the mineral assemblage consists mainly of chlorite, muscovite, sericite, plagioclase and biotite. These minerals are weakly oriented and form a non-penetrative fabric. The S_1 fabric strikes in a dominantly NW-SE direction, with a predominantly NE moderately to steeply dip and is associated

with the open to closed antiform and synform structures (Fig 4-2), that form sub-horizontal fold hinges (F_1). The wavelengths of the folds range from 20 cm to hundred metres in scale, with roughly equal fold limbs.

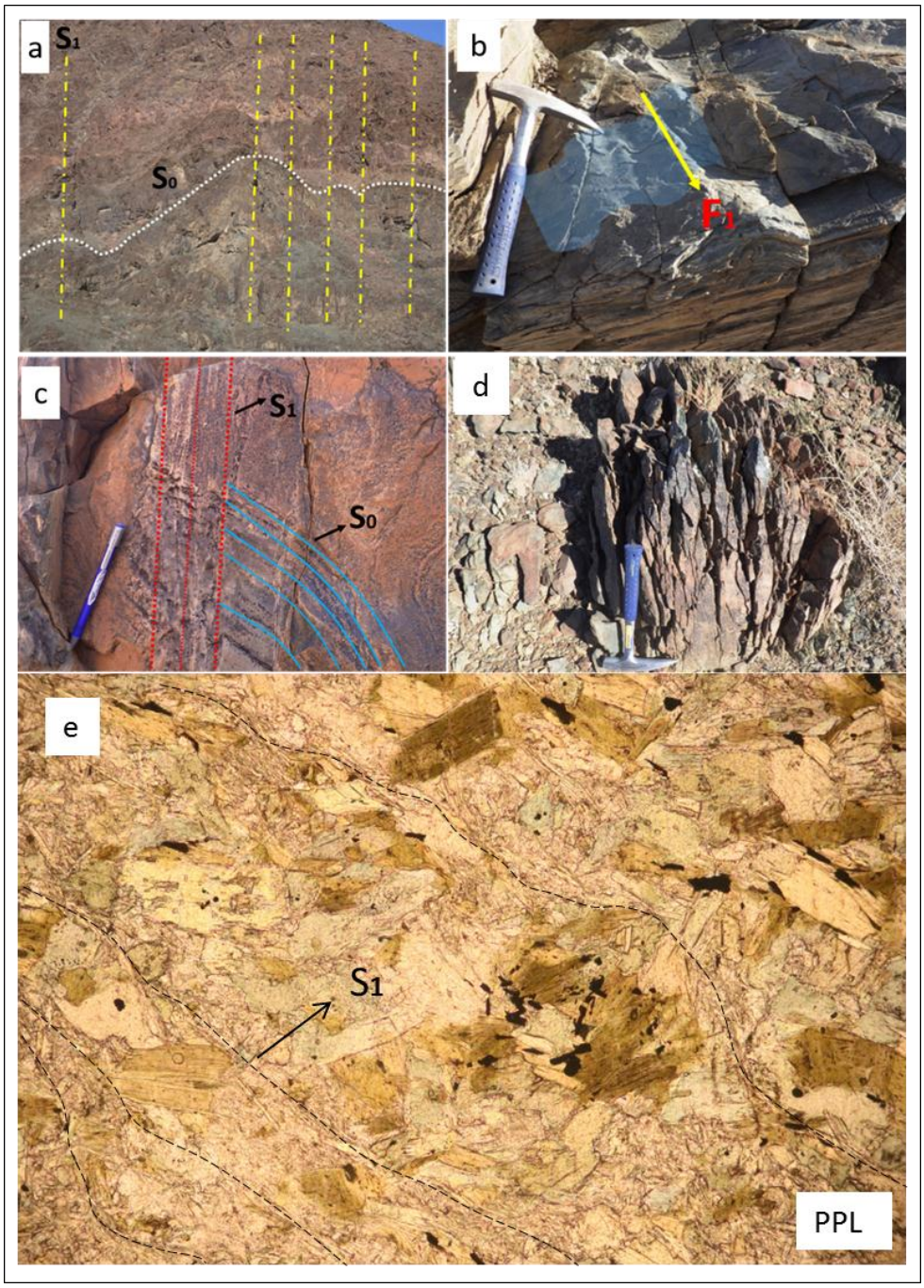

Figure 4-2: Weakly developed D_1 event fabrics within the ORG rocks in the Vioolsdrif Domain. (a) Mountain range faintly developed S_1 cleavage together with the metres scale gentle to close folds. (b) gentle to close folds of sub-horizontal fold axis (F_1) in the ORG rocks. (c) Outcrop relationship between S_0–bedding and S_1 cleavage. (d) outcrop scale photograph showing the sub-vertical NW-SE trending D_1 event foliation.(e) Photomicrograph (FOV=4.5 mm) showing the non-penetrative S1 cleavage, defined by weakly oriented mica minerals.

4.2.1.3 D2 fabric

D_2 is a brittle-ductile deformation event that transposed the pre-existing weakly developed greenschist S_1 fabric in the Pella domain into a penetrative gneissic foliation (S_2) at amphibolite facies. The gneissic texture is defined by millimetre to centimetre scale mesocratic and leucocratic bands. The amphibolite facies nature of D2 mainly demonstrated by the hornblende and garnet bearing gneisses. In places, the amphibolites facies is also represented by the semi-pelite cordierite-sillimanite bearing schists. The S_2 foliation is NW-SE trending and moderate dipping mainly to the NE. However, along the southern most boundary of the Southern Namaqua Front, the fabric is strongly overprinted by the shear fabric of the Sperlingsputs Shear Zone System. The event is also associated with a strong stretch mineral lineation denoted L_2. However, where rocks are intensely folded, an intersection lineation takes over from the stretching lineation. The L_2 lineation is a penetrative mineral lineation, mainly represented by tubular hornblende and elongated quartz aggregates and characterised by a dominant northeast moderately plunging sub-vertical to down-dip lineation on a moderate dipping foliation plane (Fig 4-3). The F_2 folds are close to tight asymmetrical, inclined, upright folds and their wavelength ranges from centimetres to metres scale.

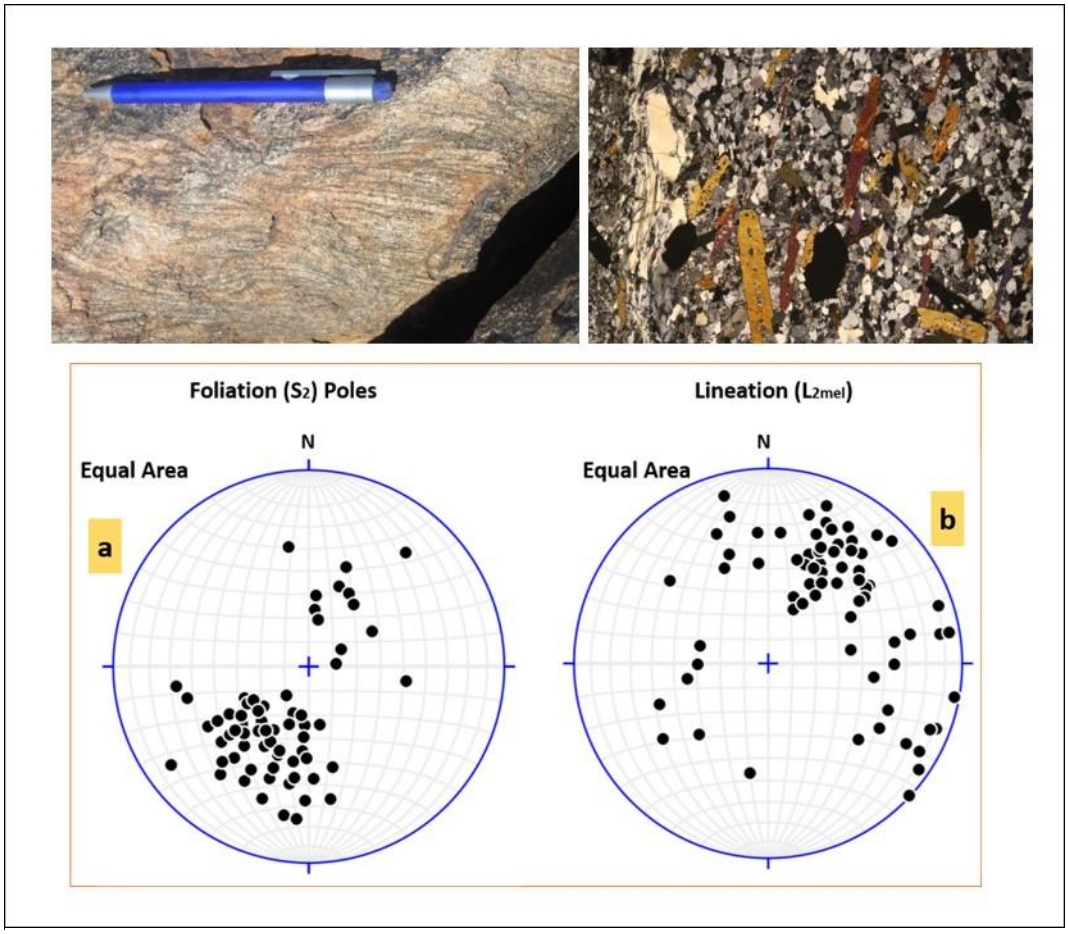

Figure 4-3: Photo macrograph, photomicrograph and stereo plots of D_2 event fabric in the study area, (a) foliation (S_2) poles stereo plot showing moderate dip foliation plane, dominantly dip toward the northeast direction. (b) Dominate down dip lineation (L_2) stereo plot, plunging toward northeast.

4.2.1.4 D3 fabric

The D_3 event is not observed in the current study area. The event is characterised by a weak to moderate developed fabrics, localised immediately south of the Marshall Rocks-Pofadder Shear Zone. The event is defined by large scale syncline and anticline fold structures (F_3) with localised foliation and lineation. These folds are striking NE-SW direction and further dragged into MRPSZ. Whilst north of the MRPSZ, the folds are elongated into NE trending dome and basin structures that are also further truncated into MRPSZ.

4.2.1.5 D_4 fabric

Shear fabrics in the study area are signed to the D_4 event. The event is defined by a shear fabric symbolized S_4, characterised by plastically deformed; ellipsoidal k-feldspar, ribbon-like quartz and flatted micas. The fabric is steeply dipping and strikes in a NW-SE direction. The dip direction of the

foliation is varying from northeast to southwest but dominantly inclined towards the southwest. However, along the margin of the rigid bodies, S_4 is mainly striking in a NNW or NNE direction.

The dominant penetrative mineral lineation occurs throughout the shear planes and has a principal southeast plunging direction, with few lineations plunging to the northwest (Fig 4-5). The mineral lineations occur either as sub-horizontal or sub-vertical (down-dip) lineations on steeply dipping shear planes (Fig 4-4). However, different types of lineations have been observed, such as intersection lineations and slickensides. Where rocks are deformed into asymmetric upright kink folds (F_4), the intersection lineation is developed between the pre-existing foliation (S_1) and the axial plane and is parallel to the local fold axis (F_4). These are mainly southeast-northwest plunging sub-vertical lineations.

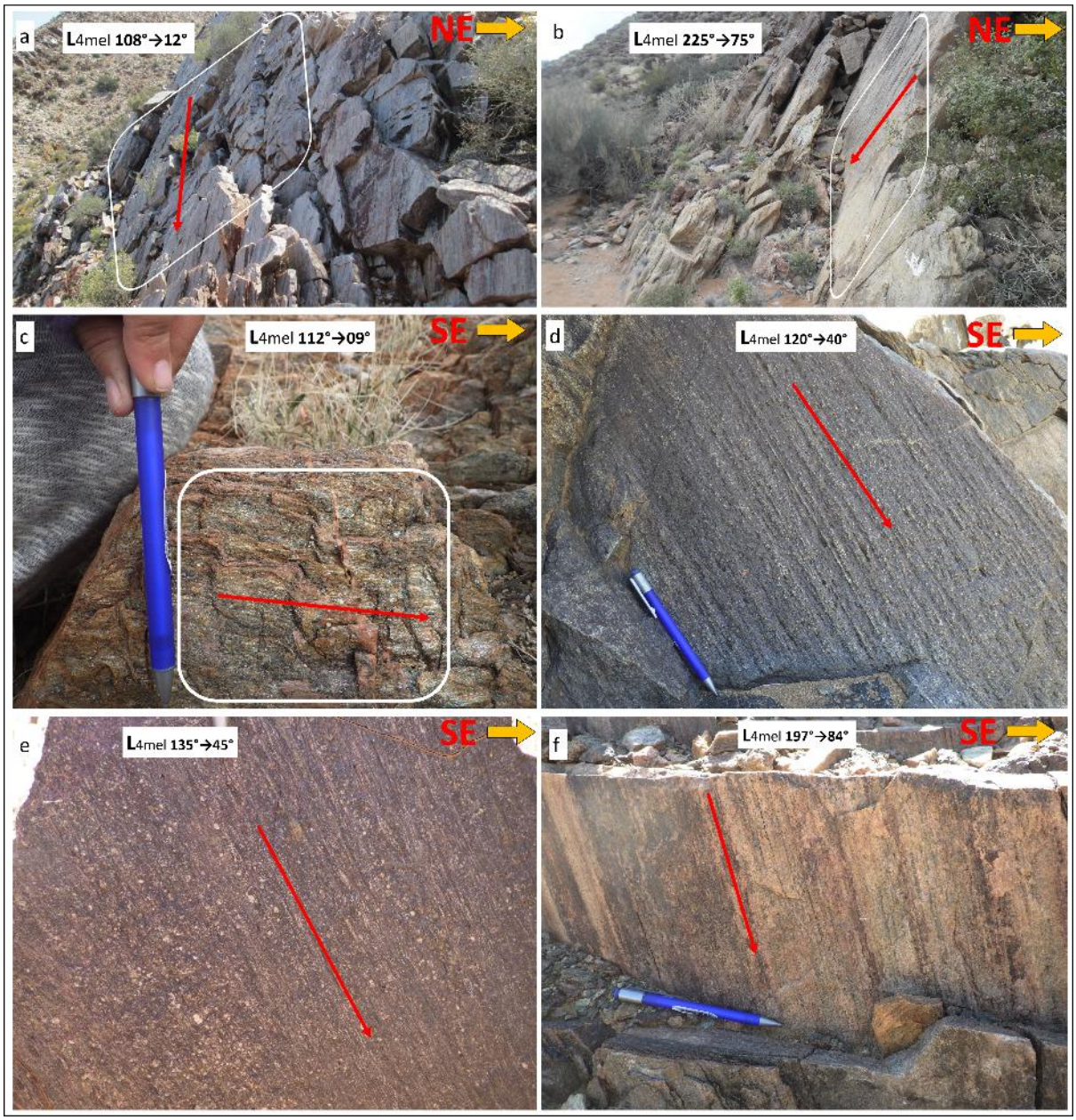

Figure 4-4: Different types of penetrative mineral elongation lineation (red arrows) along the SPSZS; (a) &(c) Sub-horizontal to horizontal mineral elongation lineation on a steeply (≥75°) dipping shear plane, (b) & (f) Down-dip mineral lineation (sub-vertical to vertical) on the margin of partly sheared granodiorite, (d) & (e) moderately plunging mineral lineation within the sheared granite of the Ramansdrif sub-suite

There is a systematic variation within the lineations as a rigid body, such as a granitoid, is approached. The lineation tends to be more sub-horizontal away from the rigid bodies, but toward and along the margin of the rigid bodies, the lineation becomes steeper (Fig 4-5), therefore steeply plunging and down-dip lineation are largely located along the margin of the rigid bodies.

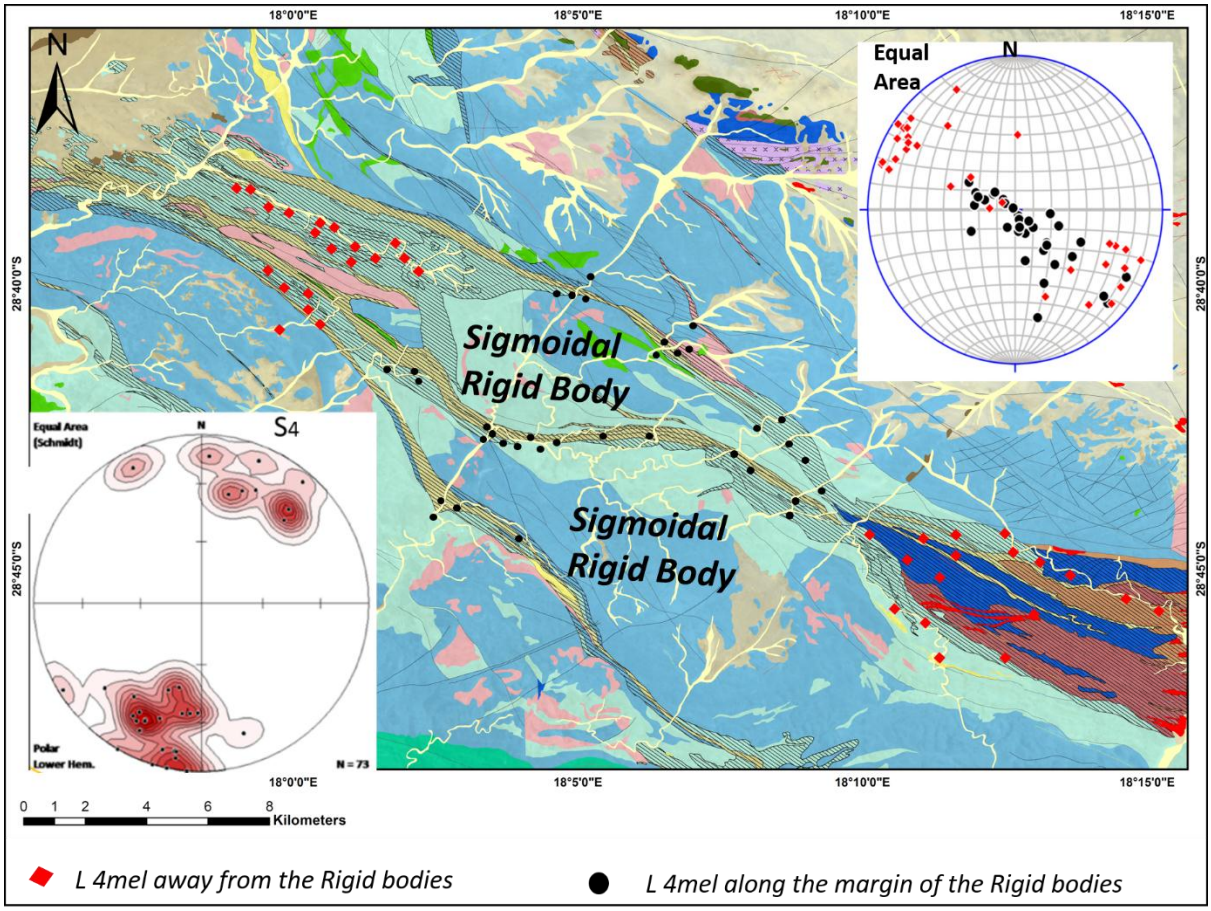

Figure 4-5: Structural readings (L_{4mel}) and (S_4) plots on the 1: 50 000 scale geological map, showing a systematic variation of mineral lineation in relation with the rigid bodies.

4.2.1.6 D_5 fabric

The D_5 event is not associated with either foliations or lineations and is characterised by brittle structures such as faults, joints and quartz veins, that are observed cross-cutting D_2, D_4 and D_1 event fabrics. The density, orientation and character of these structures varies considerably and, to some degree, systematically across the study area. The faults vary in length and width, ranging from 50 m up to tens of kilometres in length. At outcrop scale, the faults are mostly associated with zones of fracturing, tectonic breccias and fault gouge (Fig 4-6). The major fault observed in the study area is located at the central part of the study area, where it is exploited by the Kromivier. Overall, the fault is trending toward NNE direction and extends for more than 25 km. In the Haib area, these faults are observed cross-cutting and sinistrally displacing the D_4 fabric (Fig 4-6 b).

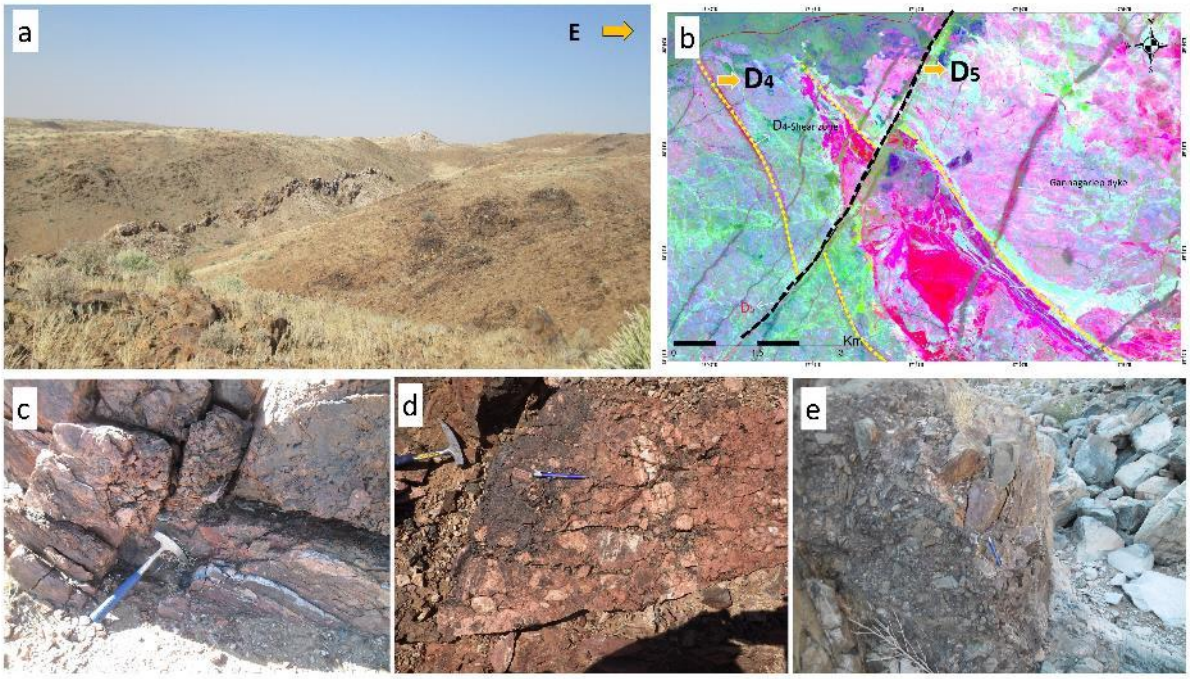

Figure 4-6: Field photographs and hyperspectral imagery of the brittle D_5 structures within the Haib area. (a) Wide angle photograph of ORG and VIS rocks, cut by a NNE striking quartz filled fault. (b) The hyperspectral imagery demonstrates the sinistral displacement of D_5 fault structure across the D_4 shear structure (Central SPSZS) in Haib Area. the image is also showing the relationship between the D_5 structure and Gannakouriep dykes. (c), (d) & (e) outcrop photographs of clast supported fault breccias, that overprinted mylonite fabric.

4.2.1.7 Summary

Fabrics observed within the study are variably distributed. The S_0 fabric is distributed throughout the Vioolsdrif domain and well preserved in the Haib area. However, the fabric is overprinted by the brittle-ductile shear fabric. The D_1 fabric is restricted within Vioolsdrif domain and has also partially reworked by the shear fabric. In the adjacent Pella domain, the S_1 fabric is completely overprinted by the penetrative S_2 gneissic fabric. Furthermore, the D_1 fabric confined to the ORG rocks and has not been observed within the Intrusive Vioolsdrif rocks. The D_2 fabric is limited to the Pella domain. The fabric tends to be weakly preserved along a wide zone of deformation between the Pella domain and Vioolsdrif domain. The D_3 fabric is not well developed in the current study area, but according to the previous work in the adjacent area by Macey et al., 2015, the fabric strongly reoriented the S_2 fabric in Pella domain. The D_4 fabric dominates the structure grain of the study area and in the study area is confined to the Vioolsdrif domain, where it forms an anastomosing array of interconnecting shear fabrics. However, on the eastern edge of the study area, the shear fabric truncates the South Namaqua Front and cross-cut the pre-existing S_2 fabric in the Pella domain.

4.2.2 Kinematic Indicators

This study only presents the kinematic indicators that are related to the D_4 event. The SPSZS contains numerous kinematic indicators at regional, outcrop and microscopic scale. Most of the kinematic indicators, such as asymmetrically inclined kink folds, riedel shears, fragmented porphyroclasts, sigma/delta clasts and C-S fabrics, were easily identified in the field. Some of these kinematic indicators, such as C-S fabric, asymmetrically folds, delta/sigma clasts, were further identified using optical light microscopy.

4.2.2.1. Asymmetric folds

Folds are common structures within the SPSZS, occurring within the core as well as along the margin of the shear zones. Asymmetric folding is the overriding folding mechanism within this shear zone system, although some symmetric folds were present. The asymmetric folds are well developed along the F-SPSZS (Fig 4-16), which coincides with the southern margin of the Southern Namaqua Front, whereby the strongly developed pre-existing D_2 gneissic foliation is deformed into NE verging, SE steeply plunging tight, inclinal folds. The folds are characterised by sharp hinges with nearly straight limbs, wavelengths between 15 cm and 1 m and a largely Z-shaped geometry (Fig 4-7 a, b & c). Where the mineral lineation was found to be sub-horizontal, the majority of the asymmetric folds suggest a dextral sense of movement. Along the shear plane where the down-dip lineation is dominant, these folds suggest there was a significant vertical component to the local shear, with an overall top to the south sense of movement (Fig 4-7 d).

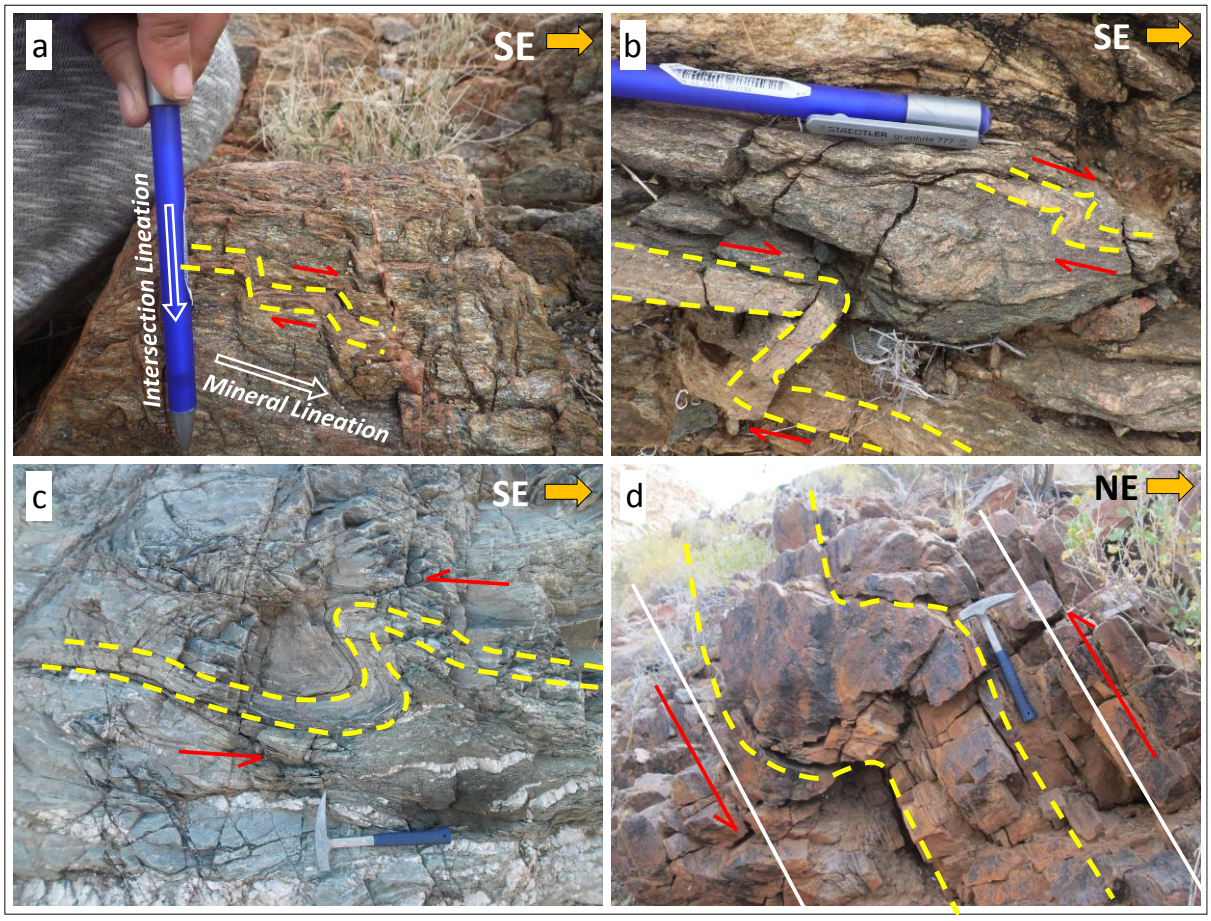

Figure 4-7: The different types asymmetric folds across the SPSZS. (a) upright kink folds along Northernmost SPSZS in the Witsputs farm, showing a dextral sense of movement. (b) closed to tight, sub-vertical, NW trending, steeply SE plunging and moderately southwest verging folds, occuring along the Northernmost SPSZS. (c) tight, SW verging folds within the Central SPSZS, yielding a sinistral sense of movement, (d) open to close, upright, moderately SW verging, NW trending folds, showing a vertical movement component to the shear zone with the top to the south.

4.2.2.2 Fragmented Porphyroclasts

Fragmented porphyroclasts are well preserved within the porphyritic granodiorite of Goodhouse Subsuite. The K-feldspar porphyroclasts within the granodiorite are elongated up to 6 cm and occasionally fractured into fragments which have been rotated into parallelism. The fragments seat in a fine-grained feldspar and quartz cataclasitic matrix. The fragments are not highly distorted, and form a domino-type fragmented porphyroclast. The sets of the minor normal faults between the fragments suggested a dextral sense of movement along the SPSZS (Fig 4-8).

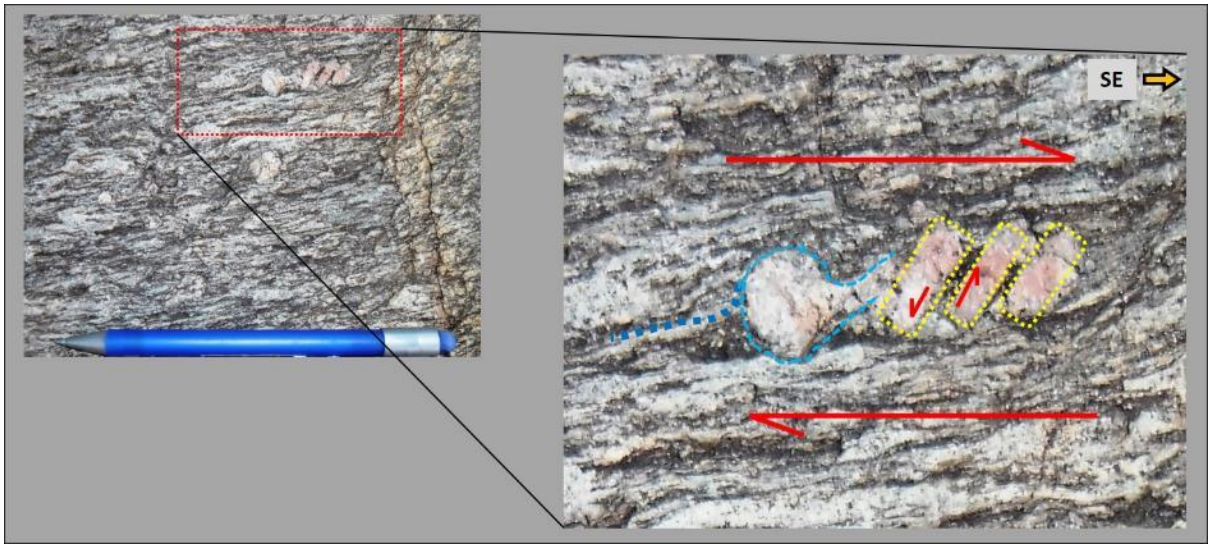

Figure 4-8: Very coarse grained biotite-rich Goodhouse porphyritic granodiorite along the Central SPSZS showing k-feldspar porphyroclasts that are deformed into domino-type fragmented porphyroclasts and suggests a dextral sense of movement to the SPSZS.

4.2.2.3 C/S fabric

Mica-rich rocks are often associated with two types of fabrics, the foliation (S) and shear bands (C). The two sets of planes are both represented at the regional, outcrop and microscope scale. At the regional scale, the two sets of planes are clearly delineated on the First Derivative Magnetic image, occurring between the Marshall Rocks-Pofadder Shear Zone and the SPSZS. From the magnetic image, the two major shear zones are shear bands and the pre-existing rotated penetrative D2 fabric is the foliation planes. At outcrop scale, the C/S fabric range from 4 cm to 50 m wide (Fig 4-9). The fabric is well preserved within the fissile biotite-hornblende gneiss along the northernmost SPSZS. The S-plane is mainly defined by centimetre to metre scale sinusoidal mica rich bands are that truncated by the shear plane. The C-plane is characterised by millimetre to centimetre scale cataclasitic to mylonitic zones. At all scales, the C/S fabric indicated a dextral sense movement to the SPSZS.

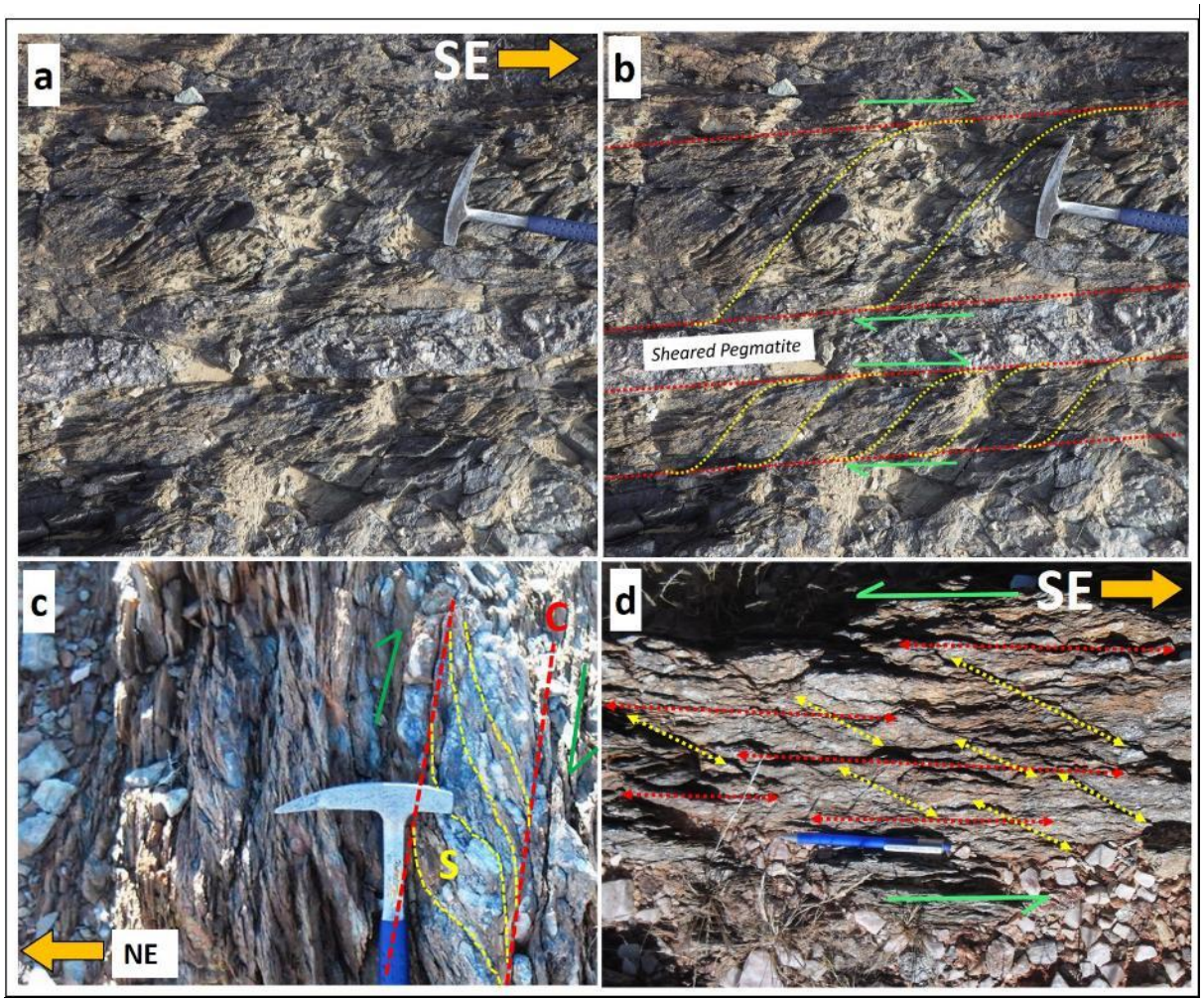

Figure 4-9: Outcrop photographs of centimetre scale C/S fabric within the mica-rich sheared intermediate rock unit, along the C-SPSZS and SW- SPSZS. (b) suggests a dextral sense of movement, (d) suggests a sinistral sense of movement and (c) display a vertical sense of movement, top to the south.

4.2.2.4 Riedel Shear Zones

Riedel shearing is observed on the eastern edge of the study area. The shear zones are very narrow, less than 50 m in thickness, and range from 100 m to hundreds of meters in trace length (Fig 4-10). They are characterised by bands of phyllonites, cataclasites and mylonites within the equigranular-porphyritic granodiorite of the Goodhouse subsuite in the Vioolsdrif domain. The Riedel shear zones occur as three set of shear zones that trend ESE, NE and NW.

The ESE trending shear zones are 11°-15° to the major shear zones (SPSZS), and are therefore understood to be R-shears. Similarly, the NE trending shear zones that are 63°-75° to the SPSZS, are then inferred to be conjugate Riedel shears (*R'-shears*). While the NW striking shear zones are the synthetic shears to the major shear zone and they form a small acute angle of about 8° to 10° to the

SPSZS and inferred to be *P-shears*. The SPSZS at both macro and microscopic observation scale is dominated by a dextral shear sense of movement. However, the Riedel shearing is independently interpreted to show a sinistral sense of movement for the SPSZS (Fig 4-10).

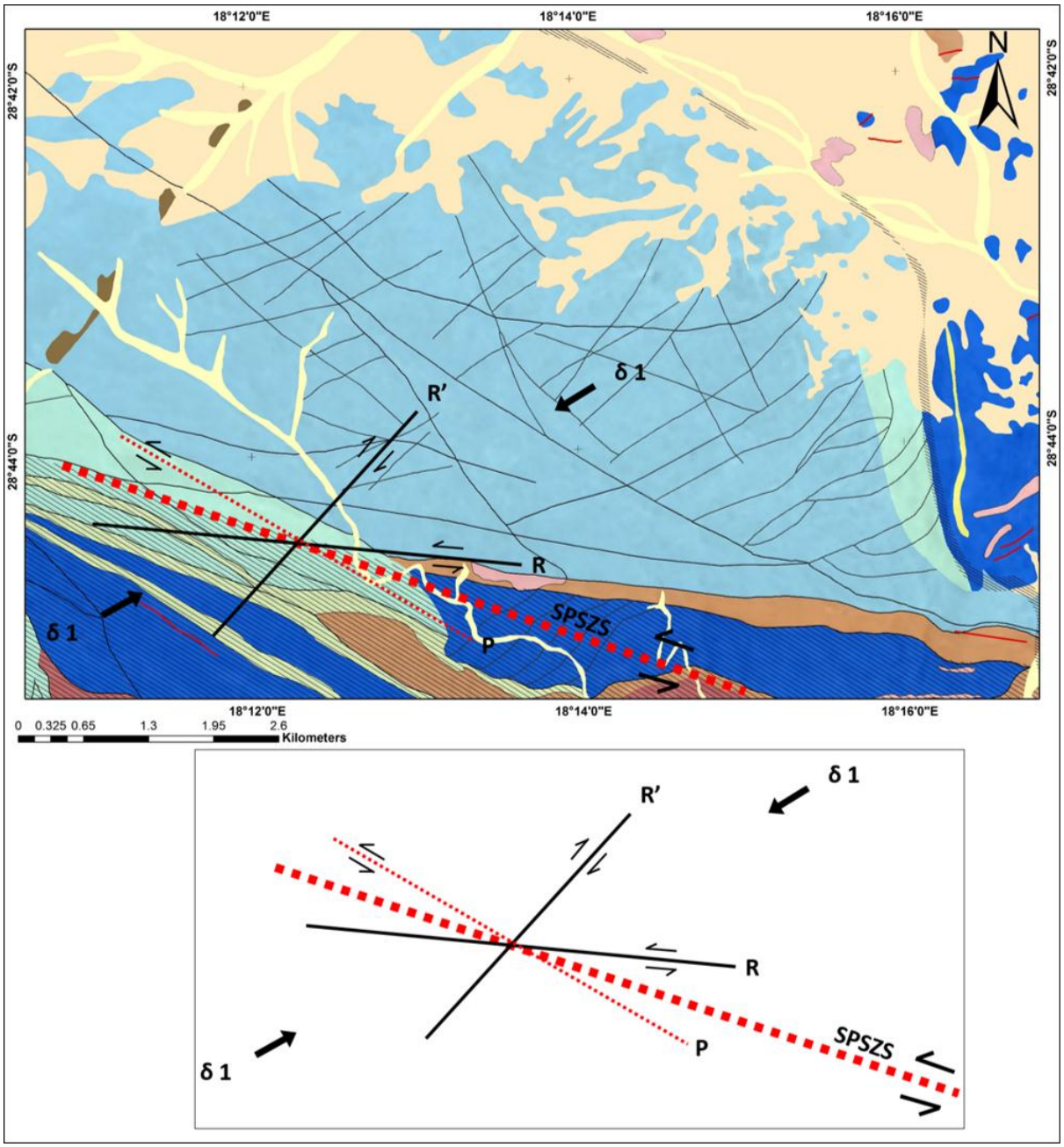

Figure 4-10: The 1: 50 000 scale structural geological map showing the Riedel shear zone in the eastern part of the study area within the equigranular-porphyritic granodiorite. Below is a summary of the Riedel shear zones (R & R"-conjugate Riedel shears and P shears) deduced from the above structural geological map.

4.2.2.5 Porphyroclasts

Porphyroclasts in the SPSZS observed at both field and microscopic scale, whereby they occur as large single crystals set in a finer grained matrix of different composition, usually base on the initial composition of the grind rock. The porphyroclasts mainly occur as naked clasts (equidimensional clasts forming sharp contact with the matrix (Fig 4-11 f)), but in places mantled clasts or strain shadows porphyroclasts characterized. The strain shadow porphyroclasts are mainly represented in sheared porphyritic granitoids of the Vioolsdrif Intrusive Suite, whereby quartz and k-feldspar crysts are shaped into sigmoidal porphyroclasts, referred as *Sigma-type porphyroclasts* (Fig 4-11 a, b & c).

From the microscopic observation, most of the porphyroclasts are pre-kinematic, moulded by S_4 and often elongated with the long axis parallel to the major shear fabric, however in few thin sections their long axis oriented oblique to S_4 (Fig 4-11 d). The inclusions within the pre-kinematic porphyroclasts are weakly oriented, with a net orientation at an angle to S_4 foliation. The syn-kinematic porphyroclasts are scarce, mostly weakly represented by the recrystallize sigmoidal quartz grain aggregates that lacks a clear porphyroclasts core and wraps around by the anastomosing mica matrix (Fig 4-11 e). The sigmoidal quartz aggregates consist of strain shadow zones that reflects a dextral sense of movement. The post-kinematic porphyroclasts also observed in the microscope, represented by isometric euhedral pyrite (Fig 4-11 g)

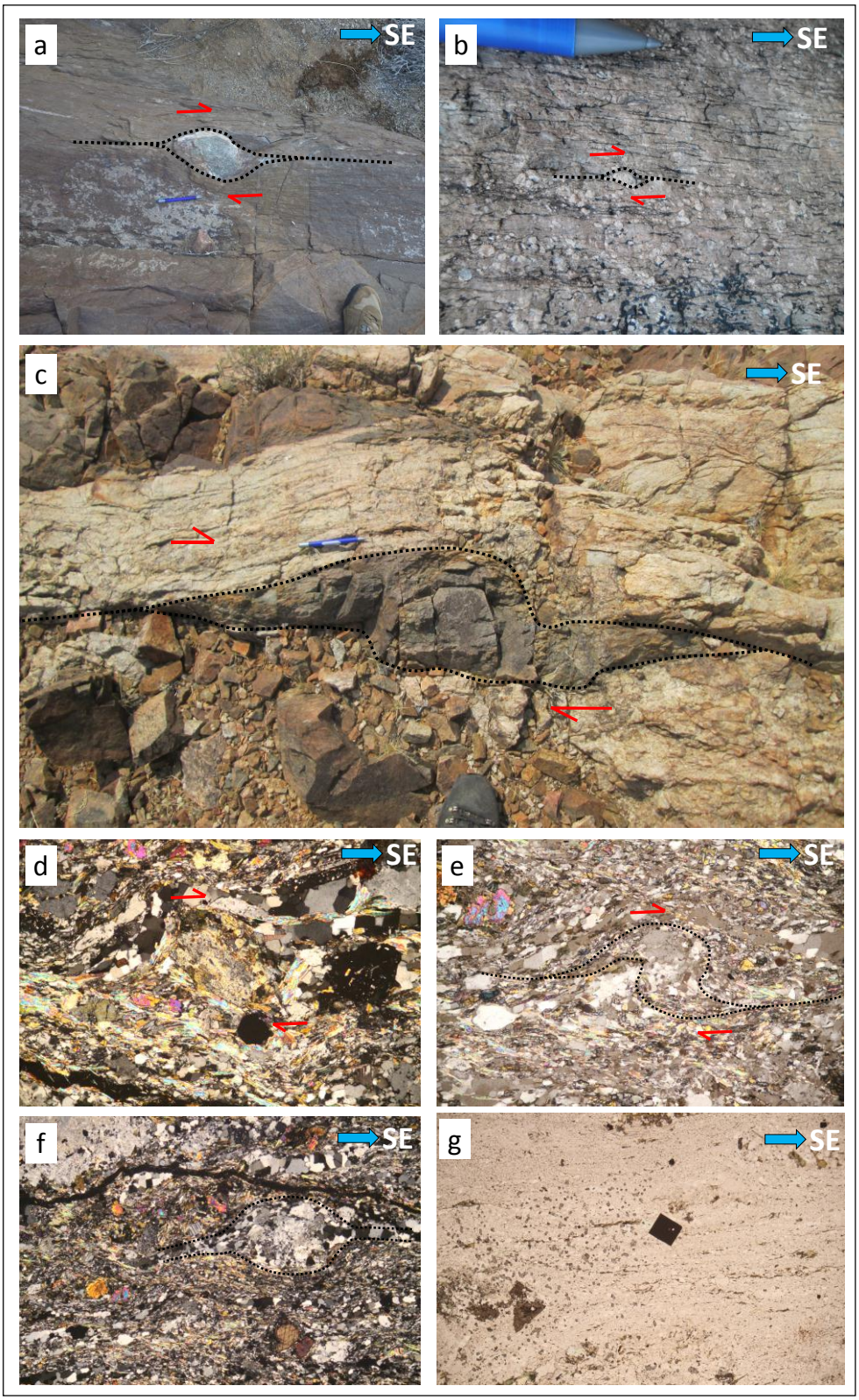

Figure 4- 11: The isometric and anisometric ellipsoidal porphyroclasts within the SPSZS. (a), (b) & (c) sigmoidal quartz and feldspar sigma type-porphyroclast, presenting a dextral sense on movement to the SPSZS, (d) pre-kinematic plagioclase porphyroclast, moulded by anastomosing S_4 foliation that defined by biotite and muscovite, (e) recrystallize sigmoidal quartz grain aggregates, wraps around by the anastomosing mica matrix, (f) isometric /ellipsoidal/ naked recrystallize quartz aggregate and (g) post- kinematic pyrite crystals

4.2.3 Fault Rock Types

In this section, all the fault rocks in the study area represented. The SPSZS consists of several ~200 m wide northwest-southeast striking high strain zones of fault rocks. The shear zones cross-cuts various types of units of the Vioolsdrif Intrusive Suite and Orange River Group. The shearing deformation is characterised by numerous deformation bands across the shear zone, namely; (1) cataclasitic bands and (2) mylonitic bands. The brittle deformation is mainly observed cross-cut the shear fabric event. The brittle zones largely consist of fissile rocks and breccias and mainly occur oblique to either cataclastic or mylonitic zones. The different deformation zones are represented within a single rock unit as well as varying across several types of lithological units (Fig 4-12). The granitoids (VIS) across the shear zone are dominated by fissile and cataclasitic textures, but are also sheared into mylonites in a few isolated cases. Whilst the ORG across the shear zone are overall sheared into mylonites and the felsic extrusive rocks are more often sheared into mylonite to ultramylonite in comparison with the intermediate and mafic rocks of the ORG.

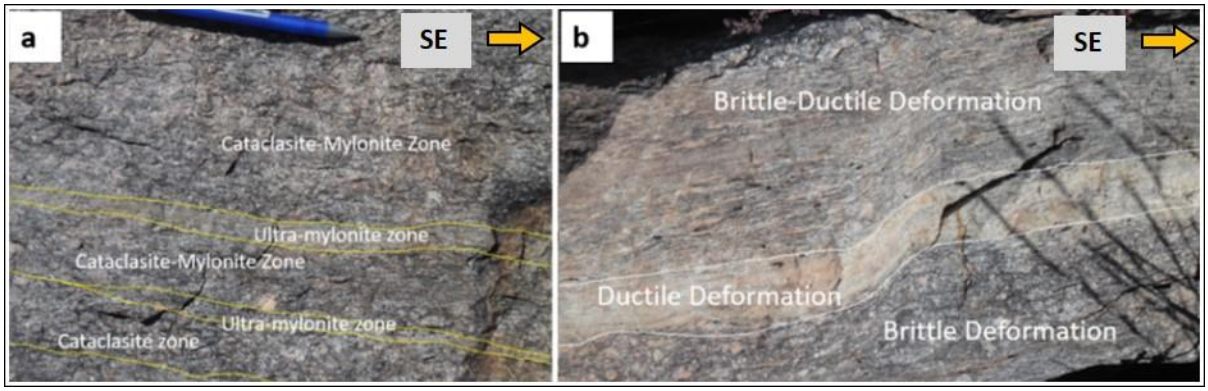

Figure 4-12: Structural variation within the granodiorite of the Goodhouse sub-suite, shown by numerous of interlayered deformation bands of mylonitic and cataclasic textures

4.2.3.1 Mylonites

Mylonites outcrop prominently in the study area and are the main fault rock type used to delineate the extent of the SPSZ. In general, they form fairly parallel, aligned and flattened grains, mineral aggregates and small shear surface, that define the D_4 event shear fabric. Many of the mineral grains in the mylonites, especial quartz grains form very lenticular individual crystals that are wrapped across the relict porphyroclasts (k-feldspar). The mylonites in the study area range from protomylonite to ultramylonite and lithology exerts a strong control over what type of mylonite is developed. The different types of mylonites are described as follows.

(a) Protomylonite

Protomylonite is the common mylonitic fault rock within the SPSZS, derived mainly from the more competent intrusive rocks of the VIS (Fig 4-13). The protomylonites are associated with conchoidal fractures and characterised by either abundant ovoidal k-feldspar or quartz porphyroclasts in a fine grained streaky matrix. The porphyroclasts are mainly k-feldspar, hornblende and ± quartz crystals that experience less grain size reduction and occur as eye-shaped augen or as irregular partially altered porphyroclasts. These porphyroclasts form more than 50% of the protomylonite and are set within the very fine-grained recrystallized quartz, sericite and ± feldspar grains forming a mortar texture. The foliation in the protomylonite is planar, but has a continuous distinctly lensoidal or anastomosing aspect, especially along the relict grains of k-feldspar. The continuous foliation in sheared intrusive rocks, especially in the granodiorite, is defined by flattened, inequant k-feldspar grains and very thin nonpenetrative stretched quartz zones. In many cases, k-feldspar porphyroclasts behave brittley, breaking into mm sized chips that are again oriented parallel to the planar fabric.

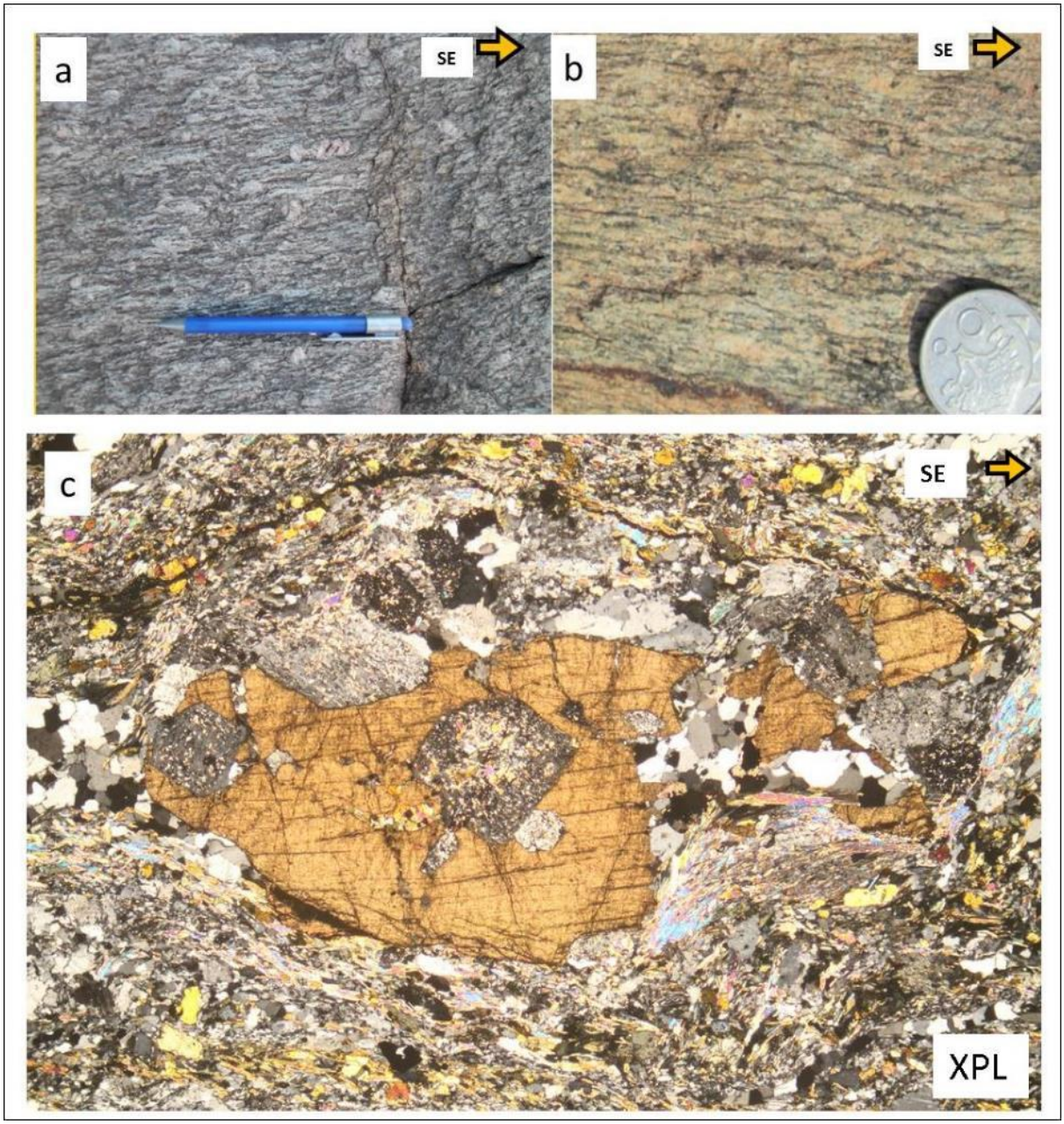

Figure 4-13: (a) & (b) protomylonites derive from porphyritic granodiorites of the Goodhouse sub-suite, associated with mm to cm scale abundant ovoidal k-feldspar porphyroclasts surrounded by anastomosing biotite, (c) photomicrograph (XPL FOV 4.5 mm) of the protomylonite derived from the porphyritic granodiorite, with a large relict hornblende surrounded by the finer protomylonite matrix

(b) Mylonite and Ultramylonite

Rocks within the SPSZS are dominantly sheared into mylonite. The volcanic rocks of the ORG in the SPSZS are highly sheared into mylonite in comparison to VIS rocks that sheared into protomylonite and cataclasite. The mylonites are mainly characterised by a fine grained matrix of either mafic, intermediate or felsic in composition mainly consists of quartz, sericite, feldspar and biotite (Fig 4-

13). The matrix forms 60% up to 85% total volume of the mylonite and associated with few remaining porphyroclasts (k-feldspar, quartz, hornblende, plagioclase, garnet). The common k-feldspar porphyroclasts are more reduced in size than the porphyroclasts observed in the protomylonite and are intensely strained into flattened crystals (Fig 4-14 b). The c-axes of these flattened porphyroclasts are NW-SE striking, parallel to the major shear fabric of the SPSZS.

The ultramylonites are characterised by a fine grained laminated texture, showing banding and micaceous fractures, based on the parental rock composition. The laminated texture is defined by mm to cm thick interlayered leucocratic and mesocratic bands (Fig 4-14 d). The recrystallized smaller grains within the ultramylonite are tightly intergrown and always grow preferentially along the planes of foliation parallel to the direction of the shearing. The k-feldspar porphyroclasts are completely reduced into smaller grains and form less than 8% of the total volume of ultramylonite.

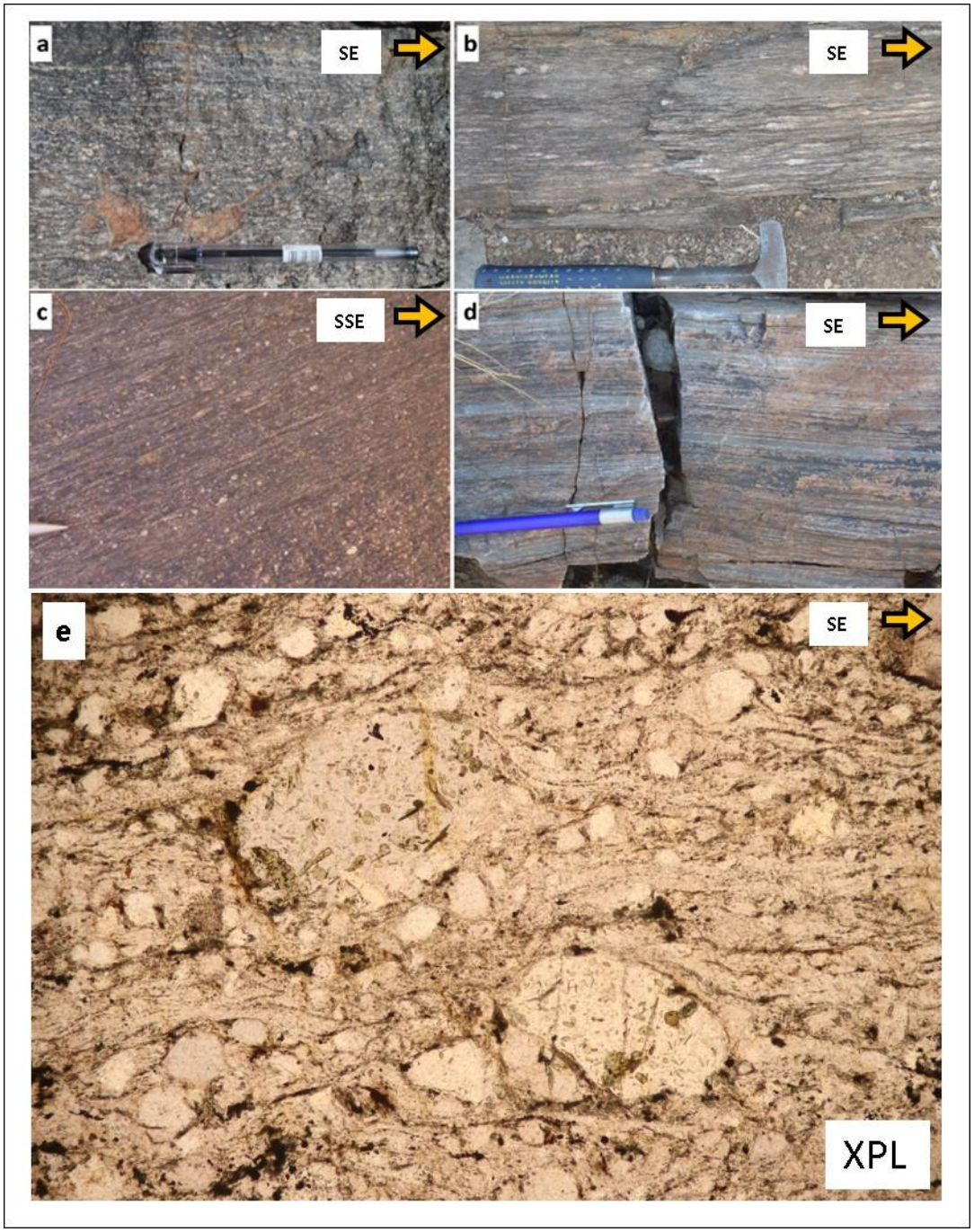

Figure 4-14: Different types of mylonites, ranging from mylonite to ultramylonite. (a) poorly to moderately developed mylonite fabric in the equigranular granodiorite, defined by mm scale deformation zone that alternate with undeformed zones. (b) & (c) strong penetrative mylonite fabric, whereby the k-feldspar megacrysts are grilled into cm scale elongated ellipsoidal porphyroclasts. (d) felsic ultramylonite, probably derived from rhyolite of the ORG rocks. (e) photomicrograph (XPL FOV 4.5 mm) of mylonite intermediate composition.

4.2.3.2 Cataclasites

Shearing in the SPSZSZ partly results in the comminution of rock to a very fine-grained strongly indurated fault rock. This fault rock is mainly characterised by a tiny angular chips of mineral grains (quartz & feldspar) of various size that set within a fine grained to glassy matrix, classified as cataclasites mostly derived primarily from the intrusive rocks of the VIS, specifically from the granodiorite and granite of the Goodhouse and Ramansdrif subsuite respectively (Fig 4- 15 a & b). The intrusive texture is completely disrupted and most of k-feldspar and quartz megacrysts have undergone grain size reduction, forming numerous irregular to sub-rounded cracked fragments. These angular porphyroclasts range from 1 mm to 10 cm in diameter with the maximum size being 25 cm. The mica minerals such biotite in the cataclasite occur as plate elongated thin layers associated with uneven fractures. The matrix in the cataclasite in most places is comminute quartz-feldspar plagioclase and takes up mainly less than 50% of the total volume of the cataclasite, but also ranges from 40 to 90 percentages. The cataclasites within the SPSZS either occur as foliated or non-foliated cataclasite. The foliated cataclasite is the common cataclasitic fault rock within the SPSZS and observed to be well-pronounced in a deformed volcanic rocks than in the deformed intrusive rocks. The foliated cataclasite have a well-developed planar fabric that is subparallel to the major shear fabric. The fabric is mainly defined by oriented mm to cm scale angular k-feldspar and quartz porphyroclasts. The foliated cataclasite is also associated with elongated wire-like opaque minerals and biotite that defining a space but discontinuous foliation. Non-foliated cataclasite is not a common product of the SPSZS. They mainly occur in lower strain area, mostly derived from porphyritic intrusive rocks, characterised by randomly oriented cm scale angular fragments of k-feldspar set within a fine grained matrix of felsic or intermediate composition. The mica minerals within the non-foliated cataclasite forms mm scale sub rounded to angular shaped non-oriented aggregates that forms spotted texture.

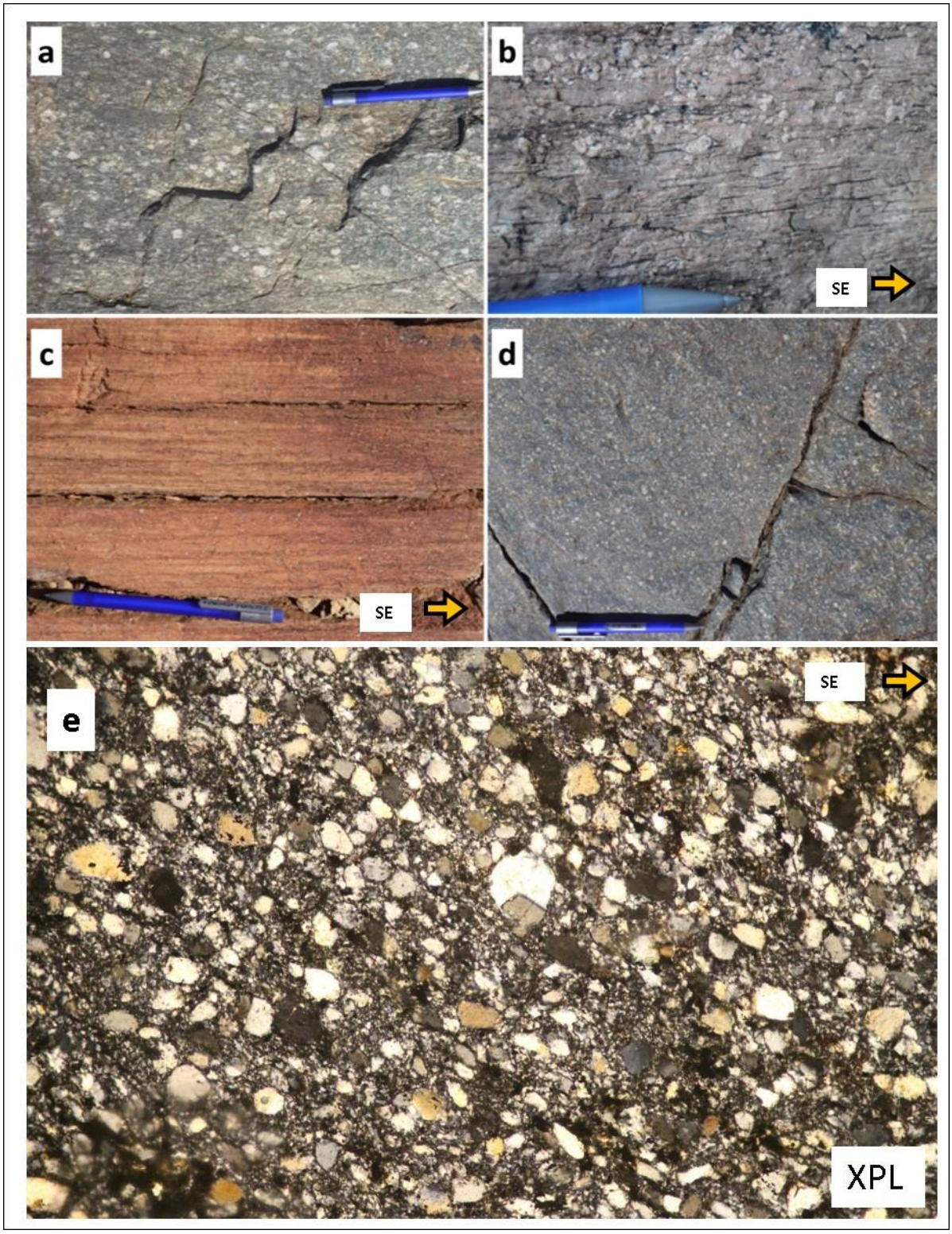

Figure 4-15: Photograph of foliated and non-foliated cataclasites taken along the Sperlingsputs Shear Zone System. (a) non-foliated cataclasite consists of various size of angular clasts of k-feldspar within a medium to fine grained medium grey matrix, (b) foliated cataclasite associated with elongated ellipsoidal k-feldspar porphyroclasts, that defined the foliation, (c) & (d) foliated cataclasite, whereby the k-feldspar porphyroclasts are comminute into mm scale clasts.(e) Photomicrograph (XPL FOV 4.5 mm) foliated cataclasite.

4.2.3.3 Breccia

In the study area, fault breccia is a common fault rock, mostly observed within the NNE trending brittle structures, that is oblique to SPSZS and cross-cut all the major fabrics within the study area, however, in places they are observed forming centimetre to metre scale layers arranged parallel to the brittle-ductile layers (mylonite and cataclasite). The breccia fault rocks that are line parallel to brittle-ductile structures are characterised by angular fragments mostly of the mylonite or cataclasite set in a very fine-grained variable brownish to dark grey in colour matrix. The fragments in most cases form the 70% of the rock volume and ranges from 1 mm to 30 cm in diameter and they are randomly oriented with their net orientation sub parallel to the major shear fabric of the SPSZS (Fig 4-16).

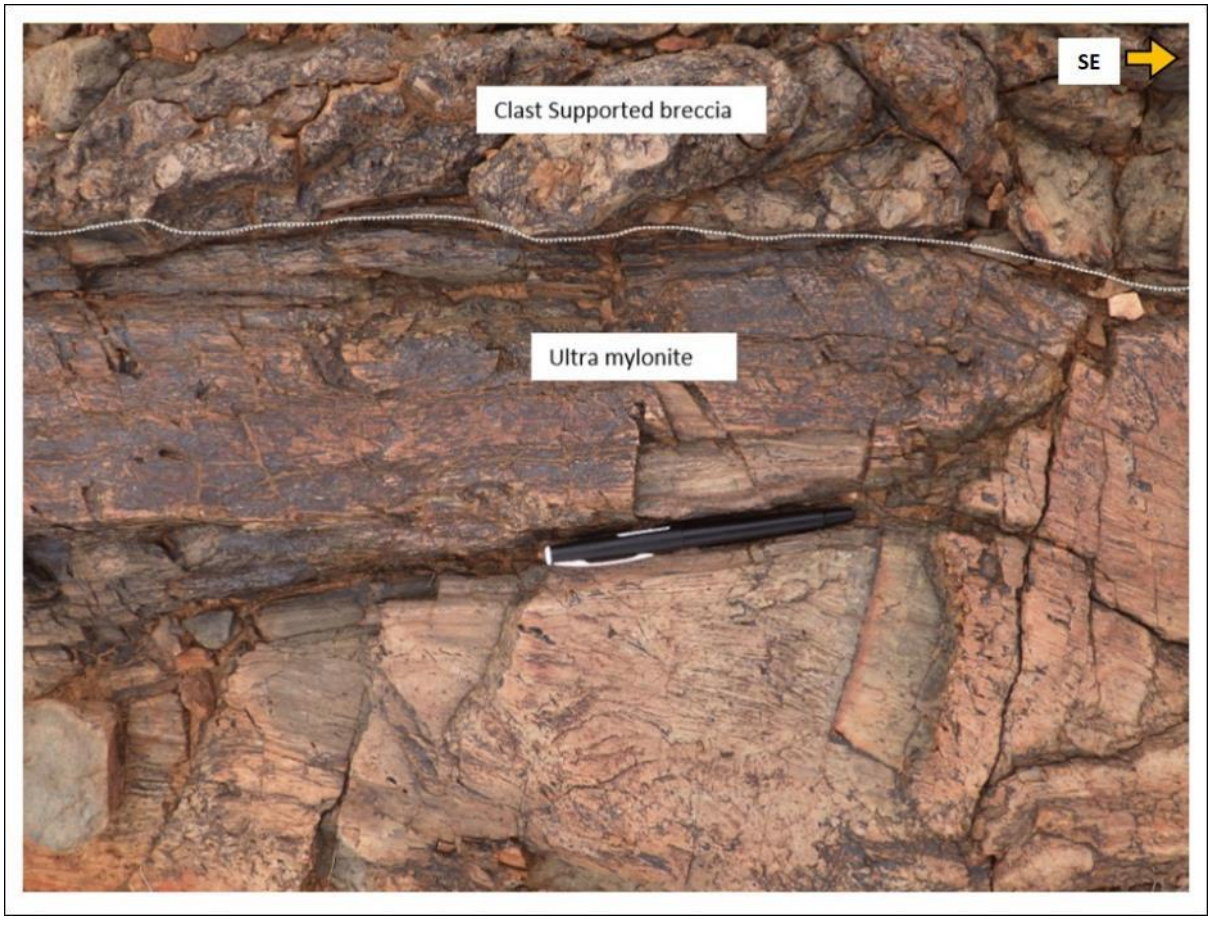

Figure 4-16: The centimetre-wide clasts supported breccia fault rock along the Frontal Sperlingsputs Shear Zone, that interlayering with the ultra mylonite.

The common NNE trending fault breccias are characterised by mm to cm scale angular fragments of the wall rocks that set in a finer grained matrix (Fig 4-17). The fragments are randomly oriented and are either of volcanic and granitoid of the ORG and VIS respectively. These fault breccias are either

matrix supported breccia or clast supported breccia. The matrix supported breccia is not common and is typically located at the centre of the fault structure. The clasts size mainly smaller less than 5 cm in diameter and they are usually rounded to angular in shape. The clasts supported breccia is common and distributed throughout the fault structure, but generally dominate the margin part of the fault structure. These fault breccia contains fragments that are sub rounded to angular in shape and are variable in size, range from 1 cm to 1 m. The fragments are crowded within a sparse fine-grained matrix in between and in places, occur with narrow mm-sized calcite-lined veins. The calcite veins are less than 2 cm and randomly oriented, with a net orientation parallel to the major trending direction of the fault structure.

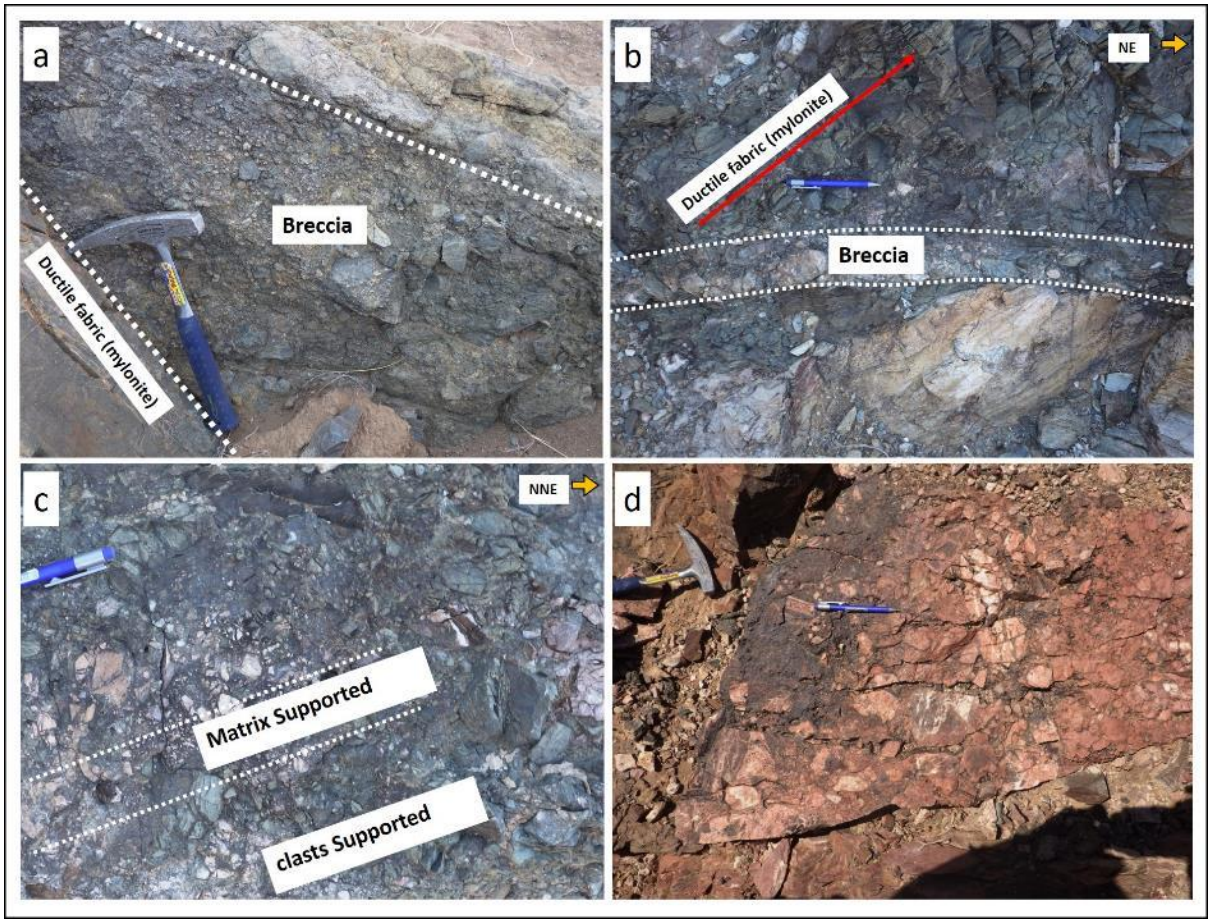

Figure 4-17: Various types of fault breccia within the NNE trending fault structure. (a) clast supported fault breccia obliqui to the ductile-brittle mylonite to cataclasite fabric, (b) fault breccia cross-cut the shear fabric, (c) the position of clast and matrix supported fault breccia in the fault structure, (d) clast supported fault breccia along the major NNE trending fault within the Haib prospecting area.

4.3 DISTRIBUTION OF STRUCTURAL ELEMENTS

4.3.1 Introduction

Individual shear zones across the SPSZS appear to have different significance. For example, one shear zone within the SPSZSZ represents the tectonic boundary between the two domains, while in places, the SPSZS is preferentially partitioned into interconnecting shear zones centred within the Vioolsdrif Domain, neither representing the tectonic boundary between domains or provinces. For this reason, the Sperlingsputs Shear Zone System is further divided into three major interconnecting shear zones, based on their role in the Richtersveld Magmatic Arc (RMA), that mainly controlled by the nucleation factors, often responsible for their present position. The shear zones of the SPSZS are mainly within the volcanic rocks of the ORG and anastomosing around the intrusive bodies of the VIS. However, the north most shear zone of the SPSZS is along the pre-existing tectonic boundary between the two domains (Fig 4-18). Therefore, the significant of the SPSZS in the RMA is not the same across the study area. In addition, the subdivision presented here is also constructed on the basis of shearing intensity, geographically location and structural variation (different arrangements and distribution of structural elements) across the shear system. The SPSZS is dominantly WNW-ESE trending, however in the western part of the study area; the SPSZS is trending NNW directions. All the above-mentioned differences in the SPSZS result in the separation of the SPSZS into three sub-divisions that are discussed in more detail below. The three sub-divisions of the SPSZS are as follow; *Southwest Sperlingsputs Shear Zones (SW-SPSZS)*, *Central Sperlingsputs Shear Zones (C-SPSZS)* and *Frontal Sperlingsputs Shear Zone (F-SPSZS)* (Fig 4-18). Because D2 and D4 event fabrics and their associated structural elements are dominant within these three shear zones, the focus of this section will be on the distribution of these structural elements.

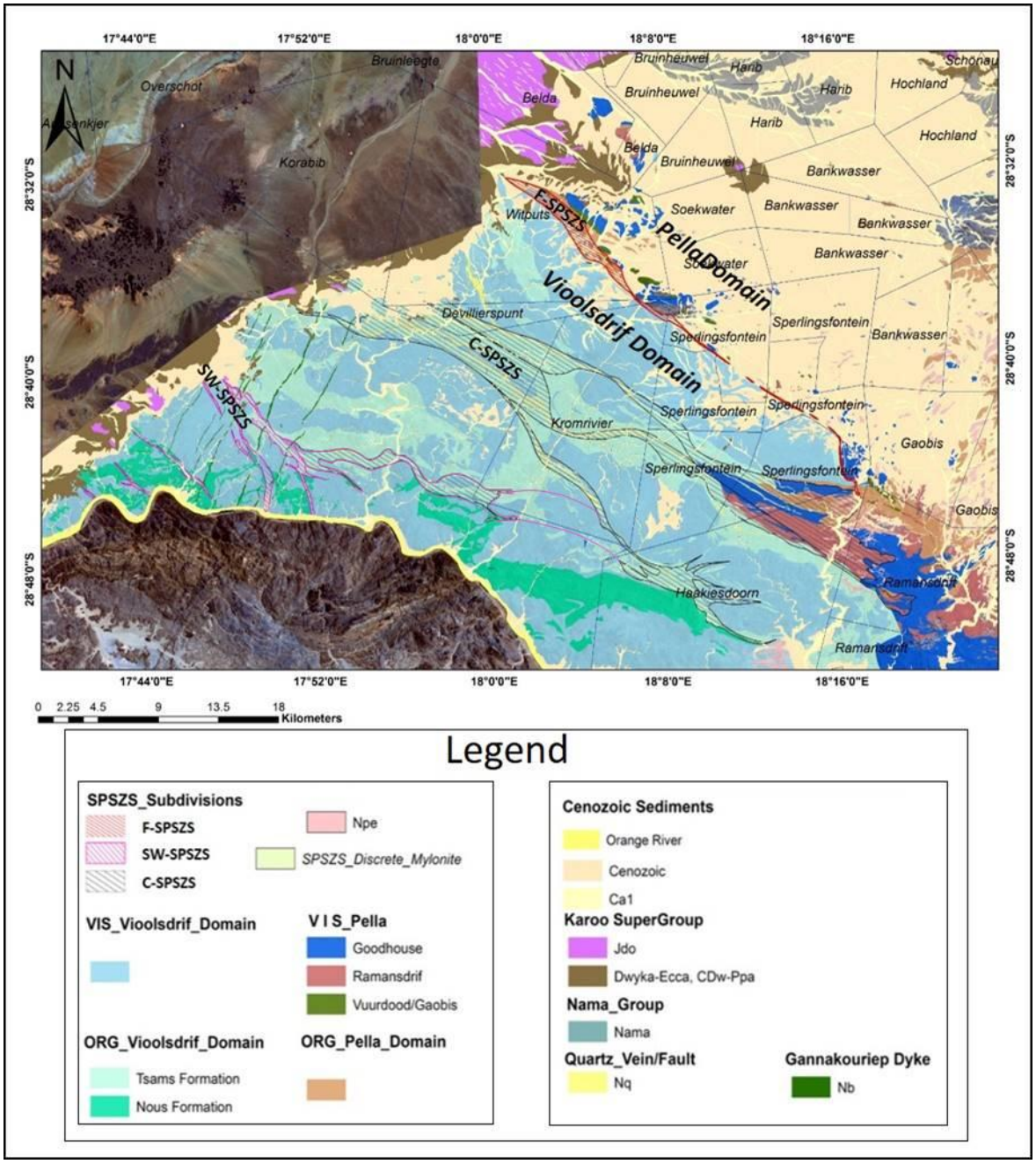

Figure 4-18: Simplified structural geological of the study area produced during this study, showing the distribution of three difference types sub-division of the SPSZS

4.3.2 South west Sperlingsputs Shear Zone

The SW-SPSZS consists of mainly two major shear zones, located in the vicinity of Haib, some 15 to 18 km east of the Noordoewer Namibian border. The shear zones in the west extend across the Orange River into South Africa, forming a set of interconnecting continuous shear zones. In the east, the same shear zones converge and merge further north with the Central Sperlingsputs shear zones to form a kilometre-wide WNW trending shear zone (Fig 4-19). The SW-SPSZS is 50 to 100 m wide and has a NNW – striking direction rather than the predominantly WNW to NW trending direction of the SPSZS. These shear zones have a habit of being wider within the extrusive rocks and narrower within the massive granitoids (Fig 4-19). The SW-SPSZ is characterised by metre-scale wide cataclasitic to mylonitic rock units. The cataclasitic texture dominates the SW-SPSZ and is mainly assigned to sheared granitoids of the Goodhouse and Ramansdrif of the VIS. The mylonite texture is more often associated with sheared extrusive rocks of the ORG.

Shear zone planes are steeply dipping and have a moderately to steeply plunging lineation, that dominantly plunges toward the southeast and northwest. However, in places the lineation is observed to be sub horizontal to horizontal as discussed in section 4.2.1.5. Numerous shear sense indicators, such as inclined close folds (Fig 4-7 d), suggest a significant vertical component to the shear zones with an overall top to the southeast sense of movement. Where the lineation is sub-horizontal, the dextral sense of movement predominates, defined by C/S fabric (Fig 4-9 b) and sigma type porphyroclasts (Fig 4-11 a) and this is consistent with the overall Sperlingsputs Shear Zone System. However, limited asymmetric folds (Fig 4-7 c) and C/S fabrics (Fig 4-9 d), which are randomly distributed, display a sinistral sense of movement.

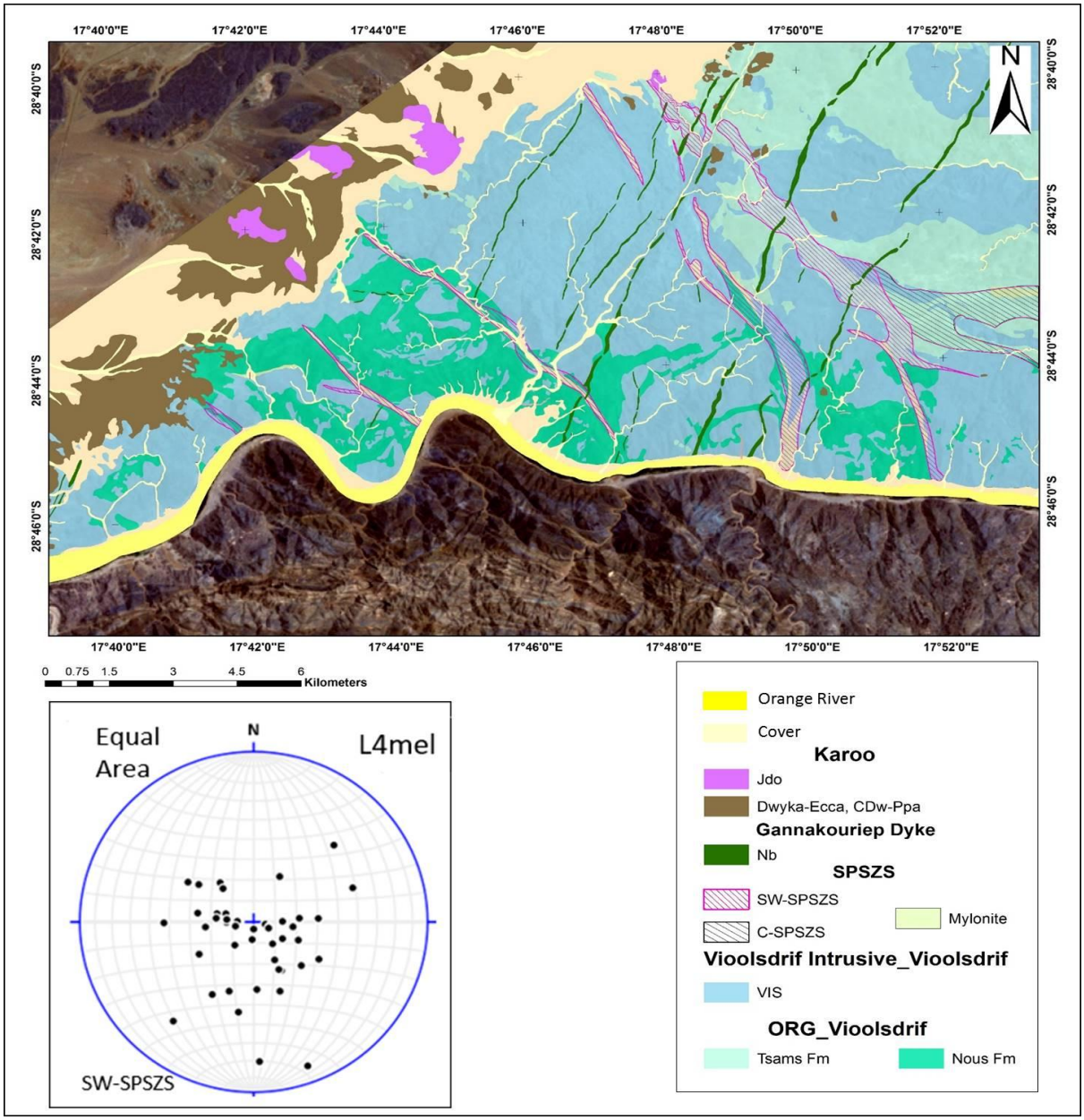

Figure 4-19: The geological map and L_{4mel} stereo plot of the SW-SPSZS, showing the extent and width variation of the shear structure in relation with intrusive and extrusive rocks. The L_{4mel} stereo plot demonstrate a dominant down dip lineation along the shear planes.

4.2.3 Central Sperlingsputs Shear Zone

The C-SPSZ is a group of anastomosing shear zones that are at the centre of the study area, and extend from the Sperlingsfontein (Sperlingsputs) farm across the Kromrivier farm into the Korabib farm (Fig 4-20). The Central Sperlingsputs shear zone varies considerably in width from approximately 50 m to 7 km wide, although locally it consists of discontinuous packages of sheared rocks in excess of 100 m wide. On the Kromrivier farm, these shear zones branch and diverge

outwards. The southern branch extends further west parallel to the Orange River and connects with the SW-SPSZS (Fig 4-20), whilst the north branch extends further northwest and lines up with other C-SPSZ to form the widest km-scale (7 km) single shear zone. These shear zones characterised by packages of interlayered felsic, intermediate and mafic rocks (mainly volcanic rocks) sheared into cataclasite, phyllonite, mylonite and ultramylonite. In comparison to the other two shear zone systems (F-SPSZS and SW-SPSZS), mylonite and ultramylonite are more densely developed in this shear zone. This shear zone is also characterised by the widest interlayered continuous discrete felsic and intermediate ultramylonites and mylonite of the three shear zone systems. The sheared rock units within the C-SPSZS dominantly wrap around the 100 m to 1 km wide rigid bodies of granitoids although rarely these rigid bodies may also contain volcanic rocks. However, the shear zones are dominantly located within the volcanic rocks rather than along the margins of the volcanic rocks and in the granitoid bodies (Fig 4-20). The C-SPSZ has a WNW-ESE striking direction, although in the vicinity of rigid bodies, the foliation tends to have a NNW to NNE striking direction. Stereonet plots indicate NW-SE as an average trending direction. The shear plane is steeper in comparison to the F-SPSZS planes and variably steeply dipping towards the NNE and SSW instead of the persistent northeasterly dip direction of the F-SPSZS. The orientation of the mineral elongation lineations along the shear zones is quite variable, primarily moderate-shallow plunging, and dominantly plunging toward the southeast. The lineation along the margin of the rigid bodies is mostly a down-dip lineation, whereas away from the rigid bodies, the lineation is dominantly shallow plugging (Fig 4-5). The dominant shallowly plunging mineral lineation, along with various shear sense indicators, such as fragmented porphyroclasts (Fig 4-8), sigma and delta type porphyroclasts (Fig 4-11 c, d), implies a substantial sub-horizontal component with an overall dextral sense of movement. However, the Riedel shear zones independently shows a sinistral sense of movement in the C-SPSZS (Fig 4-10).

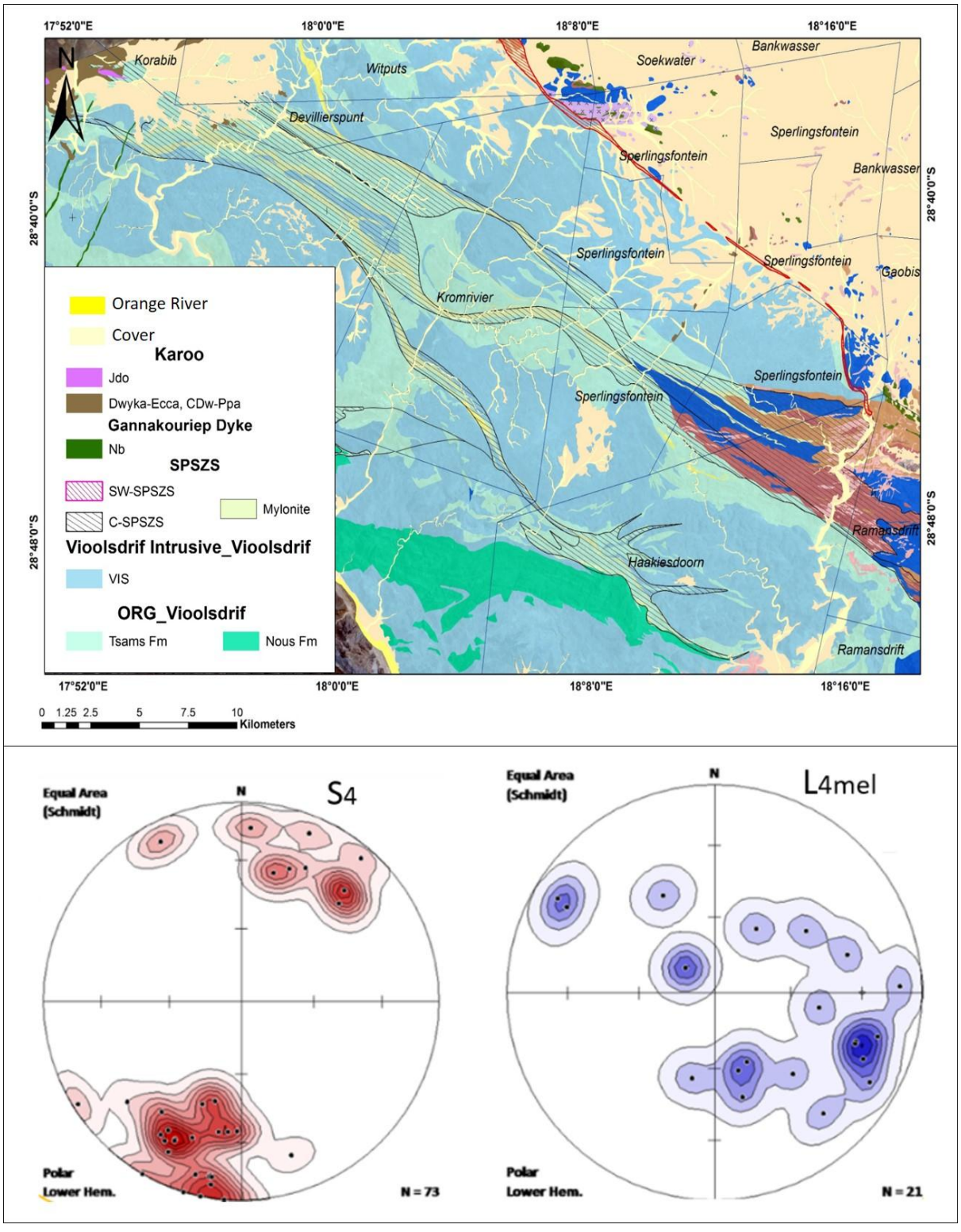

Figure 4-20: Structural geological map together with stereo net plots of the structural readings taken from the Central Sperlingsputs Shear Zone System. (S_4) foliation pole stereo plot, showing the dominate NE steeply dipping shear plane and (L_{4mel}) mineral elongation lineation stereo plot, displaying the governing sub-horizontal SE plunging lineation.

4.3.4 Frontal Sperlingsputs Shear Zone

The F-SPSZ is a single shear zone of the SPSZS that coincides with the SNF, which in this area appears to be a tectonic boundary between the lower grade greenschist-facies Vioolsdrif Domain and the high grade amphibolite-facies Pella Domain. The F-SPSZ is characterised by NW-SE striking shear planes that are moderately to steeply dipping toward the NE direction and represented by discontinuous cataclasitic, phyllonitic to mylonitic rocks. In this location there are a lot of sediments that represent Palaeozoic and quaternary deposits and these obscure the location of the F-SPSZS in many places. However, the extent of this distinct linear feature (F-SPSZ) beneath the younger sediments was further delineated using geophysical data such us aeromagnetic images. The distinct magnetic linear feature further west on the Witsputs farm, is cut off by NNE trending D_5 structures and shows dextral displacement on the order of several metres.

The shear zone is moderately to steeply dipping (50˚ - 80˚) with an overall NW-SE striking direction (Figure 4-21). The shear planes are predominately dipping toward the NE and less commonly to the SW. Linear features (mainly mineral lineations) are dominantly moderately down dip plunging lineations with a predominately southeast plunging direction. However, a horizontal lineation was also present at a few outcrops (Fig 4-4 c). The two lineations (down-dip and horizontal) together with different types of shear sense indicators, suggest a different senses of movement within the F-SPSZS. The C/S fabrics (Fig 4-9 c) suggested a significant vertical component to the shear zone with an overall top to the southwest (reverse fault) movement. The asymmetric folds and other recrystallize sigmoidal quartz grain aggregates (Fig 4-7 a, b and Fig 4-11 e), suggest a dextral sense of movement.

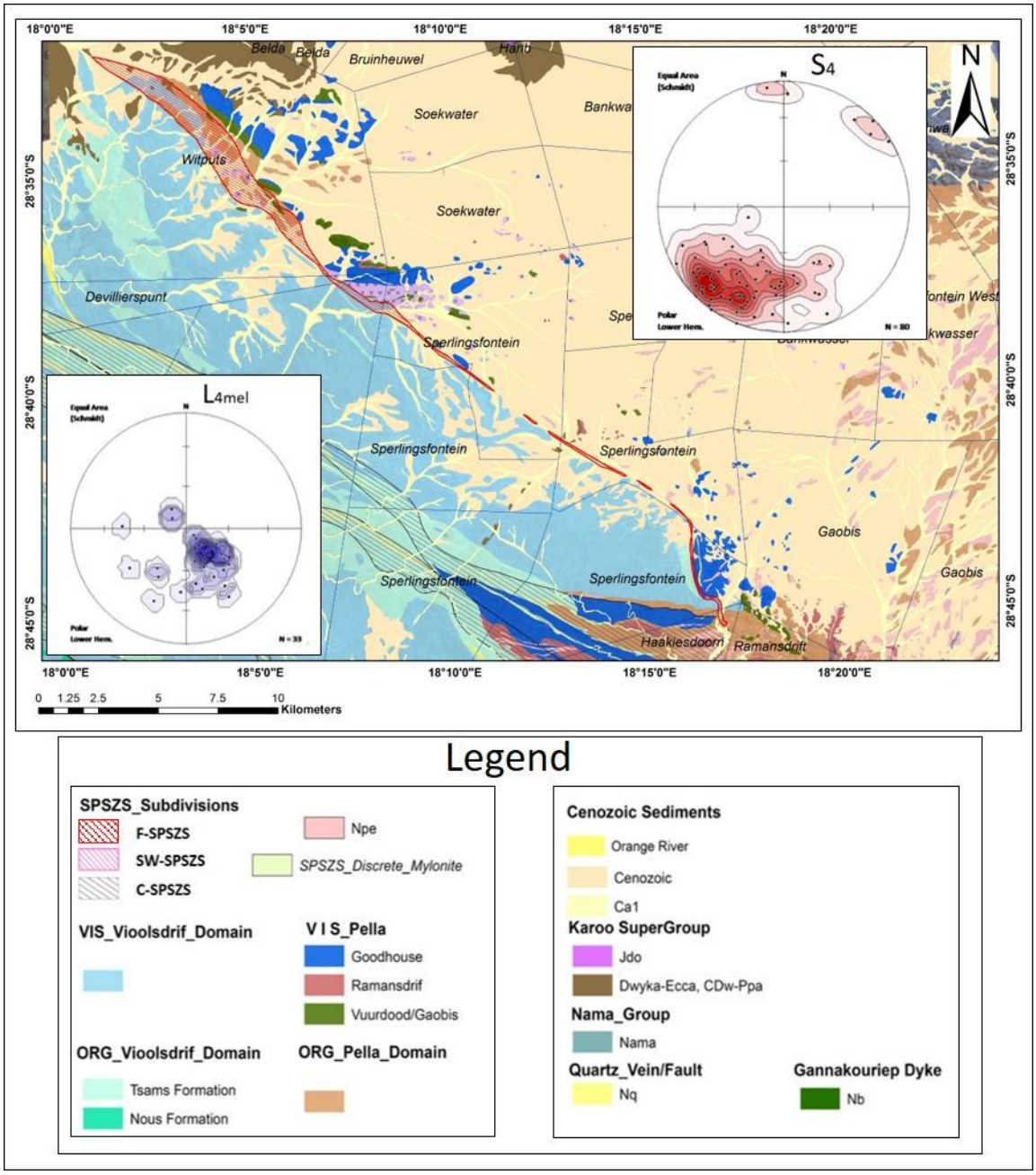

Figure 4-21: Structural geological map and stereo net plot of both foliation and lineation measurements taken from the Frontal Sperlingsputs Shear Zone. (S_4) foliation pole stereo net plot, dominated by a moderately NE dipping shear planes, (L_{4mel}) mineral elongation lineation stereo net plot showing the leading moderately SE plunging lineation.

4.3.5 The Southern Namaqua Front (SNF) in the Sperlingsputs Farm

The SNF in this study is classified as a transpositional tectonic boundary between the lower grade greenschist facies rocks of the Vioolsdrif Domain and the higher grade amphibolite facies rocks of the Pella Domain. The boundary in the current study area is poorly defined. The SNF coincides with the F-SPSZS, and is now mainly represented by the F-SPSZS (Fig 4-22). The boundary is located where the homogeneous gneissic foliation (S_2) and penetrative mineral lineation (L_2) starts to develop in the weakly deformed lower greenschist rock units and is marked by a fusion of fault rock types (cataclasite, mylonite, ultra- mylonite) that sit between the two domains (Vioolsdrif and Pella Domains). For this reason, the SNF is completely reworked by the F-SPSZS and the existing kinematic analysis of the SNF is not sufficient. However, the geometry of the SNF clearly correlates with the present position of gneissic rocks in relation to non-gneissic rock units which more or less coincides with the position of the F-SPSZS. Therefore, in the study area, the SNF has a NW-SE principal striking direction with moderately to shallow dipping shear planes, and a dominant dip toward the northeast. In the south east of the study area, the SNF appears to be narrower, < 1 km, and is dextrally dragged into the lower grade Vioolsdrif domain by the C-SPSZS (Fig 4-22).

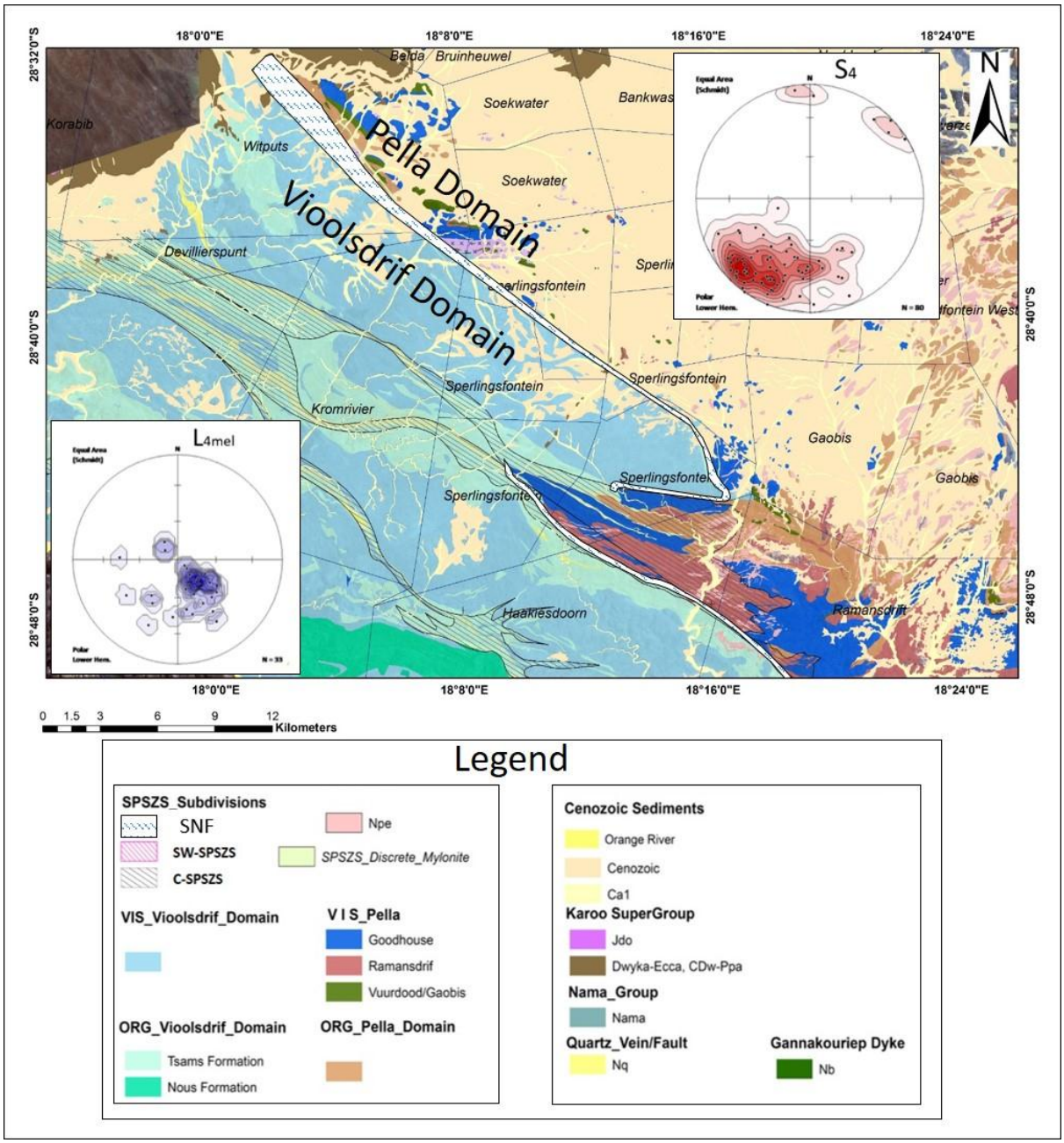

Figure 4- 22: Structural geological map and stereo net plot of both foliation and lineation measurements taken along the SNF that separate the high grade gneissic Pella Domain from the lower grade weakly deformed Vioolsdrif Domain.

4.3.6 Summary

The structural grain of the study area dominated by the SPSZS that subdivided into three major shear zones. The SW-SPSZS forms a set of NNW trending interconnecting continuous shear zones and primary dominated by cataclasitic texture. While, the C-SPSZS is the widest shear zone within the SPSZS, trending WNW direction and dominated by mylonitic texture. The F-SPSZ is characterised

by NW-SE striking shear planes that are moderately to steeply dipping toward the NE direction and represented by discontinuous cataclasitic, phyllonitic to mylonitic rocks. Both shear zones display a dextral sense movement, however, at places, especially along the margin of rigid bodies, the shear zones tend to be dominated by the vertical movement. The F-SPSZS coincides with the SNF, which in this area a tectonic boundary between the lower grade greenschist-facies Vioolsdrif Domain and the high grade amphibolite-facies Pella Domain (Fig 4-23).

4. 4 PEGMATITES DISTRIBUTION IN THE SPSZS

Pegmatites in the SPSZS occur along the shear zones, and can be traced for more than 500 m in strike, however the tracing along the strike becomes more difficult where the pegmatite forms sharp lateral termination and discontinuity. They are mainly aligned parallel to the shear foliation and in places are intruding oblique to the fabric and cross-cut the major mylonitic fabric of the SPSZS (Fig 4-23 a, b & c). Outside the SPSZS, the pegmatites are general randomly oriented with a WNW striking net direction and they occur as either irregular patches or discontinuous regular bodies within the ORG volcanism and VIS intrusive bodies. The pegmatites mostly outside the SPSZS preserved their contacts relationship with the wall rocks, which is characterised by the compositional and textural variation across. Mainly they form a cut-off sharp contact with the surrounding rocks although; in the Haib area, the pegmatites form gradational contact with the late-alkaline granites.

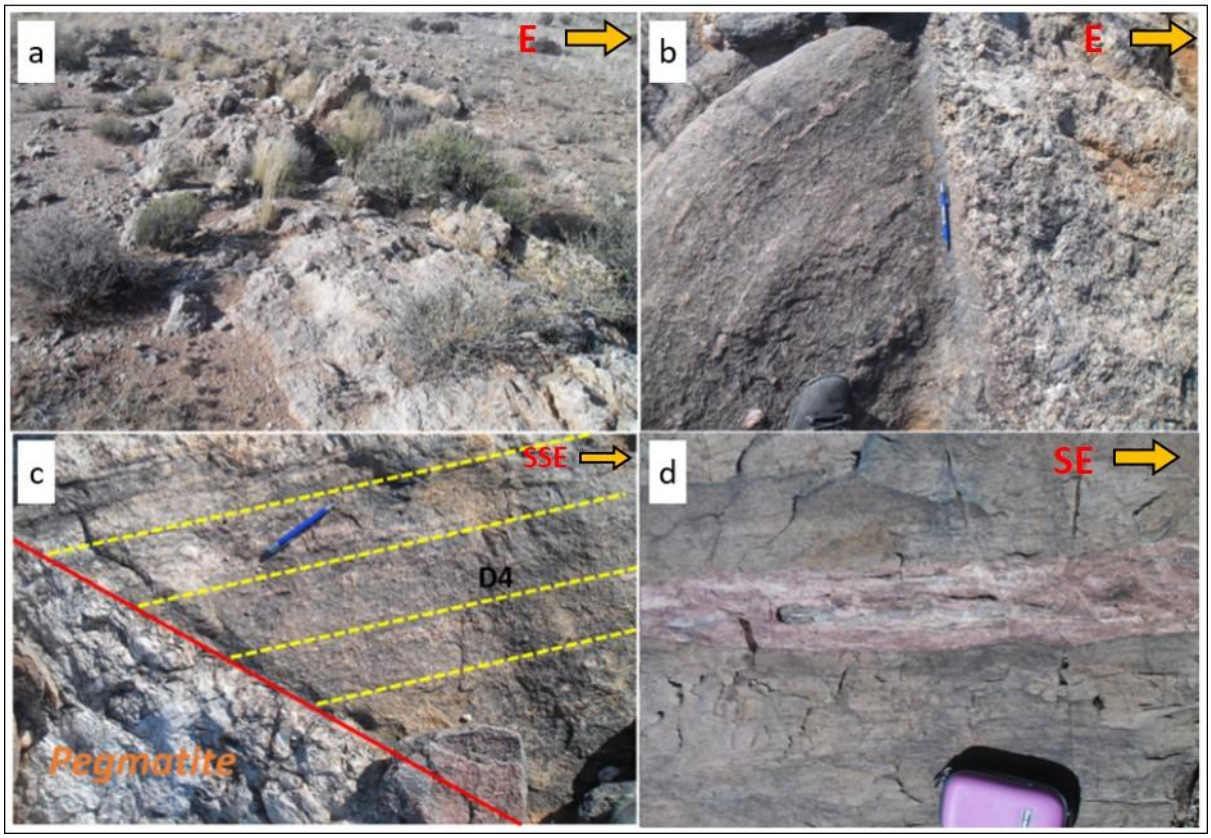

Figure 4-23: Widely distributed compositional homogeneous sheet-like pegmatites in the SPSZS. (a) meter wide fissile pegmatite align parallel to D_4. (b) & (c) Cross-cutting intrusion relationship between the un deformed/sheared pegmatites and D_4 (C-SSPSZS) in the Sperlingsputs farm. (d) the distinct D_4 mylonitic fabric along the pegmatite

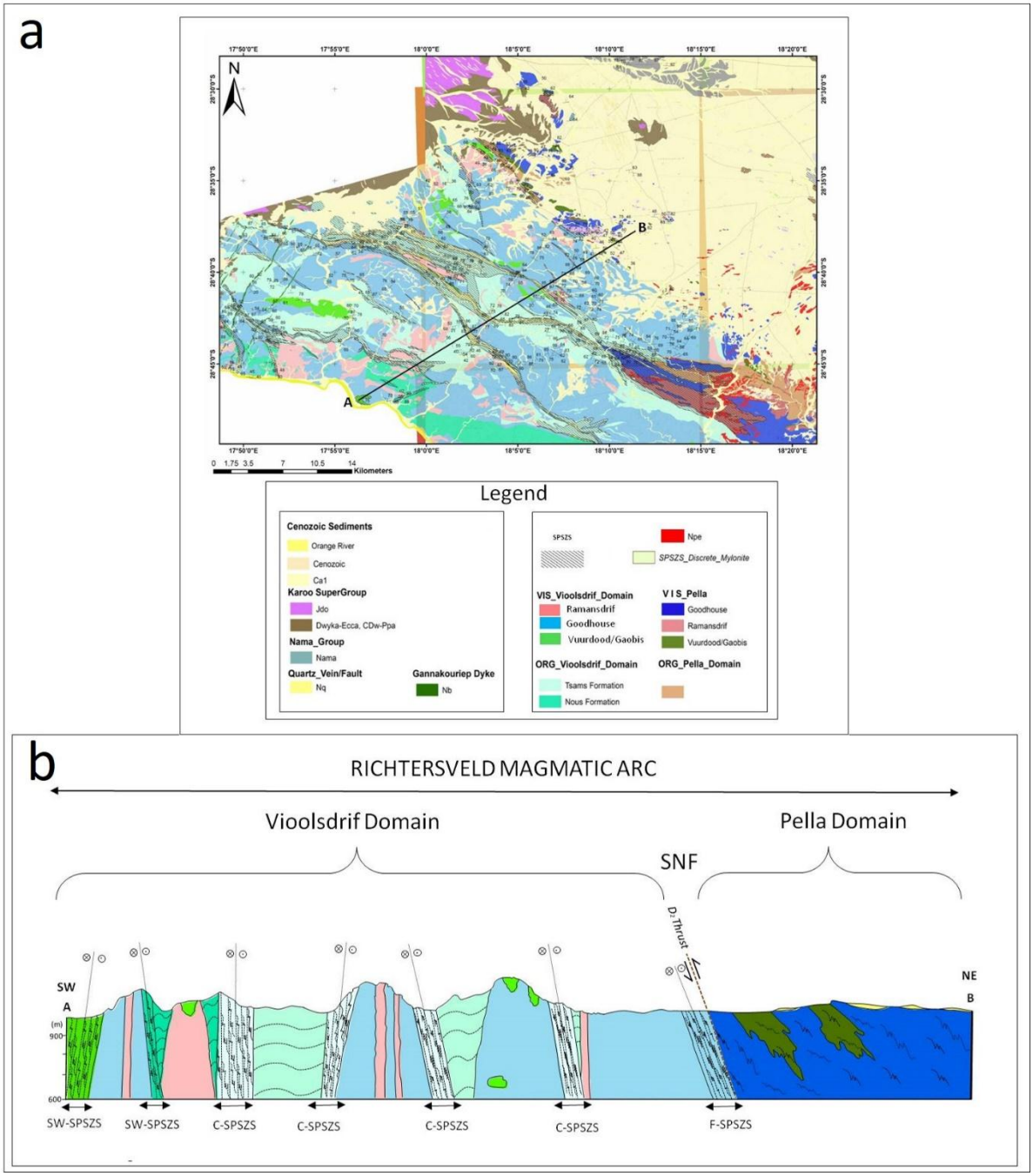

Figure 4-23: (a) Structural geological map of the study area, showing the overall lateral extent and geometry of the three subdivision of the SPSZS, (b) schematic cross-section drawn along the profile A-B, showing the nature of the SPSZS. The cross-section also shows the relationship between the F-SPSZS and the SNF.

CHAPTER 5: DISCUSSION

5.1 HOST ROCK LITHOSTRATIGRAPHIC COMPARISONS AND CORRELATIONS

5.1.1 The Haib Subgroup Lithostratigraphy

The Orange River Group within the low grade Vioolsdrif Domain has a simple stratigraphy, subdivided into four main units: (1) the De hoop Subgroup; (2) the Haib Subgroup; (3) the Hom Subgroup; and (4) the Rosyntjieberg Formation (Beukes, 1973; Blignault, 1974, 1977; Reid, 1977; Ritter, 1977, 1980; SACS, 1980). The Haib Subgroup has a variable composition, ranging from basalt to rhyolite. Previous work by Blignault, (1977) further divided the Haib Subgroup into two formations, (1) Tsams Formation on the north and (2) Nous Formation on south (Fig 3-2). The formations were distinguished base on the proportion of felsic to intermediate and mafic lavas. The Tsams formation is leucocratic to mesocratic at outcrop range and dominated by felsic lavas. While the Nous Formation is more melanocratic at outcrop scale and governed by mafic volcanic rocks (Blignault, 1977).

This study focuses on compositional, textural and structural variations along the Tsams and Nous formations to further clarify the differences between the two formations. Where the volcanic rocks are not fragmented or sheared, textures and structures such as volcanic flows, shrinkage cracks, and irregular to polygonal columnar jointing are homogeneously distributed across the two formations. The compositional variation observed within the Haib Subgroup is clearly defined by the proportion of felsic to intermediate-mafic volcanic rocks. In the south of the study area, almost along the Orange River (Fig 3-2), basaltic andesite and andesite dominate the volcanic group, and are interlayered with rhyolite and dacite, but at less than 50 m scale units. In the north of the study area, along the Sperlingsputs and Kromrivier farms, rhyolite and dacite dominate the volcanic group. In summary, the volcanic rocks in the Haib Subgroup, texturally and structurally, are homogeneously distributed, but have vary compositionally within the Vioolsdrif Domain.

Most of the volcanic rock units within the Vioolsdrif Domain are highly fragmented and sheared, and therefore there were no conclusive features to define the original stratigraphic order of the Haib Subgroup volcanic rocks in the study area. Therefore, this study suggests keeping the established stratigraphy of the Haib Subgroup (Blignault and Reid, 1977), based on compositional variation and geographical location.

5.1.2 Relationship between the Vioolsdrif and Pella domain

The study area sits within the Richtersveld Subprovince of the NMP, referred as the Richtersveld Magmatic Arc (RMA) in this study (Macey et al., 2015). The RMA in the study area is made up of volcanic of the Orange River Group and voluminous plutonic rocks of Vioolsdrif Suite that have variable texture, strain, metamorphic grade and composition. The southern part of the study area comprises weakly deformed rocks that preserved Paleoproterozoic crust of greenschist facies known as the Vioolsdrif Domain (e.g. Blignault,1977; Macey et al., 2015). While the northern part of the study area contains the highly deformed amphibolite facies gneisses known as the Pella Domain gneisses and these rocks are stratigraphic equivalent to the Vioolsdrif Domain rocks (e.g. Blignault, 1977; Reid, 1977,1997; Reid et al., 1987).

In the study area, the greenschist facies mineral assemblage dominates the Vioolsdrif domain. The intermediate rocks mainly comprises of weakly oriented igneous hornblende, biotite, plagioclase and quartz. Muscovite (±sericite), epidote and chlorite occur as secondary minerals; occur as a retrograde mineral after plagioclase, biotite and/or hornblende. While the Pella domain dominated by amphibolite mineral assemblage. The gneissic foliation is defined by the alignment of flattened recrystalline strained polygonal quartz and feldspar aggregates (display a strong undulose extinction and twinning), dark brown biotite, aligned igneous hornblende, randomly oriented overprinting hornblende that typically represented by large, unaltered poikiloblastic crystals with a well-developed prismatic cleavage. The amphibolite-facies mineral assemblage is also well preserved in pelitic rocks, consisting of cordierite, sillimanite, garnet, biotite and quartz.

Previous and recent works on geochronology and geochemical studies by Blignault and Reid (1977), Reid et al., (1987), Cilliers (1989), Minnaar (2012) and Macey et al., (2014), correlate the age group and chemical variations of the ORG and VIS rocks between Vioolsdrif and Pella Domain. In the Pella Domain, the meta-volcanic rocks and orthogneisses show near-identical major element compositions and trends to the magmatic rocks of the Vioolsdrif Domain and the REE compositions of the ORG volcanic rocks and Vioolsdrif Suite define similar, coherent patterns on chondrite-normalized plots in both domains (Macey et al., 2015).

Furthermore, Macey et al., (2015) dated and correlated the two meta-quartzites from Pella and Vioolsdrif Domains. The two meta-quartzites provide similar concordant ages in a range of 2040 ma to 1914 ma. Again the same study was done in the VIS on the Goodhouse Subsuite. In the interior of

the Vioolsdrif Domain, the Gaarseep granodiorite provide concordant age 1879 ± 7 ma and the Gaobis diorite orthogneiss from the Pella Domain shows over a similar concordant age of 1835 ± 8 Ma. All the above suggested that the two domains are made up of same rock units that have deformed at different metamorphic grade.

In summary, the Vioolsdrif Domain deformation is limited to D_1 deformation, Late-Namaqua (D_4) shear zone and Brittle D_5 event (Gariep Orogence event after Macey et al., 2015). While the Pella Domain preserved a penetrative gneissic structures of the Namaqua Orogeny, that probably obliterated the D_1 event structures. Both Domains subsequently subjected to the Late-Namaqua transcurrent D_4 shear zone (1000 – 960 Ma after Toogood, 1976; Melcher et al., 2008; Lambert, 2013), that reoriented and mylonitised the pre-existing structure of both D_1 and D_2 events. However, in the study area, the Pella Domain only subjected to D_4 on the eastern edge of the study whereby the gneissic rocks were sheared and dextrally dragged into the lower grade Vioolsdrif domain by C-SPSZS (Fig 3-1).

5.2 CHARACTERISATION OF THE SPSZS

5.2.1 General Features of the SPSZS

The SPSZS is characterised by a northwest-southeast trending anastomosing arrays of interconnected structures, which have undergone heterogeneous deformation. The shear zone system is defined by high strain zones of variable fault rocks, namely; ultramylonite, protomylonite, cataclasites and ± breccia. The deformation mechanism within the SPSZS ranges from brittle to brittle-ductile deformation, with the brittle-ductile structures dominating the shearing system. These structures were at all scales, from sub-microscopic to a wide zone of intense deformation, that are tens of meters wide. The SPSZS is defined by a low grade greenschist facies mineral assemblages, consisting of chlorite, sericite, plagioclase, muscovite and biotite. In the field the SPSZS is also defined by a sub-vertical to vertical shear planes, that associated with either down-dip lineation or sub-horizontal lineation. The down-dip lineation is observed mainly along the margins of rigid bodies, whilst the sub-horizontal lineations are mostly away from the rigid bodies (Fig 4-5). Several shear sense indicators (see section 4.2.2) demonstrated that the SPSZS is dominated by a dextral sense of movement. However, limited kinematic indicators, such as Riedel shear zones, asymmetric folds, delta and stigma type porphyroclasts, that are randomly distributed display a sinistral sense of movement in the SPSZS. In addition, some of the individual shear zones across the SPSZS play a

significant role in the RMA. The F-SPSZS reworked the SNF and now marks the tectonic boundary between the Vioolsdrif and Pella Domains in the study area.

5.2.2 Development of the sub-vertical down-dip lineation

The SPSZS is associated with two types of lineation, a sub-horizontal lineation and a sub-vertical to down dip lineation. The development of the sub-vertical lineation in a large scale dextral SPSZS is ambiguous on the net sense of movement of the shear zone at large, since it doesn't correlate with the simple shear components. Lineations are known to be useful in ascertaining the history of deformation (Josep et al., 2001). However, numerous studies suggest that the interpretation of the significance of lineations in rocks is not straightforward (Piazolo and Passchier, 2002). Some lineations are mirrors to strain axes or kinematic trajectories and others appear to have little kinematic significance. For example in a transpressional regime, the orientation of stretching lineation development sometimes may not necessarily correlate with the direction of simple shear component of deformation (Tikoff and Greene, 1997) and this implies that the lineation can be either parallel or perpendicular to the follow direction of the shear zone.

The SPSZS is a dextral large-scale anastomosing array of shear zones in the Namaqua Sector of the Namaqua Metamorphic Province. These shear zones are dominated by a lateral movement and are associated in places with a down-dip lineation. The vertical lineation in the SPSZS is perpendicular to the major flow direction of the shear zone. This is common in shear zones and might suggest that the dominant lineation formed is not a stretching lineation (Tikoff and Greene, 1997). However, the development of a vertical lineation may still imply a kinematic trajectory. The stereo net plot of the L_4 lineation, shows that there is a systematic variation in the plunge of lineations towards the rigid bodies (Fig 4-5). A dominate vertical lineation along the margin of rigid bodies in a lateral sense movement shear zone require an independent interpretation. Therefore, vertical lineations interpreted to be due to a localised vertical component to the shear zone along the rigid bodies.

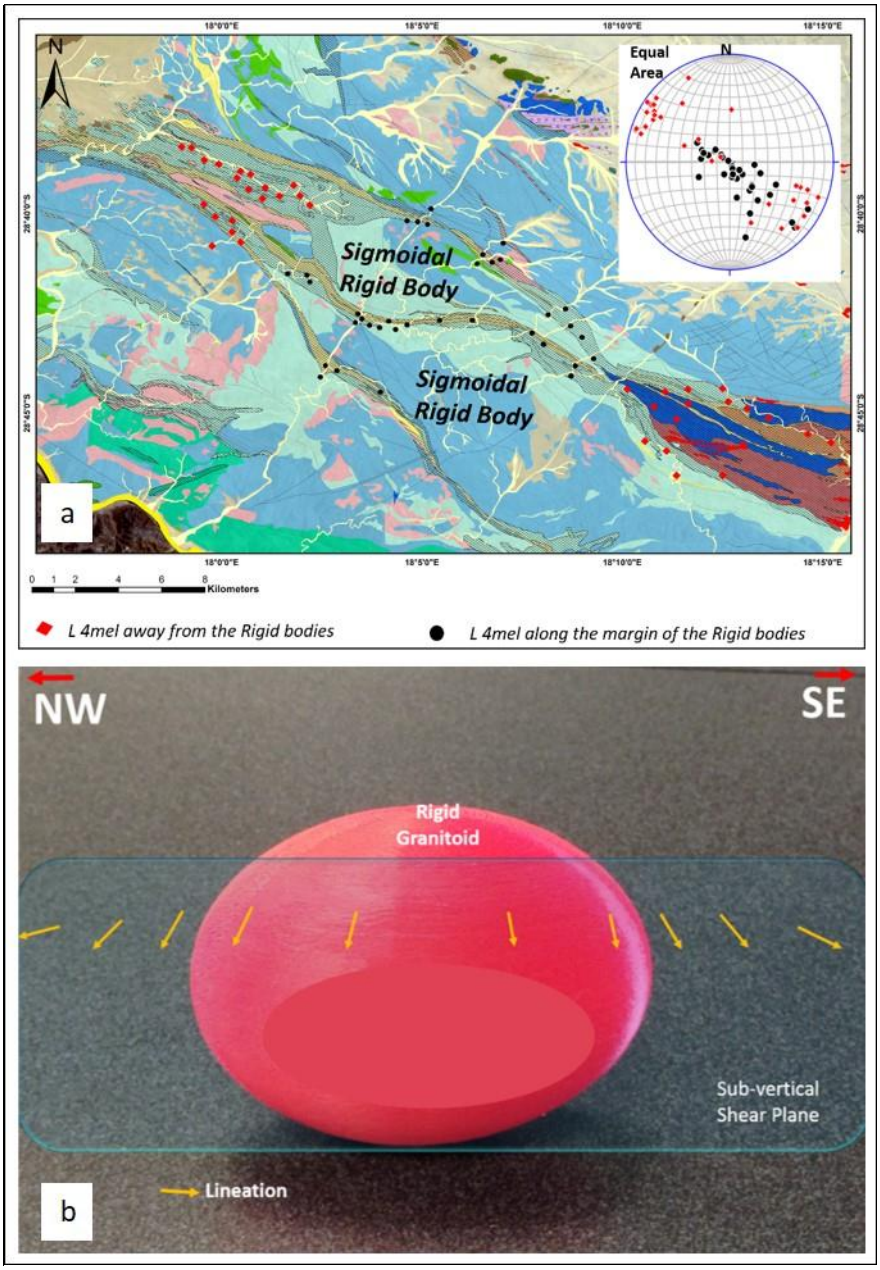

Figure 5 - 1: Different types of penetrative mineral elongation lineation; (a) Structural readings (L_{4mel}) plots on the 1: 50 000 scale geological map, showing a systematic variation of mineral lineation in relation with the rigid bodies, (b) a sketch demonstrating the change of lineation toward and along the rigid bodies.

5.2.3 Timing of the Sperlingsputs Shear Zone System

The timing of the SPSZS is based on the geometry and behaviour of pegmatites within and toward the shear zone system. The timing is further based on the relationship between the SPSZS and other Late-Namaqua Shearing (Marshall Rocks-Pofadder Shear Zone) and their significant to the orientation of the pre-existing penetrative D_2 fabric between the two shear zone system. The F-

SPSZS cross-cut and truncate the D_2 penetrative gneissic fabric, thus post-dates the D_2 (~1200 to 1100 ma) fabrics.

The SPSZS is associated with large sheared and undeformed pegmatite intrusions like other Late-Namaqua D_4 shear zones, such as Marshall Rocks-Pofadder shear zone (Lambert, 2013) and Eureka shear zone (Angombe, 2016). The relationship between the pegmatites and SPSZS is clear at outcrop scale. The pegmatites observed were sheared into mylonite and cataclasite along the SPSZS, however in places, they clearly cross-cut the mylonitic fabric of the SPSZS (Fig 3-15). This may suggest that the pegmatite intruded syn- to post-shearing. Furthermore, at regional scale, pegmatites observed coincide with some of the km-scale C/S fabrics that are located between SPSZS and MRPSZ. The C/S fabrics were clearly delineated from the geophysical data such us aeromagnetic images (Fig 5-2). Furthermore, the SPSZS shares a similar geometry, metamorphic grade and structural elements with the MRPSZ and Eureka Shear Zones. All the above-mentioned features are implying the SPSZS and MRPSZ formed from the same tectonic event.

The MRPSZ is also associated with a series of pegmatite intrusions that are largely sheared into ultra-mylonite and in places sharply cross-cut the MRPSZ mylonitic fabric (Lambert, 2013 and Macey et al., 2015). Geochronological studies on the pegmatite intrusions along the MRPSZ by Lambert (2013) gave concordant ages in the range of 1005-970 Ma. Since the SPSZS shares similar features with the MRPSZ, the interpretation is that the two were formed from the same tectonic event, hence the SPSZS is interpreted to occur around 1005-970 Ma.

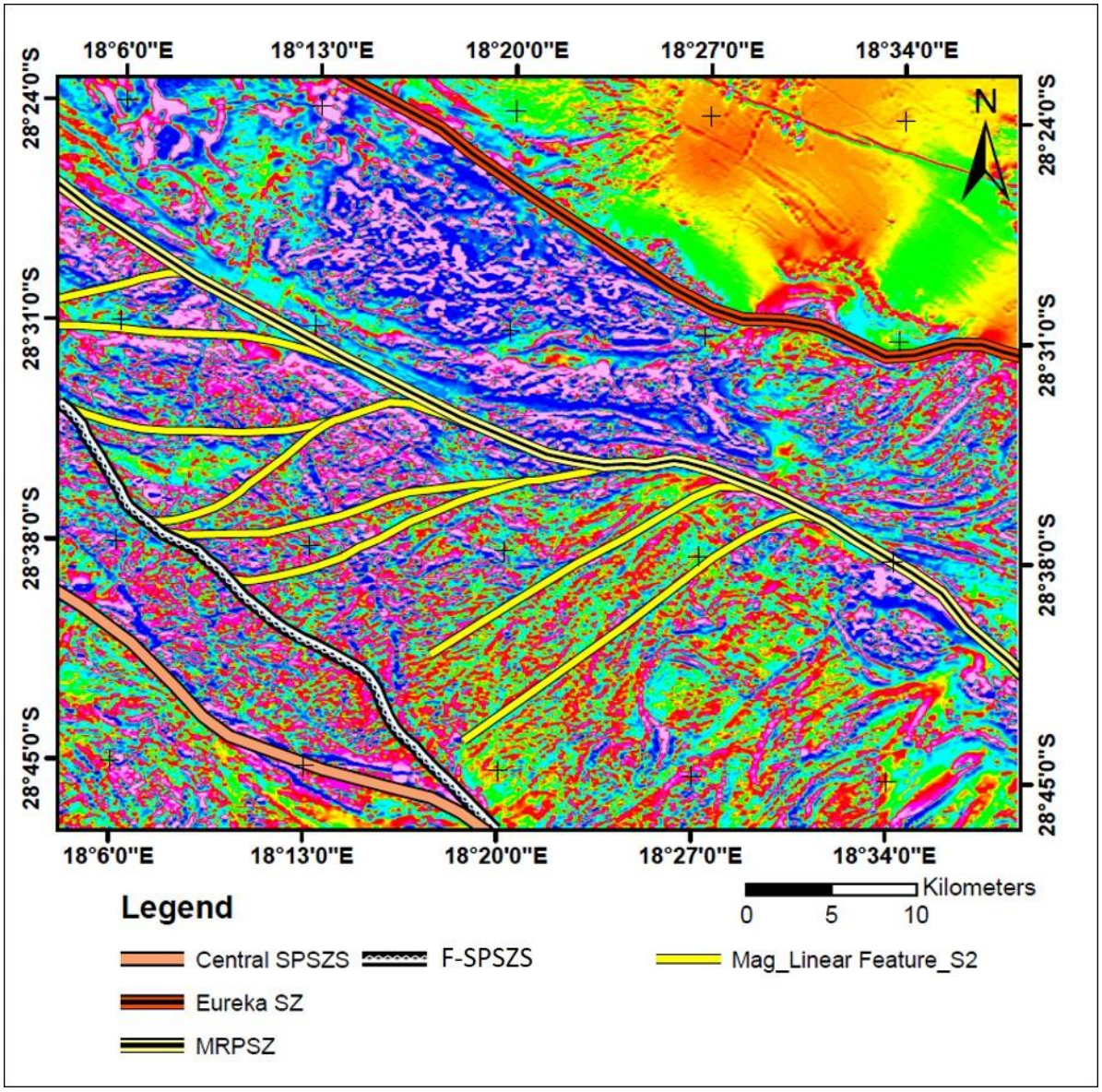

Figure 5 -2: the Kilometre scale C/S fabric formed between the SPSZS, MRPSZ and ESZ, delineationed from the Aeromagnetic image.

5.3 WHAT DETERMINED THE POSITION OF THE SPSZS?

5.3.1 The role of lithology

The SPSZS have successions of different types of fault rocks, that reflects a combinations of factors such as strain rate, presence of fluids, pressure, temperature and rock character (Tullis and Yund, 1980, Schmid and Handy, 1991). Based on field and microscopic observation the formation of fault rock types is lithologically controlled.

The shearing intensity is not homogeneously distributed across the different lithological units. The shearing is mainly present within the fine-grained volcanic rocks of the ORG, however in some places, the granitoids and gabbroic units of the VIS are also partially sheared. In many instances, the volcanic rocks form continuous metre wide discrete mylonite-ultramylonite zones (Fig 4-20), centred by cataclasite zone that are either derived from volcanic rocks or granitoids. Feldspar porphyroclasts of the granitoids are not completely sheared, but rather form centimetre scale elongated ellipsoidal porphyroclasts. The ultramylonites are mainly felsic in composition therefore, the ultramylonite zones are interpreted mainly to be derived from felsic equivalents of the ORG i.e. rhyolite or dacitic-rhyolite, instead of the corresponding Ramansdrif Granite of the VIS. The intermediate rocks (andesite and dacite) of the ORG in the SPSZS are largely sheared into either cataclasite or mylonite, but dominantly cataclasite. However due to scarce mafic volcanic rocks such as basalts in the study area, it was difficult to draw a firm conclusion since there is no sufficient information to determine their overriding texture in the SPSZS. The VIS mainly occurs as rigid bodies in SPSZS, but when sheared is dominantly cataclasite.

In conclusion, the differences in the yield strength of rocks led to formation of various types of fault rocks within the SPSZS. Least competent rocks, such as rhyolite, dacitic-rhyolite are intensely sheared, whilst the most competent rocks such as granitoids are weakly sheared into cataclasite.

5.3.2 Role of Pre-existing Structural Anisotropies

The SPSZS are preferentially located in the Orange River Group volcanic belt and along the pre-existing Southern Namaqua Front (SNF). The volcanic rocks are widely sheared, in comparison to Vioolsdrif granitoids and form continuous anastomosing mylonitic zones of about 10 to 100 metres wide. The granitoids in the SPSZS are dominated by fissile texture while the volcanic are extensively sheared into mylonites and cataclasites.

More often, the SPSZS step-over and wrap around the granitoid margins. Such mode of shearing, led to the anastomosing feature of the SPSZS. Generally, extrusive rocks are less competent compared to the intrusive rocks, therefore the SPSZS is widely distributed in the ORG volcanic than in the VIS granitoids. This is also proven by the elongated k-feldspar porphyroclast fragments, within the granitoids that show a domino-type fragmentation (Fig 4-8). Such simple fragmentation tends to dominate when the porphyroclasts suffered a small internal strain, hence at higher strain the mosaic fragmentation takes over (Duebendorfer and Christensen 1998; Babaie and La Tour 1998).

Therefore, pre-existing structures and rheology are concluded to be the main factors responsible for the nucleation of the SPSZS and the forming of fault rock types.

5.4 IMPACT OF D2 VS D4 EVENTS

5.4.1 Assignment of fault rocks to deformation events

The study area has been affected by at least four deformation events namely; D_1, D_2, D_4 and D_5. The D_1 deformation event is characterised by a weakly developed fabric within the lower grade Vioolsdrif Domain and completely transposed into penetrative gneissic texture in Pella Domain. This deformation event consists of open to isoclinal folds that are associated with a weakly developed cleavage. The event did not show any evidence of shearing; therefore, there is no fault rock of this episode within the study area. According to Joubert (1986), D_2 deformation episode represents the main deformation in the NMP making it the main fabric forming event within the NMP and is associated with thrusting event that juxtapose units of different metamorphic grades (Clifford et al., 1995). The thrust structure is mainly represented by various types fault rocks, ranging from cataclasite to ultra mylonite (Macey et al., 2015). In the study area, the D_2 fabrics are restricted to Pella Domain and the thrust event is represented by the juxtaposition of high-grade amphibolite facies Pella Domain rocks onto the lower grade greenschist facies of Vioolsdrif rocks along the Southern Namaqua Front that could be associated with fault rocks. However, the SNF in the study area is completely reworked by the SPSZS (D_4), which is the late-shearing event of the Namaqua Orogeny (Macey et al., 2014). Therefore, in this study area there is no fault rock assigned to D_2 deformation event. The D_4 event dominated the study area and is restricted to the Vioolsdrif Domain. This event is characterised by a lower greenschist facies grade and a NW trending-brittle-ductile shear fabric, represented by various types of fault rocks, such as cataclasite, mylonite, phyllonite, ultramylonite and ± fault breccia (Blignault, 1977 and Macey et al., 2015). Most of the fault rocks observed within the study area match with the main features of the D_4 shearing event such as, cataclasite, mylonite and some of the breccia. The D_4 fault breccia are those aligned parallel to the shear fabric and are in contact or interlayered with the cataclasite and mylonite layers within the shear zone . In addition, D_4 fault breccias are Dmainly consist of clasts of cataclasite and mylonite in most cases. All the fault breccias that are oblique to the D_4 shear fabric or cross-cut the shear fabric are assigned to D_5 deformation episode, which is known to be a Neoproterozoic brittle deformation episode (Macey et al., 2013).

5.5 THE RELATIONSHIP BETWEEN THE SNF AND SPSZS

Previous work by Blignault (1977) and Macey et al., (2014), pronounced the Southern Namaqua Front equivalent to Late-Namaqua Shear zones, such as Eureka Shear Zone (Macey et al., 2015 and Moses, 2016) and Marshall Rocks-Pofadder Shear Zone (Joubert, 1975; Lambert, 2013). However, the SNF in this study classified as a transposition tectonic boundary between the Vioolsdrif and Pella Domains, that was responsible for the juxtaposition of high-grade amphibolite facies rocks onto the lower grade greenschist facies rocks. In contrast, the SPSZS is a Late-Namaqua shear zones, characterised by the anastomosing arrays of interconnecting shear zones that dominated by lateral dextral sense of movement.

The high grade gneissic rock observed in the Pella Domain are stratigraphic equivalents of the lower grade rocks of the Vioolsdrif domain. This implies that the rocks within the two domains formed at either different pressure or different temperature conditions. The low-grade metamorphism (Vioolsdrif rocks) took place at shallow depths, whilst the high-grade metamorphism (Pella rocks) took place at deeper depths. Thus, the two domains primarily form at different depths, but currently in the study area the two domains occur adjacent to each other; Vioolsdrif Domain on the southwest and Pella domain on the northeast. The tectonic contact between the Pella and Vioolsdrif Domains coincides with the Frontal Sperlingsputs Shear Zone, which is known to have a horizontal sense of movement.

The above suggest that the Pella Domain is thrusted upward from the deep depth to shallow depth. Therefore, in this study the SNF is interpreted to be the transposition tectonic boundary, where by the transportation of allochthonous Pella rocks took place. Since the SPSZS is a dextral sense of movement shear system, it is unlikley that it has a significant contribution to the current position of the Pella Domain rocks. Previous work by Joubert (1986) described the D_2 deformation phase as the main fabric-forming event in the NMC, associated with regional thrusting and crustal shortening around 1200 Ma. The thrusting is responsible for juxtaposition of units of differing metamorphic grades (the Okiepean episode, after Clifford et al., 1995; LFROT after Macey et al., 2014). Thus this study suggests that the Southern Namaqua Front is equivalent to D_2 a regional thrust such as the Lower Fish River Thrust Zone, which is the tectonic boundary between Pella and Kakamas Domain, and interpreted to occur around 1200 Ma. In addition to this, Lambert (2013) and Moses (2016) described the LFROTZ's basal thrust, reworked by the Late-Namaqua shear zones (D_4), the Eureka Shear Zone and Marshall Rocks-Pofadder Shear Zone respectively. A similar mechanism occurred in

the current study area, whereby the Southern Namaqua Front was completely reworked by the Frontal Sperlingsputs Shear Zone as a zone of existence of pre-existing anisotropies.

5.6 THE RELATIONSHIP BETWEEN THE SPSZS, MRPSZ AND EUREKA SHEAR ZONE

The three shear zone systems share similar geological features; although, they play different roles in the evolution the NMC. Both shear zone systems contain similar fault rocks, such as cataclasite, phyllonite, mylonite and ultra mylonite, indicating a combination of brittle and ductile deformation mechanism (Davis and Reynolds, 1996). The ESZ dominated by a cataclasite brittle shear fabric (Angombe, 2016), whilst, MRPSZ is broadly governed by the mylonite ductile shear fabric (Lambert, 2013; Macey et al., 2015). The SPSZS characterised by the network of metre to kilometre wide interconnecting shear zones, which are either comprise by mylonite or cataclasite shear fabrics. The three shear zone systems (SPSZS, MRPSZ, and ESZ) are trending from NW to SE and WNW to ESE. This implies that they share similar principal stress. The SPSZS on overall is striking NW direction, but in places appears to trend NNW direction, especial along the margin of the rigid bodies. Their shear planes are dominantly sub-vertical to vertical, associated with both down-dip and sub-horizontal mineral stretching lineation, where by in both cases, the dominant sense of shearing interpreted to be lateral dextral sense of movements. However, in the present of rigid bodies, the SPSZS is dominated by an oblique lateral dextral sense of movement. In addition, these shear zone systems, both consist of pegmatites that are aligned parallel to the shear foliation, sheared into mylonite and ultramylonite. However, the pegmatites at some areas intrude oblique to the fabric, cross-cutting the shear fabric. This implies that the pegmatites are syn- to post-tectonic to the shearing.

The above-observed similarities led to the conclusion that both SPSZS, ESZ and MRPSZ were formed from the same tectonic event. The geochronology studies on the pegmatite intrusion along the MRPSZ by Lambert (2013) gives a concordant age in a range of 1005-970 ma. Even though the three shear zone systems share similar geological features, each shear zone system has a difference significant to the NMC evolution. The MRPSZ in the Sandfontein area partly transposed the basal thrust of the Fish River-Onseepkans Thrust zone, which is a transitional tectonic boundary between the rocks of Pella and Kakamas Domains. The LFROT in the east (northeast of Tantalite Valley) coincided with the ESZ and is completely transposed into phyllonites (Angombe, 2016). The Frontal Sperlingsputs shear zone, coincided with the SNF, which is a transposition tectonic boundary between the Vioolsdrif and Pella Domains (Fig 5-3). Therefore, these shear zone systems interpreted to be playing different roles in the evolution of the NMC.

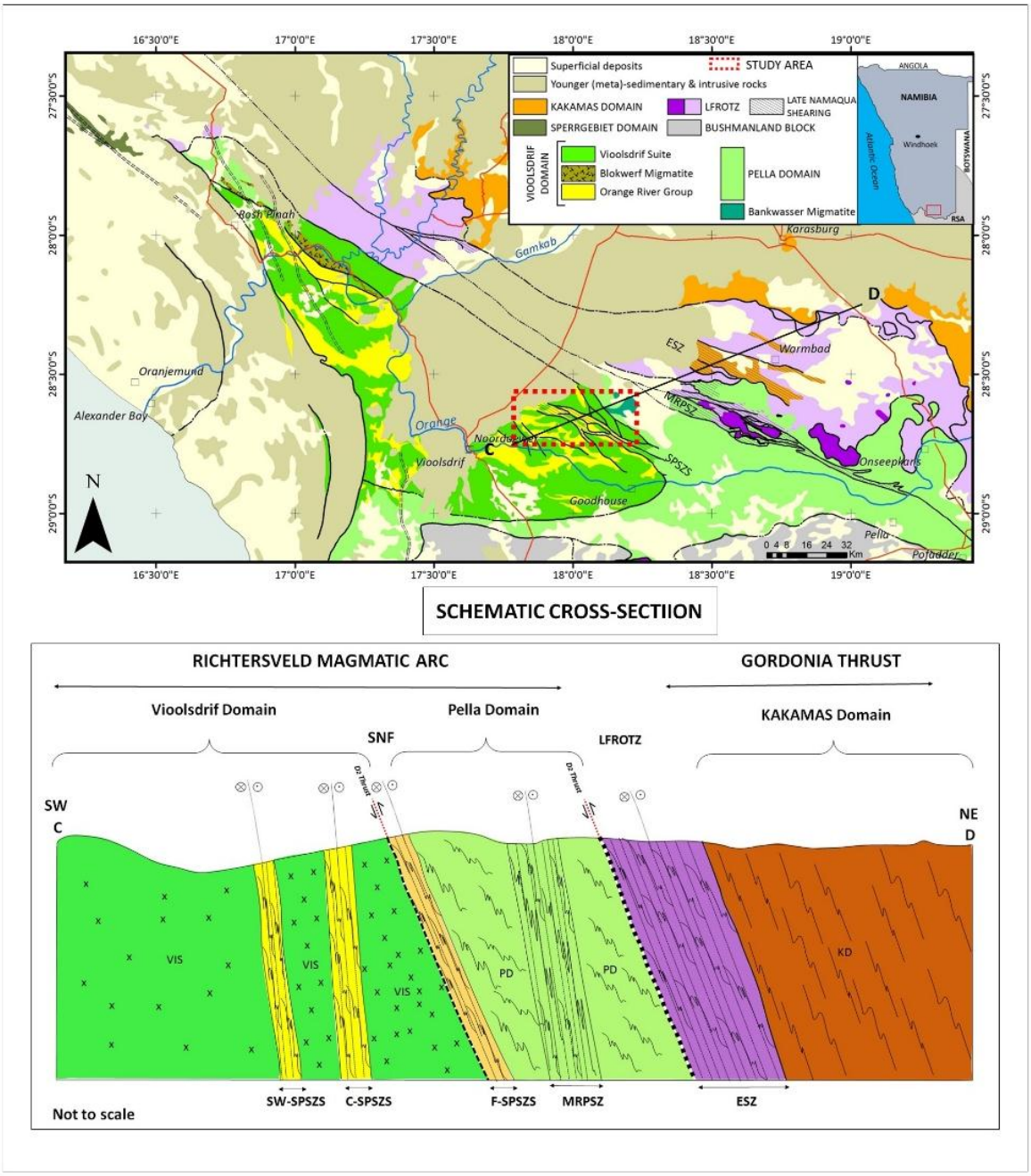

Figure 5-23: Interpreted schematic cross-section, showing the major roles the three major shear zones (SPSZS, MRPSZ, ESZ) play within the Namaqua Metamorphic Province in southern Namibia.

CHAPTER 6: CONCLUSIONS

The research project entails a detailed lithological and structural analysis that led to the classification of various lithologies, identification of different shear zones (e.g. Sperlingsputs Shear Zone System) and production of detailed 1:50 000 geological map (Appendix A). The main conclusions of this study are:

- The basement geology of the study area comprises of the Orange River Group (ORG) and Vioolsdrif Intrusive Suite (VIS) rocks. The ORG ranges from rhyolitic to basaltic in composition and predominantly andesitic lavas. The VIS range from granitoids to gabbroic in composition and is dominated primarily by the granodiorites.
- The study area consists of two distinct regions of equivalent stratigraphic units with different metamorphic grades i.e. (1) the southern part that preserve greenschist facies Palaeoproterozoic crustal rocks of the ORG and VIS, limited to D_1 deformation, referred as the Vioolsdrif Domain. (2) The northern part that comprises of amphibolite facies penetrative gneissic rocks of the ORG and VIS, referred as the Pella Domain and preserve Namaqua Orogeny fabrics that probably obliterated the D_1 event structures.
- The two regions are subsequently subjected to the Late-Namaqua transcurrent D_4 shear zones, that reoriented and mylonitised the pre-existing structure of both D_1 and D_2 events.
- The Sperlingsputs Shear Zone System (SPSZS) is a kilometre-scale networking NW-SE laterally extending dextral zone that is part of D_4 deformation event. The SPSZS is a brittle-ductile shear zone, characterised by anastomosing arrays of interconnected structures of heterogeneous deformation zone, that are defined by high strain zones of variable fault rocks ranging from Utramylonite to Cataclasite.
- The main vertical lineation (down-dip lineation) along the SPSZS in this study area is interpreted as a result of localised vertical movement along the margin of the rigid bodies. However, traces of down-dip lineation at other localities does not correlate with the simple shear components of the SPSZS, and is interpreted to be insignificant to the overall SPSZS sense of movements.
- The pre-existing structures and rheology are concluded to be the main factors responsible for the nucleation of the SPSZS and the forming of fault rocks type.

- This study interpreted the SPSZS to have occurred simultaneously with MRPSZ and ESZ at around 1005-970 Ma, based on the geometry, sense of movement, deformation mechanism and metamorphic grade.
- The low grade Vioolsdrif Domain and the high grade Pella Domain are adjacent to each other, this suggest that the Pella Domain is thrusted upward from greater depth to shallow depth during the regional thrusting D_2 deformation event. Therefore, in this study the SNF interpreted to be the transposition tectonic boundary, where by the transportation of allochthon Pella rocks took place around 1200 Ma.
- The SPSZS has no impact on the thrusting of the Pella Domain rocks over the Vioolsdrif Domain rocks, but it has a significate contribution to the lateral movement on rocks of both domains.

REFERENCES

Angombe, M.T., 2016. The lithostratigraphy and structural components of the Eureka Shear Zone, southern Namibia. Case study of the Eureka Shear Zone in Namibia. University of Stellenbosch.

Babaie, H.A., LaTour, T.E., 1998. Semi-brittle and cataclastic deformation of hornblende-quartz rocks in the ductile shear zone. Tectonophysics 229, 19-30.

Bai, Q., Mackwell, S. J. and Kohlstedt, D. L., 1991. High-temperature creep of olivine single crystals. Mechanical results for buffered samples. Journal of Geophysical Research 96, 2441-2463.

Bak, J., Korstgard, J. and Sorensen, K. A., 1975. Major shear zone within the Nagssugtoqidian of West Greenland. Tectonophysic 27. 191-209.

Beukes, G.J., 1973. 'n Geologiese ondersoek van die gebied suid van Warmbad, Suidwes-Afrika, met spesiale verwysing na die metamorf-magmatiese assosiasies van die Voorkambriese gesteentes. D.Sc. Thesis, University of the Orange Free state, Bloemfontein, p. 333. Bloemfontein.

Blignault, H.J., Van Aswegen, G., Van Der Merwe, S.W., and Colliston, W.P., 1983. The Namaqualand geotraverse and environs: part of the Proterozoic Namaqua mobile belt. Geological Society of South Africa, Special Publication 10, p. 1-29 (with one unbound map).

Blignault, H.J., 1974. The tectonic zonation of part of the Namaqua Province in the lower Fish River / Narubis cross-section. In: A. Kröner (comp.), Tenth and Eleventh Annual Reports: 1972 and 1973, Precambrian Research Unit, University of Cape Town, p. 43 - 45.

Blignault, H.J., 1977. Structural-metamorphic imprint on the part of the Namaqua mobile belt in South West Africa. Bulletin, Precambrian research, University of Cape Town 23, 197.

Carreras, J., 2001. Zooming on Northern Cap de Creus shear zones. Journal of Structural Geology 23, 1457–1486.

Cilliers, F.H., 1987. Isotope characteristics of the sulphide-bearing sequence of the Areachap Group in the Boksputs area, northern Cape. M.Sc. Thesis, University of the Orange Free State, Bloemfontein, p. 172.

Clifford, T.N., Barton, E.S., Retief, E.A., Rex, D.C. and Fanning, C.M, 1995. A crustal progenitor for the intrusive anorthosite-charnockite kindred of the cupriferous Koperberg suite, Okiep district, Namaqualand, South Africa; new isotope data for the country rocks and intrusives. Journal of Petrology 36, p. 231-258.

Colliston, W.P., Praekelt, H.E. and Schoch, A.E., 1989. A broad perspective (Haramoep) of geological relations established by sequence mapping in the Proterozoic Aggeneys Terrane, Bushmanland, South Africa. South African Journal of Geology, 92(1), p. 42 - 48.

Colliston, W.P., Praekelt, H.E. and Schoch, A.E., 1991. A progressive ductile shear model for the Proterozoic Aggeneys Terrane, Namaqua Mobile Belt, South Africa. Precambrian Research, 49, p. 205 - 215.

Colliston, W.P. and Schoch, A.E.,1996. Proterozoic metavolcanic rocks and associated metasediments along the Orange River in the Pofadder Terrane, Namaqua metamorphic belt. South African Journal of Geology, 99(1), p. 1 - 17.

Colliston, W.P. and Schoch, A.E., 2000. Mid-Proterozoic tectonic evolution along the Orange River on the Border between South Africa and Namibia. Communication of the Geological Survey of Namibia 12, 53-62.

Colliston, W.P., Schoch, A.E., 2013. Wrench-shearing during the Namaqua Orogenesis-Mesoproterozoic late stage deformation effects during Rodinia assembly. Precambrian Research 232, 44–58.

Cornell, D.H., Thomas, R.J., Moen, H.F.G., Reid, D.L., Moore, J.M., Gibson, R.L., 2006. The Namaqua-Natal Province, in: In: Johnson, M.R, Anhaeusser, C.R and Thomas, R.J. (Eds.), The Geology of South Africa. Geological Society of South Africa. Johannesburg/Council for Geoscience, Pretoria. pp. 325–343.

Cornell, D.H. and Pettersson, Å., 2007a. Ion probe dating of the Achab Gneiss, a young basement to the Central Bushmanland ore district?: African Journal of Earth Sciences, v. 47, p. 112–116.

De Villiers, J. and SÖhnge, P.G., 1959. The geology of the Richtersveld. Memoir, Geological Survey of South Africa, 48, 266 p.

De Villiers, J. and Burger, A.J., 1967. Note on the minimum age of certain granites from the Richtersveld area. Annals of the Geological Survey of South Africa, 6, pp. 83 - 84.

Duebendorfer, M., Christensen, C.h., 1988. Plastic to brittle deformation of microscline during deformation and cooling of a granitic pluton. Princeton university press, New Jersey, 176-179

Durham, W.B. and Goetze, G., 1977. Plastic flow of oriented single crystals of olivine. Mechanical data. Journal of Geophysical Research 82, 5737-5753.

Eglington, B.M., Armstrong, R.A., 2003. Geochronological and isotopic constraints on the Mesoproterozoic Namaqua-Natal Belt: Evidence from deep borehole intersections in South Africa. Precambrian Research 125, 179–189.

Frimmel, H.E., 2000. Formation of late Mesoproterozoic Supercontinent: The South Africa-East Antarctica connection, in: The precambrian Earth: Tempos and events.

Geringer, G.J., Humphreys, H.C. and Scheepers, D.J., 1994. Lithostratigraphy, protolithology, and tectonic setting of the Areachap Group along the eastern margin of the Namaqua Mobile Belt, South Africa. *South African Journal of Geology,* **97**(1), pp. 78-100.

Gevers, T.W., Partridge., F.C. and Joubert, G.E., 1937. The pegmatite area south of the Orange River in Namaqualand. Mem.geol.Surv.S. Afr., 32, 172 pp

Hartnady, C.J.H., Joubert, P. and Stowe, C.W., 1985. Proterozoic crustal evolution in southwestern Africa. Episodes, 8, pp. 236 - 244.

Hugo, P.J., 1970. The pegmatites of the Kenhardt and Gordonia districts, Cape Province. Memoir, Geological Survey of South Africa, 58, 94 p.

Humphreys, H.C., Van Bever Donker, J.M., 1987. Aspects of deformation along the namaqua province eastern boundary, kenhardt district, South Africa. Precambrian Research 36, 39–63.

Jackson, M.P.A., 1976. High-grade metamorphism and migmatization of the Namaqua Metamorphic Complex around Aus in the southern Namib Desert, South West Africa. Bulletin, Precambrian Research Unit, University of Cape Town, 18, 299 p.

Jacobs, J., Thomas, R., Weber, K., 1993. Accretion and indentation tectonics at the southern margin of the Kaapvall craton during Kibaran (Greenville) orogeny. Geology 21, 203–206.

Jacobs, J., Thomas, R.J., 1994. Oblique collision at about 1.1 Ga along the southern margin of the Kaapvaal continent, south-east Africa. Geologische Rundschau 83, 322–333.

Josep, M. P., Ben, A. and Van der Pluijm., 2001. Evaluating magnetic lineations (AMS) in deformed rocks. Tectonophysics 350, 283-298.

Joubert, P., 1971. The regional tectonism of the gneisses of part of Namaqualand. University of Cape Town, Bulletin of the Precambrian Research Unit 10, 220 pp.

Joubert, P., 1986. The Namaqualand Metamorphic Complex - A summary. In: C.R. Anhaeusser and S. Maske (Eds.) Mineral Deposits of South Africa, Vols I & II, Geological Society of South Africa, pp. 1395 - 1420.

Katsuyoshi, M. and David, M., 2004. The role of pre-existing mechanical anisotropy on shear zone development within oceanic mantle lithosphere. Journal of Petrology 45, 405-414.

Lambert, C.W., 2013. Granitic melt transport and emplacement along transcurrent shear zones : Case study of the Pofadder Shear Zone in South Africa and Namibia. University of Stellenbosch.

Macey, P.H., Minnaar, H., Miller, J.A., Lambert, C.W., Groenewald, C., Indongo, J., Angombe, M.T., Hendrik, S., Shifotoka, G., Diener, J., le Roux, P., Frei, D., 2015. The Precambrian Geology of the Region South of Warmbad from Haib to Velloorsdrif, Southern Namibia, An Explanation to 1:50 000 Geological Map Sheets 2818AC, 2818AD, 2818CA, 2818CB,2818CC,2818CD,2818DA, 2819CA,2819CB, 2819CC, 2819CD and 2819DA.

Macey, P.H., Thomas, R.J., Minnaar, H.M. Gresse, P.G., Lambert, C.W., Groenewald, C.A., Miller, J.A., Indongo, J.L., Angombe, M., Shifotoka, G., Frei, D., Diener, J.F.A., Kisters, A.F.M., Dhansay, T. Smith, H., Doggart, S., Le Roux, P., Hartnady, M.I. and Tinguely, C., 2017. Origin and evolution of the ~1.9 Ga Richtersveld MagmaticArc, SW Africa, Precambrian Research

Marais, J.A.H., Agenbacht, A.L.D., Prinsloo, M. and Basson, W.A., 2001. Geology of the 2916 Springbok sheet: Explanation, sheet 2916 Springbok (1: 250 000), Council for Geoscience, 103 p

McCourt, S., Armstrong, R.A., Grantham, G.H., Thomas, R.J., 2006. Geology and evolution of the Natal belt, South Africa. J. Afr. Earth Sci. 46, 71–92.

McDaid, J., 1978. The geology of the northern part of Diamond area No.1, SWA. 14th and 15th Annual Reports of the Precambrian Research Unit, University of Cape Town, pp. 124–140.

Mclaren, A.H., 1988. The geology of the area east of the pofadder with emphasis on the shearing associated with the Poffader Lineament. Bulletin, Precambrian research, University of Cape Town 35, 1–123.

Means, W.D., 1995. Shear zones and rock history. Tectonophysics 247, 157–160.

Melosh, B.L., Rowe, C.D., Smit, L., Groenewald, C., Lambert, C.W., Macey, P., 2014. Snap, crackle, Pop: Dilational fault breccias record seismic slip below the brittle-plastic transition. Earth and Planetary Science Letters 403, 432–445.

Minnaar, H., 2011. Composition and the evolution of the Proterozoic Vioolsdrif batholith (Including the Orange River Group), Northern Cape Province, South Africa. Department of Geology, University of the Free State.

Minnaar, H., Botha, P.M.W. and Roberts, D., 2008. The geology of the Alexander Bay area: Explanation to sheet 2816 Alexander Bay (1: 250 000). Council for Geoscience, 178 p.

Minnaar, H., 2012. Composition and Evolution of the Proterozoic Vioolsdrif Batholith (including the Orange river group), Northern cape province, South Africa. University of the Free State.

Moen, H.F.G., Toogood, D.J., 2007. Geology of the Onseepkans Area. Pretoria, South Africa: Council for Geoscience.

Miller, R.M., 2008. The geology of Namibia. Hand book, Geological Survey of Namibia, 3 volumes.

Passchier, C., Trouw, R., 2005. Micro-tectonics, Second. ed. Springer, Berlin.

Piazolo, S. and Passchier, C.W., 2002. Controls on lineation development in low to medium-grade shear zones. Journal of Structural Geology 24, 24-44.

Ramsay, J.G., 1980. Shear zone geometry: A review. Journal of Structural Geology 2, 83–99

Reid, D.L., 1977. Geochemistry of Precambrian igneous rocks in the lower Orange River region. Bulletin (P.hD. thesis), Precambrian Research Unit, University of Cape Town, 22, 397 p.

Ritter, U., 1980. The Precambrian evolution of the eastern Richtersveld. Bulletin, Precambrian Research Unit, University of Cape Town, 26, 276 p.

Robb, L.J., Armstrong, R.A., and Waters, D.J., 1999. Nature and duration of mid-crustal granulite-facies metamorphism and crustal growth: evidence from single zircon U-Pb geochronology in Namaqualand, South Africa. Journal of Petrology 40, 1747-1770.

SACS (South Africa Committee for stratigraphy) 1980. Stratigraphy of South Africa. Part 1 (Compiler LE Kent), Lithostratigraphy of the Republic of South Africa, South West Africa / Namibia and the Republics of Bophuthatswana, transkei and Venda. Handbook, Geological Survey of South Africa, 8, 690 p.

Schmid, S. M., and M. R. Handy (1991), Towards a genetic classification of fault rocks: Geological usage and tectonophysical implications, in Controversies in Modern Geology: Evolution of Geological Theories in Sedimentology, Earth History and Tectonics, edited by D. W. Mueller, J. A. McKenzie, and H. Weissert, pp. 339–361, Academic, San Diego, Calif.

Schutte, I.C., 1972. The main pegmatites of the area between Steinkopf, Vioolsdrif and Goodhouse, Namaqualand. Memoir, Geological Survey of South Africa, 60.

Simpson, C., De Paor, D.G., 1993. Strain and kinematic analysis in general shear zones. Journal of Structural Geology 15, 1–20.

Stephen, A.N., 2011. Types of Metamorphism. Petrology 2120

Stowe, C.W., 1983. The Upington Geotraverse and its implications for Craton Margin Tectonics. In: B.J.V. Botha (Editor). Namaqualand Metamorphic Complex. Special Publication of the Geological Society of South Africa, 10, p. 147 - 171.

Strydom, D., Colliston, W.P., Praekelt, H.E., Schoch, A.E., Van Aswegen, G., Pretorius, J.J., Beukes, G.J., De Villiers, B., Watkeys, M.K. and Botes, F.J., 1987. The tectonic units of parts of Namaqualand, Bushmanland and southern South West Africa/Namibia. 1:250 000 scale map, Bushmanland Research Project, Department of Geology, University of the Orange Free State.

Tikoff, B., Green, D., 1997. Stretching lineation in transpressional shear zones. Journal of Structural Geology 19, 29-39.

Thomas, R.J., Agenbacht, A.L.D., Cornell, D.H., Moore, J.M., 1994. The Kibaran of southern Africa: Tectonic evolution and metallogeny. Ore Geology Reviews 9, 131–160.

Toogood, D.J., 1976. Structural and Metamorphic Evolution of a Gneiss Terrain in the Namaqua Belt Near Onseepkans, South West Africa. Bulletin of the Precambrian Research unit, 19, 1–189.

Tullis, J., and R. A. Yund (1980), Hydrolytic weakening of experimentally deformed Westerly granite and Hale albite rock, J. Struct. Geol., 2, 439–451.

Van Aswegen, G., Strydom, D., Colliston, W.P., Praekelt, H.E., Blignault, H.J., Schoch, A.E., Botha, B.J.V. and Der Merwe, S.W., 1987. The structural-stratigraphic development of part of the Namaqua Metamorphic Complex - an example of Proterozoic major thrust tectonics. In: A. Kröner (Ed.) Proterozoic Lithosphere Evolution. American Geophysical Union, Geodynamics Service, pp. 207 - 216.

Van Bever Donker, J.M., 1983. The Neusspruit lineament, Upington geotraverse, possible boundary between the Namaqualand Metamorphic Complex and the Namaqua Front. In: B.J.V. Botha (Editor). Namaqualand Metamorphic Complex, Special Publication, Geological Society of South Africa, 10, p. 193 - 198.

Von BackstrÖm, J.W. and De Villiers, J., 1972. The geology along the Orange River Valley between Onseepkans and the Richtersveld. Explanation of sheets 2817D (Vioolsdrif), 2818C (Goodhouse), 2818D (Dabenoris) and 2819C (Onseepkans), Geological Survey of South Africa, 101 p.

Wendt, A.S., Mainprice, D., Rutter, E. and Wirth, R., 1998. A joint study of experimental deformation and experimentally induced microstructures of pretextured peridotites. Journal of Geophysical Research 103, 18205-18221.

White, S. H., Burrows, S. E., Carreras J., Shaw, N.D. and Humphreys, F. J., 1979. Mylonite in the ductile shear zones. Journal of Structural Geology 2, 175-187.

APPENDICES

Appendix A

Attached detailed 1: 50 000 scale Geological Map of the study area

Appendix B

List of samples for petrographic, geochemical and structural analysis

WAYPOINT	LAT	LONG	SAMPLE #	MAJOR UNIT	ROCK UNIT	PHOTO	Structural Samples	Petrography (thin section)	Geochemistry
JLI14 011	-28,716317	18,138173	JI14 001	ORG	META-ANDESITE	P108-804-806		X	X
JLI14 012	-28,718821	18,134195	JI14 002	ORG	META-BASALT	P108-808-809		X	X
JLI14 013	-28,71645	18,12894	JI14 003	ORG	META-RHYOLITE	P108-815-816		X	X
JLI14 015	-28,719045	18,123164	JI14 004		DIORITE	P108-819-822			
JLI14 016	-28,718716	18,120198	JI14 005	ORG	META-TUFFA	P108-8023-8024		X	X
JLI14 017	-28,71975	18,11823333	JI14 006	ORG	META-RHYOLITE	P108-8025-8026		X	X
JLI14 29	-28,704288	18,245528	JI14 007	VIOOLSDRIF/GOODHOUSE	META-GRANODIORITE	P108-866-870			
JLI14 32	-28,74386667	18,15731667	JI14 008	GANNAGARIEP DYKE	DIORITE			X	
JLI14 33	-28,663769	18,163812	JI14 009	VIOOLSDRIF/GOODHOUSE	META-GRANODIORITE				
JLI14 34	-28,64931	18,160557	JI14 010A		META-GABBRO	P108-877-890		X	
JLI14 34	-28,64931	18,160557	JI14 010B		BT-QTZ-FLD GNEISS				
JLI14 35	-28,660762	18,162767	JI14 011	GANNAGARIEP DYKE	DIORITE	P108-891-895			
JLI14 39	-28,735693	18,187084	JI14 012A	ORG	META-RHYOLITE	P108-919-925			
JLI14 39	-28,735693	18,187084	JI14 012B	ORG	META-ANDESITE (porhyritic)			X	X
JLI14 40	-28,740332	18,189802	JI14 013	ORG	META-ANDESITE (porhyritic)	P108-926-930			
JLI14 40	-28,740332	18,189802	JI14 014A	ORG	META-ANDESITE (fissile)			X	
JLI14 40	-28,740332	18,189802	JI14 014B	ORG	META-ANDESITE (Magnetite Bearing)				
JLI14 41	-28,743621	18,190616	JI14 015	ORG/VIOOLSDRIF	Meta-rhyolite/	P108		X	

					Ramsdrif granite	935-938			
JLI14 52	-28,752423	18,153119	JI14 016	VIOOLSDRIF	KHOROMUS	P108-984-1001		X	
JLI14 58	-28,73775	18,17643333	JI14 017	ORG	META-RHYOLITE	P108-1035-1043		X	
JLI14 60	-28,731032	18,176596	JI14 018	ORG	META-INTERMEDIATE LAVA	P108-1046-1049		X	
JLI14 60	-28,731032	18,176596	JI14 019	ORG	META-ANDESITIC LAVA	P108-1046-1049		X	X
JLI14 66	-28,72639	18,158357	JI14 020	ORG	META-INTERMEDIATE MYLONITE		X	X	
JLI14 67	-28,734511	18,155762	JI14 021	VIOOLSDRIF/GOODHOUSE	META-GRANODIORITE				
JLI14 73	-28,717925	18,241989	JI14 022	VIOOLSDRIF/GOODHOUSE	META-GRANODIORITE	P108-1081-1094			
JLI14 80	-28,73789	18,229338	JI14 023	VIOOLSDRIF	RAMSDRIF GRANITE				
JLI14 87	-28,721573	18,222698	JI14 024	VIOOLSDRIF	RAMSDRIF GRANITE				
JLI14 90	-28,636759	18,125264	JI14 025	VIOOLSDRIF	RAMSDRIF GRANITE	P108-1164-1165			
JLI14 91	-28,631674	18,127365	JI14 026	VIOOLSDRIF/GOODHOUSE	META-GRANODIORITE	P108-1166-1170			
JLI14 92	-28,631237	18,128339	JI14 027	VUURSDRIF SUBSUITE	META-LEUCO-GABBRO	P108-1171-1178			
JLI14 94	-28,624836	18,124777	JI14 028	GANNAGARIEP DYKE	DIORITE				
JLI14 98	-28,610818	18,125121	JI14 029		META-GABBRO	P108-1201-1209			
JLI14 99	-28,614554	18,13151	JI14 030	VIOOLSDRIF/GOODHOUSE	META-GRANODIORITE				
JLI14 100	-28,618609	18,136436	JI14 031		META-GABBRO	P108-1212-1215			
JLI14 102	-28,624374	18,138008	JI14 032	VIOOLSDRIF/GOODHOUSE	META-GRANODIORITE	P108-1216-1218			
JLI14 103	-28,626651	18,13945	JI14 033	VUURSDRIF SUBSUITE	META-LEUCO-GABBRO				
JLI14 112	-28,70276667	18,09111667	JI14 034A	ORG	DACITE (porhyritic pyroclastic)	P108-1256-1261		X	
JLI14 112	-28,70276667	18,09111667	JI14 034B	ORG	DACITE (limited pyroclastic)				
JLI14 112	-28,70276667	18,09111667	JI14 034C	ORG	DACITE (btwn A & B)				X
JLI14 114	-28,707239	18,085285	JI14 035	ORG	BASALTIC-ANDESITIC LAVA			X	X
JLI14 115	-28,70859	18,084186	JI14 036		FELSIC-CATACLASITE-MYLONITE		X	X	
JLI14 118	-28,720464	18,041399	JI14 037	ORG	INTERMEDIATE LAVA			X	X
JLI14 119	-28,719705	18,040442	JI14 038	ORG	DACITIC-ANDESITIC LAVA	P108-1290-1319	X	X	
JLI14 122	-28,719705	18,040442	JI14 039	VIOOLSDRIF/GOODHOUSE	SHEARED GRANODIORITE	P108 1334-1339	X	X	
JLI14 126	-28,7158	18,03596667	JI14 040	ORG	META-RHYOLITE	P108-1350-		X	X

						1357			
JLI14 127	-28,71601667	18,0332	JI14 041	VIOOLSDRIF/GOODHOUSE	SHEARED GRANODIORITE	P108-1372-1384	x	x	
JLI14 128	-28,715342	18,02968	JI14 042	ORG	META-RHYOLITE	P108-1385-1388		x	x
JLI14 134	-28,73036667	18,01781667	JI14 043	ORG	DACITIC-ANDESITIC LAVA				
JLI14 135	-28,73036667	18,01781667	JI14 044	ORG	DACITIC-ANDESITIC LAVA			x	
JLI14 137	-28,73608333	18,02381667	JI14 045	ORG	DACITIC-ANDESITIC LAVA	P108-1411-1414		x	x
JLI14 139	-28,74004	18,03202	JI14 046	ORG	L-TECTONISE META-RHYOLITE			X	X
JLI14 144	-28,734292	18,04124	JI14 047	ORG	META-ANDESITE			X	x
JLI14 145	-28,733404	18,041719	JI14 048		FELSIC-ULTRA-MYLONITE		X	x	
JLI14 146	-28,732241	18,042325	JI14 049	ORG	BASALTIC-ANDESITIC ULTRA-MYLONITE		x	X	
JLI14 146	-28,732241	18,042325	JI14 050	ORG	BASALTIC-ANDESITIC ULTRA-MYLONITE (hrn bearing)			x	x
JLI14 147	-28,72915	18,044283333	JI14 051	ORG	CATACLASITIC BASALTIC-ANDESITIC (Oriented sample)		x	X	
	-28,712133333	18,056683333	JI14 052	ORG	BASALTIC-ANDESITIC LAVA (Within a Rigid body)			X	X
JLI14 150	-28,701012	18,058013	JI14 053	ORG	BASALTIC-ANDESITIC LAVA			x	X
JLI14 152	-28,69591	18,063412	JI14 054	VIOOLSDRIF	PORPHYRITIC RAMSDRIF GRANITE				
JLI14 153	-28,68955	18,066744	JI14 055	ORG	PORPHYRITIC META-RHYOLITE			X	x
JLI14 162	-28,675902	18,088192	JI14 056	GANNAGARIEP DYKE	DIORITE				
JLI14 163	-28,67979	18,09534	JI14 057		Sub-volcanic intermediate medium grained rock unit				
JLI14 166	-28,728468	18,180062	JI14 058		Chlorite-kfd phenocrystal sheared rock	P108-1451-1460			
JLI14 171	-28,740622	18,182012	JI14 059	VIOOLSDRIF	META-GRANODIORITE (SNF)	P108-1469-1477			
JLI14 172	-28,741875	18,181612	JI14 060		INTER-LAYERING QTZ-Kfd-UTRA-MYLONITE	P108-1478-1486			
JLI14 174	-28,743721	18,181646	JI14 061	VIOOLSDRIF	QUARTZ FELDSPATHIC GNEISS				
JLI14 176	-28,748636	18,17957	JI14 062	VIOOLSDRIF	RAMSDRIF GRANITE & GOODHOUSE (Highly sheared)				
JLI14 178	-28,7507	18,17695	JI14 063	ORG	PORPHYRITIC ANDESITIC LAVA			x	X
JLI14 187	-28,681852	18,153648	JI14 064	VIOOLSDRIF	RAMSDRIF GRANITE				
JLI14 188	-28,675808	18,149975	JI14 065	VIOOLSDRIF	PORPHYRITIC RAMSDRIF GRANITE				
JLI14 193	-28,690129	18,135297	JI14 066		MILKY COLOR PORPHYRITIC GRANITE	P108-1565-1574			
JLI14 193	-28,690129	18,135297	JI14 067		PINK COLOR PORPHYRITIC GRANITE	P108-1565-			

						1574			
JLI14 208	-28,74655	18,07508333	JI14 068	VIOOLSDRIF	EQUIGRANULAR GRANODIORITE	P108-1639-1643			
JLI14 209	-28,746648	18,071573	JI14 069		CATACLASITIC - MYLONITIC ROCK UNIT		x	X	
JLI14 212	-28,743349	18,066589	JI14 070A	ORG	SHEARED ANDESITIC LAVA			X	
14 JLI213	-28,742595	18,064619	JI14 070B	ORG	CATACLASITIC-MYLONITIC RHYOLITE			X	
JLI14 215	-28,743388	18,06281	JI14 071	ORG	CATACLASITE (RHYOLITE)		X	x	
JLI14 216	-28,74421667	18,06236667	JI14 072	ORG	FISSILE ANDESITE				
JLI14 221	-28,630163	18,092127	JI14 074	VIOOLSDRIF	EQUIGRANULAR RAMSDRIF GRANITE				
JLI14 225	-28,678384	18,120242	JI14 075	VIOOLSDRIF	PORPHYRITIC GRANODIORITE	P108-1730-32			
JLI14 226	-28,668825	18,130419	JI14 076	VIOOLSDRIF	PORPHYRITIC RAMSDRIF GRANITE				
JLI14 229	-28,66061667	18,13383333	JI14 077A		FELDSPATHIC GRANITE (contact)				
JLI14 229	-28,66061667	18,13383333	JI14 077B		FELDSPATHIC GRANITE (centre)				
JLI14 229	-28,66061667	18,13383333	JI14 078	VIOOLSDRIF	GRANODIORITEGRANITE OR RAMSDRIF				
WAYPOINT	LAT	LONG	SAMPLE #	MAJOR UNIT	ROCK UNIT	PHOTO			

Appendix C

Geochemical Data

SAMPLE ID	SUITE/GROUP	Na2O+K2O	LATITUDE (DD)	LONGITUDE (DD)	SAMPLE LITHOLOGY	SiO_2	TiO_2	Al_2O_3	Fe_2O_3 (t)	FeO	Fe2O3	MnO	MgO	CaO	Na_2O	K_2O	P_2O_5	Cr_2O_3	L.O.I.	Total
CHM 274	ORG	4,52	-28,8105	18,1017	Fine-grained mesocratic lava	62,16	0,55	13,96	6,74			0,14	4,07	7,18	4,02	0,50	0,21	0,03	0,64	100,21
CG1388	ORG		-28,8569	18,3126	Andesitic lava	66,74	0,56	15,62	4,46			0,10	1,75	3,85	2,97	3,41	0,16	below detection	0,55	100,17
CHM 293	ORG		-28,8004	18,2617	Melanocratic lava	66,16	0,54	15,36	4,30			0,09	1,94	4,17	3,53	3,34	0,16	below detection	0,50	100,09
CHM 295	ORG		-28,8078	18,2549	Leucocratic lava	68,23	0,50	14,52	3,08			0,08	1,21	2,32	3,31	4,98	0,13	below detection	1,71	100,08
CHM 277	ORG		-28,7963	18,1096	Very fine-grained grey gneiss	71,57	0,59	13,73	2,90			0,05	0,73	2,78	3,62	3,32	0,18	below detection	0,53	10392,00
CHM 275	ORG		-28,8006	18,1081	Melanocratic fine-grained gneiss	55,93	0,79	16,84	7,92			0,13	2,80	6,92	3,78	2,94	0,29		0,64	99,00

CG1387	ORG		-28,8569	18,3126	Meso fine grey lava	71,89	0,38	15,11	2,67			0,05	0,89	2,97	3,90	1,50	0,09		0,65	100,12
JI14047	ORG	4,98	-28,7343	18,0412	Meta-andesite	55,30	0,76	15,69	9,03			0,16	4,35	7,53	2,58	2,40	0,29	0,00	1,14	99,24
JI14035	ORG	6,05	-28,7072	18,0853	Basaltic-andesitic lava	57,48	0,65	16,03	7,10			0,11	4,05	6,30	3,20	2,85	0,25	0,02	1,02	99,05
JI14002	ORG	4,40	-28,7188	18,1342	Meta-basalt	57,79	0,64	13,84	8,09			0,16	5,30	7,97	2,81	1,60	0,24	0,04	0,69	99,17
JI14046	ORG	6,39	-28,7400	18,0320	L-tectonise meta-rhyolite; Agglomeritic lava	58,06	0,74	16,94	7,11			0,13	3,53	5,68	3,26	3,13	0,28	0,01	0,74	99,62
JI14045	ORG	5,48	-28,7361	18,0238	Dacitic-andesitic lava	58,09	0,69	16,28	6,96			0,12	3,98	6,67	2,28	3,20	0,28	0,02	1,01	99,59
JI14052	ORG	6,44	-28,7121	18,0567	Basaltic-andesitic lava (within a rigid body)	58,31	0,76	16,46	6,52			0,10	2,49	6,63	3,26	3,18	0,28	0,00	0,96	98,97
JI14001	ORG	5,35	-28,7163	18,1382	Meta-andesite	61,75	0,65	15,20	6,22			0,15	2,83	5,63	3,37	1,98	0,24	0,01	1,38	99,40
JI14034C	ORG	6,78	-28,7028	18,0911	Dacite (btwn a & b)	63,07	0,61	16,10	5,18			0,13	1,70	4,55	3,50	3,28	0,25	0,00	1,13	99,50
JI14005	ORG	7,27	-28,7187	18,1202	Meta-tuffa	64,62	0,51	14,56	4,64			0,10	2,02	4,01	3,29	3,98	0,13	0,01	1,30	99,18
JI14037	ORG	7,76	-28,7205	18,0414	Intermediate lava	65,70	0,83	14,46	4,58			0,07	1,26	3,90	2,25	5,52	0,26	0,01	0,50	99,32
JI14053	ORG	6,58	-28,7010	18,0580	Basaltic-andesitic lava	65,77	0,54	14,33	4,66			0,10	1,71	4,07	3,76	2,81	0,19		0,69	98,65
JI14040	ORG	7,70	-28,7158	18,0360	Meta-rhyolite	65,90	0,62	15,88	4,01			0,08	1,03	3,64	3,52	4,17	0,20		0,58	99,63
JI14043	ORG	7,84	-28,7304	18,0178	Dacitic-andesitic lava	66,35	0,55	16,22	3,28			0,06	1,04	3,65	2,95	4,89	0,13		0,47	99,59
JI14050	ORG	4,30	-28,7322	18,0423	Basaltic-andesitic ultra-mylonite (hrn bearing); Hbl-porphyroblastic lava	66,86	0,49	14,82	4,43			0,09	2,33	5,31	2,69	1,61	0,12	0,01	0,95	99,70
JI14042	ORG	7,73	-28,7153	18,0297	Meta-rhyolite	68,20	0,52	15,61	2,87			0,06	0,70	3,14	3,29	4,44	0,11	0,00	0,44	99,38
JI14055	ORG	9,23	-28,6896	18,0667	Porphyritic meta-rhyolite	68,46	0,52	14,62	2,49			0,05	0,56	1,97	3,55	5,68	0,11		1,04	99,05
JI14110	ORG	7,92	-28,5700	18,0273	Qtz porphyritic rhyolite	77,93	0,19	11,99	0,92			0,04	0,07	0,63	3,37	4,55	0,06	0,00	0,19	99,94
JI14006	ORG	8,13	-28,7198	18,1182	Meta-rhyolite	69,71	0,47	14,75	2,53			0,06	0,62	2,56	3,23	4,90	0,10	0,00	0,70	99,62

JI14003	ORG	7,04	-28,7165	18,1289	Meta-rhyolite	70,57	0,47	14,44	2,55			0,05	0,81	2,37	3,75	3,29	0,10		1,14	99,54
JI14012B	ORG	6,98	-28,7357	18,1871	Meta-andesite (porhyritic)	66,30	0,51	15,22	4,48			0,11	1,51	3,85	3,49	3,50	0,19	0,01	0,36	99,53
JI14013	ORG	6,46	-28,7403	18,1898	Meta-andesite (porhyritic)	67,69	0,44	14,96	3,94			0,09	1,56	3,24	3,16	3,29	0,16	0,00	0,93	99,47
JI14019	ORG	6,63	-28,7310	18,1766	Meta-andesitic lava	64,52	0,56	15,25	5,30			0,12	1,93	4,60	3,63	3,00	0,21	0,01	0,51	99,64
JI14063	ORG	6,16	-28,7507	18,1770	Porphyritic andesitic lava	61,81	0,68	16,47	5,97			0,11	1,78	5,78	2,94	3,21	0,27	0,00	0,53	99,55
CHM20	ORG		-28,8339	17,9182	Andesite	58,10	0,74	17,66	4,10	4,36	3,28	0,12	3,45	6,53	3,29	2,22	0,24	0,00	0,00	100,00
CHM21	ORG		-28,8410	17,9130	TrachyAndesite	62,01	0,79	15,80	3,86	3,11	3,08	0,09	2,11	4,40	4,78	3,46	0,36	0,00	0,00	100,00
CHM22	ORG		-28,8482	17,9114	Andesite	62,95	0,66	15,14	3,62	3,34	2,89	0,10	3,65	5,01	2,99	3,05	0,21	0,00	0,00	100,00
CHM29	ORG		-28,8824	17,7921	Basaltic trachyAndesite	55,59	0,77	15,78	4,54	5,69	3,62	0,15	5,75	8,43	2,26	1,76	0,20	0,00	0,00	100,00
CHM31	ORG		-28,8224	17,7828	Basaltic trachyAndesite	54,58	0,71	14,53	4,64	6,08	3,71	0,15	7,85	8,14	2,33	1,71	0,21	0,00	0,00	100,00
CHM32	ORG		-28,8162	17,6402	Rhyolite	69,75	0,65	14,57	2,23	1,54	1,78	0,09	0,79	2,69	3,33	4,67	0,14	0,00	0,00	100,00
CHM256	ORG		17,9172	-28,8336	Melanocratic lava	55,71	0,76	16,10	8,57			0,14	4,35	6,60	2,49	2,90	0,24	0,01	2,20	100,08
CHM257	ORG		17,9181	-28,8339	Melanocratic lava	56,13	0,74	16,78	7,76			0,13	3,42	7,17	2,78	2,32	0,24	0,00	1,80	99,28
CHM258	ORG		17,9183	-28,8359	Melanocratic lava	52,04	0,65	14,17	7,55			0,13	6,41	6,69	3,02	3,24	0,28	0,04	4,75	98,96
CHM259	ORG		17,9183	-28,8359	Porphyrytic Rhyolite	77,54	0,14	11,85	0,99			0,00	0,20	0,03	2,34	5,77	0,01	0,00	0,59	99,48
CHM260	ORG		17,9160	-28,8377	Porphyrytic Rhyolite	72,41	0,33	13,51	1,96			0,06	0,42	1,74	2,85	4,92	0,07	0,00	1,94	100,20
CHM261	ORG		17,9139	-28,8400	Porphyrytic Rhyolite	58,25	0,71	15,57	5,67			0,09	2,18	4,79	3,91	3,91	0,32	0,00	3,67	99,08
CHM262	ORG		17,6673	-28,8048	Mesocratic lava	53,38	0,74	14,43	9,46			0,16	6,69	9,08	2,25	1,41	0,20	0,03	2,01	99,84
CHM263	ORG		17,6625	-28,8059	Mesocratic lava	53,03	0,77	15,08	10,11			0,18	4,83	7,82	2,78	1,59	0,22	0,03	2,39	98,84
CHM264	ORG		17,6609	-28,8019	Melanocratic lava	54,07	0,66	13,92	9,53			0,14	6,87	5,70	1,96	2,30	0,15	0,07	4,65	100,02
CHM265	ORG		17,6590	-28,7997	Melanocratic lava	55,62	0,73	14,20	8,85			0,15	6,29	7,55	2,05	1,65	0,19	0,04	2,39	99,69

CHM266	ORG		17,6558	-28,7999	Melanocratic lava	57,17	0,70	13,83	8,40			0,13	6,66	6,22	2,38	1,43	0,18	0,04	2,54	99,69
CHM267	ORG		17,6500	-28,7936	Mesocratic lava	69,97	0,42	14,55	3,14			0,06	1,57	2,47	3,34	2,87	0,12	0,01	1,78	100,29
CHM268	ORG		17,8490	-28,8473	Felsic lava	71,15	0,37	14,07	2,16			0,08	0,50	1,88	3,57	4,74	0,06	0,00	1,67	100,25
CHM269	ORG		17,8512	-28,8483	Felsic lava	77,93	0,24	12,32	1,28			0,01	0,25	0,32	3,60	4,11	0,03	0,00	0,42	100,52
DR-02	ORG		-28,7938	17,6489	FRAGMENTAL VOLCANIC ROCK	62,34	0,58	14,28	3,75	3,95	3,00	0,11	6,44	4,25	1,92	2,98	0,15	0,00	0,00	100,00
DR-03	ORG		-28,7940	17,6492	FRAGMENTAL VOLCANIC ROCK	61,84	0,83	15,30	3,66	3,18	2,92	0,09	6,03	2,43	2,80	4,37	0,19	0,00	0,00	100,00
DR-04	ORG		-28,7938	17,6491	FRAGMENTAL VOLCANIC ROCK	70,95	0,72	13,11	2,44	2,03	1,95	0,08	2,05	3,21	4,29	1,44	0,15	0,00	0,00	100,00
DR-05-1	ORG		-28,7938	17,6495	FRAGMENTAL VOLCANIC ROCK	50,97	0,96	19,38	4,98	5,02	3,98	0,20	7,57	3,90	2,18	5,58	0,25	0,00	0,00	100,00
DR-05-2	ORG		-28,7941	17,6498	FRAGMENTAL VOLCANIC ROCK	66,18	0,76	14,71	2,93	2,51	2,34	0,10	3,60	3,15	3,54	2,91	0,17	0,00	0,00	100,00
DR-05-3	ORG		-28,7938	17,6493	FRAGMENTAL VOLCANIC ROCK	70,04	0,76	12,78	2,57	2,28	2,05	0,09	2,42	4,10	3,20	2,10	0,17	0,00	0,00	100,00
DR-05-4	ORG		-28,7940	17,6491	FRAGMENTAL VOLCANIC ROCK	69,64	0,77	13,26	2,55	2,22	2,04	0,09	2,33	4,03	3,04	2,40	0,18	0,00	0,00	100,00
DR-05-5	ORG		-28,7935	17,6488	FRAGMENTAL VOLCANIC ROCK	58,39	0,85	17,05	3,88	3,77	3,10	0,14	5,17	4,85	2,47	4,01	0,20	0,00	0,00	100,00
DR-05-6	ORG		-28,7942	17,6495	FRAGMENTAL VOLCANIC ROCK	64,30	0,63	14,12	3,50	3,19	2,79	0,13	6,06	2,43	2,40	3,81	0,14	0,00	0,00	100,00
DR-06	ORG		-28,7940	17,6494	FRAGMENTAL VOLCANIC ROCK	69,42	0,63	14,28	2,58	2,10	2,06	0,07	1,34	3,83	4,46	1,63	0,17	0,00	0,00	100,00
DR-07	ORG		-28,7944	17,6500	FRAGMENTAL VOLCANIC ROCK	65,96	0,78	14,58	3,15	2,74	2,52	0,09	3,26	3,59	3,43	2,84	0,20	0,00	0,00	100,00
DR-08	ORG		-28,7939	17,6498	FRAGMENTAL VOLCANIC ROCK	53,81	0,73	13,84	4,49	5,41	3,59	0,17	11,30	6,06	1,40	3,49	0,20	0,00	0,00	100,00
DRL-11	ORG		-28,7941	17,6496	FRAGMENTAL VOLCANIC ROCK	67,71	0,67	14,38	2,92	2,36	2,33	0,08	2,27	3,39	5,57	1,06	0,17	0,00	0,00	100,00
DRL-121	ORG		-28,8075	17,8618	Dacite	66,14	0,50	15,03	3,04	2,48	2,42	0,08	2,60	3,91	2,69	4,03	0,11	0,00	0,00	100,00
DRL-122	ORG		-28,8083	17,8666	Dacite	66,22	0,49	15,03	3,07	2,45	2,45	0,08	2,48	3,66	2,66	4,36	0,10	0,00	0,00	100,00
DRL-123	ORG		-28,8041	17,6602	Basaltic andesite	56,80	0,81	15,61	4,59	5,37	3,66	0,14	5,89	6,85	2,33	2,34	0,20	0,00	0,00	100,00
DRL-125	ORG		-28,8036	17,6604	Basaltic andesite	57,25	0,82	15,58	4,59	5,38	3,67	0,14	5,59	6,77	2,26	2,33	0,20	0,00	0,00	100,00

DRL-126	ORG		-28,8081	17,6613	Basaltic andesite	56,40	0,84	15,75	4,52	5,45	3,61	0,13	6,06	7,07	2,37	2,13	0,19	0,00	0,00	100,00
DRL-127	ORG		-28,7984	17,6616	Basaltic andesite	59,07	0,78	15,53	4,27	4,58	3,41	0,13	4,53	6,64	1,59	3,58	0,15	0,00	0,00	100,00
DRL-14	ORG		-28,7937	17,6488	FRAGMENTAL VOLCANIC ROCK	70,96	0,59	13,57	2,53	1,86	2,02	0,07	1,39	2,32	6,42	0,63	0,17	0,00	0,00	100,00
DRL-15	ORG		-28,7936	17,6492	FRAGMENTAL VOLCANIC ROCK	60,75	0,80	17,52	3,37	3,07	2,69	0,11	4,23	3,72	5,24	1,68	0,18	0,00	0,00	100,00
DRL-17	ORG		-28,7941	17,6496	FRAGMENTAL VOLCANIC ROCK	67,08	0,47	13,49	3,19	3,08	2,55	0,07	3,39	4,86	4,22	0,67	0,11	0,00	0,00	100,00
DRL-20	ORG		-28,7936	17,6490	FRAGMENTAL VOLCANIC ROCK	63,33	0,60	14,96	2,77	2,53	2,21	0,12	3,67	6,44	1,47	4,38	0,30	0,00	0,00	100,00
DRL-21	ORG		-28,7942	17,6501	FRAGMENTAL VOLCANIC ROCK	63,48	0,64	16,27	3,02	2,76	2,42	0,07	3,43	4,23	2,78	3,69	0,24	0,00	0,00	100,00
DRL-22	ORG		-28,7545	17,7152	FRAGMENTAL VOLCANIC ROCK	56,93	0,79	17,59	3,99	4,22	3,19	0,12	3,88	6,80	1,55	4,62	0,31	0,00	0,00	100,00
DRL-23	ORG		-28,7581	17,6955	FRAGMENTAL VOLCANIC ROCK	61,61	0,74	16,62	3,56	2,94	2,84	0,10	2,22	5,16	3,91	3,58	0,27	0,00	0,00	100,00
DRL-41	ORG		-28,7445	17,7139	Basaltic andesite	59,02	0,64	15,76	3,79	4,37	3,03	0,10	5,07	7,17	1,91	2,74	0,20	0,00	0,00	100,00
DRL-42	ORG		-28,7464	17,7165	Basaltic andesite	55,64	0,70	14,51	4,50	5,51	3,59	0,15	8,02	7,17	1,92	2,58	0,20	0,00	0,00	100,00
DRL-43	ORG		-28,7990	17,6482	Basaltic andesite	55,97	0,72	14,73	4,53	5,65	3,61	0,13	8,24	6,52	2,58	1,66	0,18	0,00	0,00	100,00
DRL-45	ORG		-28,7983	17,6560	Basaltic andesite	57,55	0,74	15,22	4,31	5,31	3,44	0,14	6,22	7,18	2,30	1,72	0,19	0,00	0,00	100,00
DRL-48	ORG		-28,8046	17,6600	Basaltic andesite	57,38	0,81	15,88	4,51	5,20	3,60	0,14	5,65	6,64	2,04	2,48	0,19	0,00	0,00	100,00
DRL-49	ORG		-28,7680	17,7360	Basaltic andesite	53,22	0,71	14,87	4,42	6,43	3,53	0,17	8,35	9,52	1,96	1,02	0,22	0,00	0,00	100,00
DRL-50	ORG		-28,7554	17,7478	Basaltic andesite	53,84	0,72	14,84	4,44	6,12	3,54	0,16	8,49	8,66	2,02	1,38	0,22	0,00	0,00	100,00
DRL-55	ORG		-28,7481	17,7204	Non-porphyritic Rhyolite	74,31	0,26	14,00	1,48	1,12	1,18	0,03	1,19	1,30	3,62	2,92	0,07	0,00	0,00	100,00
DRL-56	ORG		-28,7519	17,7244	Andesite	59,82	0,66	15,96	3,68	3,47	2,94	0,10	3,85	6,20	4,83	1,91	0,27	0,00	0,00	100,00
DRL-57	ORG		-28,8334	17,9865	Basaltic andesite	56,10	0,71	15,27	4,14	5,37	3,31	0,14	7,11	8,00	2,41	1,37	0,24	0,00	0,00	100,00
DRL-62	ORG		-28,8294	17,8670	Andesite	59,38	0,66	16,38	3,67	3,63	2,93	0,10	4,92	5,62	2,60	3,56	0,22	0,00	0,00	100,00

DRL-65	ORG		-28,7544	17,7358	Basaltic andesite	55,26	0,77	14,91	4,39	5,99	3,51	0,16	7,95	7,87	1,28	2,11	0,19	0,00	0,00	100,00
DRL-66	ORG		-28,7575	17,7320	Dacite	67,46	0,69	16,13	2,10	1,81	1,68	0,06	1,02	4,86	3,29	2,76	0,23	0,00	0,00	100,00
DRL-67	ORG		-28,7502	17,7385	Basaltic andesite	57,78	0,82	15,79	3,99	4,74	3,19	0,12	5,65	7,17	2,24	2,24	0,28	0,00	0,00	100,00
DRL-68	ORG		-28,7560	17,7275	Dacite	66,39	0,45	14,64	2,77	2,33	2,21	0,06	3,88	3,30	3,73	2,86	0,14	0,00	0,00	100,00
DRL-89	ORG		-28,8274	18,0613	Andesite	61,23	0,72	18,38	2,92	2,49	2,33	0,08	1,55	5,63	3,53	3,76	0,31	0,00	0,00	100,00
DRL-93	ORG		-28,8329	17,8392	Dacite	64,95	0,82	14,88	3,59	2,93	2,87	0,10	2,04	4,46	3,05	3,73	0,17	0,00	0,00	100,00
RT-01	ORG		-29,0000	16,0000	Porphyry	68,61	0,49	16,00	2,13	1,65	1,70	0,05	1,38	2,84	3,79	3,36	0,12	0,00	0,00	100,00
RT-02	ORG		-29,0000	16,0000	Porphyry	68,44	0,45	15,31	2,87	2,16	2,29	0,05	1,15	2,46	3,09	4,49	0,10	0,00	0,00	100,00
RT-03	ORG		-29,0000	16,0000	Porphyry	68,55	0,45	15,51	2,44	1,95	1,95	0,04	1,27	3,25	3,06	3,86	0,10	0,00	0,00	100,00
DRA-01	ORG		-28,8352	17,9876	FRAGMENTAL VOLCANIC ROCK	62,90	0,95	17,18	3,26	2,25	2,60	0,08	1,54	2,72	2,25	7,23	0,29	0,00	0,00	100,00
DRA-05	ORG		-28,8359	17,9866	Non-porphyritic Rhyolite	72,84	0,69	12,96	2,01	1,37	1,60	0,04	1,00	1,79	2,23	5,33	0,15	0,00	0,00	100,00
DRA-06	ORG		-28,8350	17,9900	Non-porphyritic Rhyolite	73,65	0,36	13,67	1,55	0,89	1,23	0,04	0,31	0,59	3,65	5,56	0,04	0,00	0,00	100,00
DRA-06A	ORG		-28,8354	17,9884	Non-porphyritic Rhyolite	73,70	0,36	14,07	1,03	0,58	0,82	0,03	0,22	0,86	3,23	6,10	0,04	0,00	0,00	100,00
DRA-06B	ORG		-28,8354	17,9890	Non-porphyritic Rhyolite	73,78	0,35	13,68	1,38	0,79	1,10	0,03	0,33	0,86	4,05	4,98	0,05	0,00	0,00	100,00
DRA-06C	ORG		-28,8354	17,9896	Non-porphyritic Rhyolite	73,93	0,37	14,04	0,95	0,53	0,76	0,07	0,28	0,52	3,73	5,73	0,05	0,00	0,00	100,00
DRA-06D	ORG		-28,8361	17,9905	Non-porphyritic Rhyolite	74,55	0,37	13,81	1,20	0,73	0,96	0,04	0,39	0,67	2,54	5,90	0,04	0,00	0,00	100,00
DRA-06E	ORG		-28,8354	17,9912	Non-porphyritic Rhyolite	74,81	0,27	13,10	1,11	0,61	0,89	0,03	0,20	0,65	3,52	5,90	0,02	0,00	0,00	100,00
DRL-112	ORG		-28,6273	17,8553	Dacite	62,79	0,68	17,11	3,01	2,51	2,40	0,07	2,59	4,50	3,77	3,35	0,24	0,00	0,00	100,00
DRL-113	ORG		-28,6295	17,8450	Andesite	60,06	0,77	15,52	4,12	4,23	3,29	0,14	4,88	5,38	2,16	3,29	0,27	0,00	0,00	100,00
DRL-115	ORG		-28,6330	17,8536	Andesite	62,44	0,65	16,96	3,02	2,74	2,41	0,09	2,54	5,22	2,62	4,10	0,23	0,00	0,00	100,00

DRL-47	ORG		-29,0000	16,0000	Andesite	66,26	0,51	16,92	2,07	2,06	1,66	0,08	1,09	6,70	2,06	2,48	0,18	0,00	0,00	100,00
DRL-58	ORG		-28,8366	17,9871	Non-porphyritic Rhyolite	76,15	0,20	13,74	1,00	0,69	0,80	0,03	0,45	0,98	3,60	3,30	0,06	0,00	0,00	100,00
DRL-69	ORG		-28,6465	17,8959	Non-porphyritic Rhyolite	80,89	0,20	11,22	0,64	0,45	0,51	0,03	0,43	0,53	3,60	2,07	0,06	0,00	0,00	100,00
DRL-70	ORG		-28,6481	17,8908	FRAGMENTAL VOLCANIC ROCK	54,55	0,67	13,74	4,42	6,34	3,53	0,15	10,17	7,63	1,83	1,18	0,21	0,00	0,00	100,00
DRL-71	ORG		-28,6362	17,8651	Dacite	63,58	0,66	17,01	3,15	2,73	2,51	0,06	1,84	4,62	3,18	3,56	0,24	0,00	0,00	100,00
DRL-72	ORG		-28,6231	17,8471	FRAGMENTAL VOLCANIC ROCK	53,80	0,64	13,19	4,24	5,80	3,38	0,16	12,37	6,75	1,81	1,90	0,19	0,00	0,00	100,00
DRL-73	ORG		-28,6733	18,0879	Andesite	58,84	0,74	16,98	4,08	4,07	3,26	0,11	3,43	6,25	3,06	2,97	0,28	0,00	0,00	100,00
DRL-74	ORG		-28,7308	17,9654	Basaltic andesite	55,12	0,73	15,04	4,41	5,48	3,52	0,15	7,38	7,98	2,13	2,16	0,28	0,00	0,00	100,00
DRL-75	ORG		-28,7368	17,9651	Dacite	65,18	0,76	16,72	2,58	1,79	2,06	0,06	1,18	3,31	3,01	5,73	0,19	0,00	0,00	100,00
DRL-76	ORG		-28,7492	17,9699	Non-porphyritic Rhyolite	72,40	0,36	14,12	1,44	0,91	1,15	0,05	0,61	1,87	2,96	5,50	0,06	0,00	0,00	100,00
DRL-77	ORG		-28,7436	17,9670	FRAGMENTAL VOLCANIC ROCK	60,14	0,59	18,78	2,38	2,42	1,90	0,07	3,79	6,55	3,40	2,15	0,21	0,00	0,00	100,00
DRL-78A	ORG		-28,7512	17,9992	Dacite	66,27	0,54	15,06	2,95	2,37	2,35	0,08	2,34	3,76	3,04	4,04	0,15	0,00	0,00	100,00
DRL-78B	ORG		-28,7552	17,9997	Andesite	64,73	0,66	15,73	3,41	2,84	2,72	0,08	1,82	4,23	3,58	3,40	0,21	0,00	0,00	100,00
DRL-78C	ORG		-28,7585	18,0003	Andesite	64,25	0,61	15,78	3,61	3,73	2,89	0,19	3,48	4,14	2,55	2,23	0,14	0,00	0,00	100,00
DRL-79	ORG		-28,7466	17,9683	Non-porphyritic Rhyolite	68,20	0,47	15,77	1,96	1,38	1,57	0,06	1,07	3,02	3,79	4,58	0,09	0,00	0,00	100,00
DRL-81	ORG		-28,7002	18,0337	FRAGMENTAL VOLCANIC ROCK	55,62	0,68	14,73	4,36	5,50	3,48	0,16	6,96	8,58	3,38	0,67	0,24	0,00	0,00	100,00
DRL-92	ORG		-28,8445	17,8245	Rhyolite	69,95	0,44	14,94	1,77	1,16	1,41	0,04	0,94	2,42	3,67	4,94	0,09	0,00	0,00	100,00
DRL-94	ORG		-28,8434	17,8350	Rhyolite	69,90	0,47	14,92	1,93	1,38	1,54	0,05	0,84	2,70	3,44	4,64	0,11	0,00	0,00	100,00
DRP-03	ORG		-28,6783	17,8450	Dacite	69,84	0,36	15,29	2,16	1,65	1,72	0,05	1,31	2,68	2,22	4,75	0,12	0,00	0,00	100,00
DRP-04	ORG		-28,6868	17,9230	Andesite	61,09	0,67	16,17	4,02	4,14	3,21	0,16	4,03	4,94	1,86	3,55	0,17	0,00	0,00	100,00

DRP-10	ORG		-28,7054	17,8703	Andesite	64,59	0,58	15,79	3,38	3,28	2,70	0,12	2,84	4,55	2,70	2,70	0,14	0,00	0,00	100,00
DRP-12	ORG		-28,7130	17,9288	Andesite	63,21	0,63	15,70	3,74	3,56	2,98	0,14	3,37	4,41	2,39	3,41	0,17	0,00	0,00	100,00
RT-04	ORG		-29,0000	16,0000	Dacite	63,74	0,59	15,60	3,38	2,97	2,70	0,09	2,88	4,33	2,10	4,84	0,17	0,00	0,00	100,00
RT-05	ORG		-29,0000	16,0000	Dacite	63,94	0,60	15,51	3,49	3,01	2,78	0,10	2,73	4,43	2,14	4,59	0,16	0,00	0,00	100,00
RT-06	ORG		-29,0000	16,0000	Dacite	64,05	0,60	15,71	3,55	3,05	2,84	0,10	2,50	4,27	2,24	4,51	0,13	0,00	0,00	100,00